S. Shylesh, W. R. Thiel, and V. Schünemann

DOI: 10.1002/anie.200905684

Nanocatalysts

Magnetically Separable Nanocatalysts: Bridges between Homogeneous and Heterogeneous Catalysis

Sankaranarayanapillai Shylesh, Volker Schünemann, and Werner R. Thiel**

Keywords:
catalysis · heterogenization · magnetic properties · magnetic separation · nanoparticles

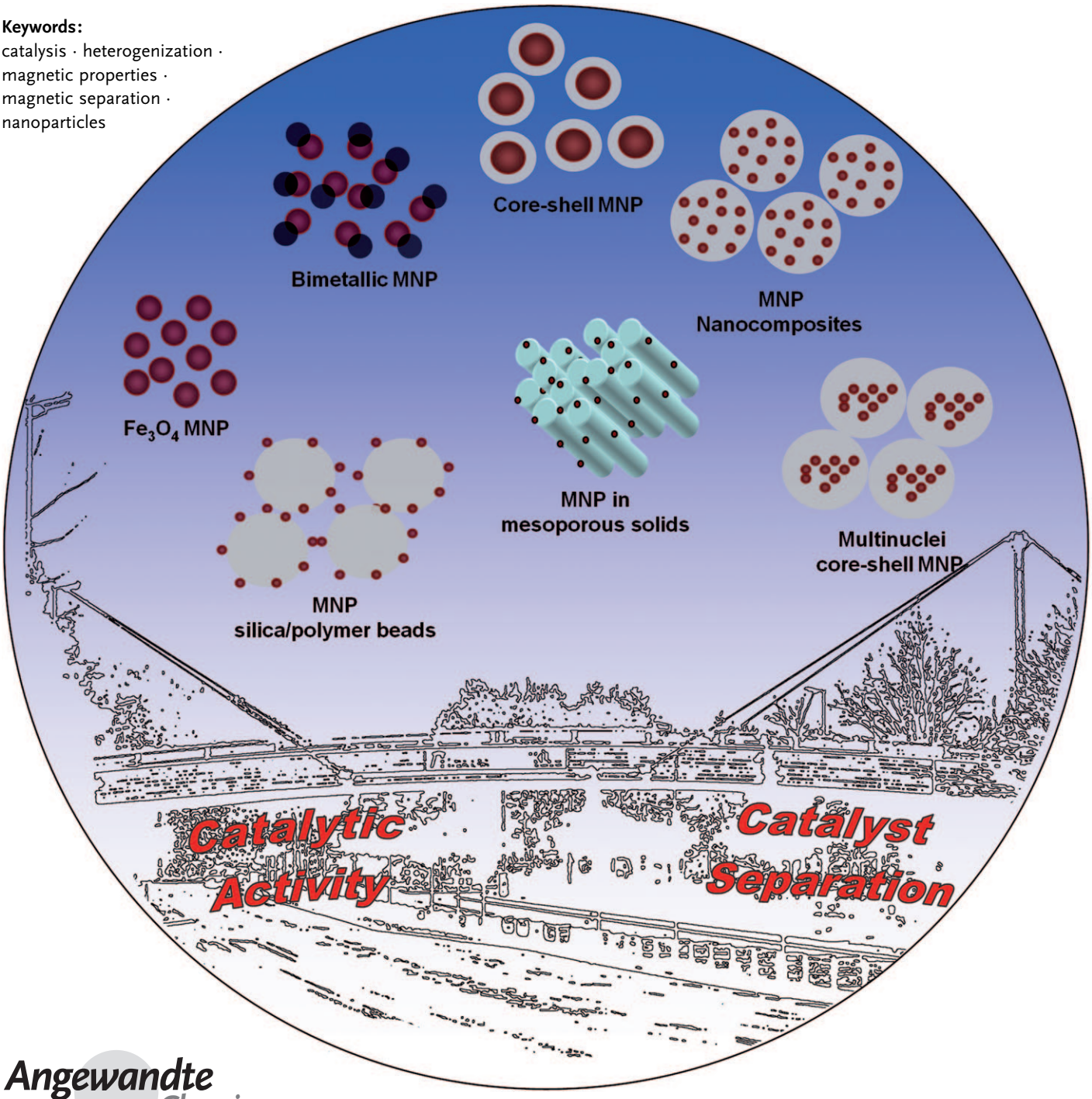

Recovery and reuse of expensive catalysts after catalytic reactions are important factors for sustainable process management. The aim of this Review is to highlight the progress in the formation and catalytic applications of magnetic nanoparticles and magnetic nanocomposites. Directed functionalization of the surfaces of nanosized magnetic materials is an elegant way to bridge the gap between heterogeneous and homogeneous catalysis. The introduction of magnetic nanoparticles in a variety of solid matrices allows the combination of well-known procedures for catalyst heterogenization with techniques for magnetic separation.

From the Contents

1. Introduction

Nanochemistry is an exponentially growing research field in modern science that involve the synthesis and application of nanoparticles of different sizes and shapes.[1] Nanoparticles are different from their bulk counterparts and exhibit unique properties. A typical well-known example is the fluorescence emission from semiconductor nanocrystals (quantum dots, QDs) which is dependent on the particle size and covers the entire visible spectrum.[2] Decreasing the size of a particle results in a larger share of the atoms being located on the surface, which can increase the influence of surface effects on the material properties. It has, for example, been shown theoretically and experimentally that decreasing the size of a crystalline metal particle will confine the electron motion. In parallel, the electronic bands of the crystal get gradually quantized, thereby resulting in an increase in the band-gap energy.[3] As described by El-Sayed, new properties, which are possessed neither by the bulk solid nor by the molecules or atoms forming the solid, are expected to be observed under these size transitions. This makes nanochemistry interdisciplinary—integrating different areas of research from material science to biomedicine.[4]

Colloidal metallic nanoparticles have widely been used for catalytic transformations, and represent something like the frontier between homogeneous and heterogeneous catalysis— these system are often referred to as "quasihomogeneous" (or soluble heterogeneous) systems.[5–11] A series of reduction techniques using molecular hydrogen,[12] alcohols,[13] or $NaBH_4$[14] have been reported for the synthesis of colloidal metal nanoparticles. Since nanoparticles possess a large fraction of their atoms on the external surface, they have to be stabilized by capping agents such as polymers,[15] surfactants,[16] dendrimers,[17] and ionic liquids.[18] Applications in catalysis are clear as these systems offer high surface areas and a high concentration of low-coordinated sites and surface vacancies, which are required for high catalytic performances.[19] Besides the inherent size–activity relationship, the particle shape also has to be taken into account.[20] For example, hexagonal Pt(111) surfaces were reported to be about 3–7 times more active for aromatization reactions than cubic Pt(100) surfaces.[21] Thus, controlling the particle morphology is widely utilized to tune their activity and selectivity.[22]

Reaction time, temperature, and the concentration of reactants added during particle synthesis allow control over the particle size[23] as well as particle ripening.[24] Unprotected nanoparticles are usually unstable and coagulation is unavoidable during the catalytic transformation.[25] To produce stable nanoparticles and to retain their high activity it is necessary to terminate the particle growth and to stabilize the surface. Protection has been achieved through the addition of capping agents or by immobilization in solid materials with high specific surface areas.[23,26,27] Capping agents used for this purpose are mainly polymers or long-chain alkyl surfactants with polar head groups that bind to the nanoparticle surface through covalent or electrostatic interactions. The stabilization itself is explained by electrostatic or steric effects or by a combination of both (Figure 1). A wealth of catalytic applications of such nanosystems have been reported, the catalytic reduction of nitrobenzene, for example.[28] Catalysis of olefin hydrogenation and CO oxidation at low temperatures by Au nanoparticles,[29] and the catalysis of C–C coupling[30] or hydrosilylation reactions of olefins[31] by Pd nanoparticles are further examples.

Alternatively, nanoparticles have been immobilized or grafted onto inorganic supports to improve their stabilization and recycling ability.[23,32] Porous materials also allow control over the particle growth according to the pore size and the enhancement of the dispersion and concentration of the

[*] Dr. S. Shylesh, Prof. W. R. Thiel
Fachbereich Chemie, Technische Universität Kaiserslautern
Erwin-Schrödinger-Strasse 52, 67663 Kaiserslautern (Germany)
Fax: (+49) 631-2054647
E-mail: thiel@chemie.uni-kl.de
Prof. V. Schünemann
Fachbereich Physik, Technische Universität Kaiserslautern
Erwin-Schrödinger-Strasse 56, 67663 Kaiserslautern (Germany)

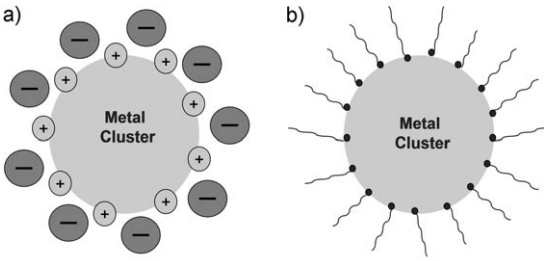

Figure 1. Methods for the stabilization of nanoparticles: a) electrostatic and b) steric stabilization.

active sites in the host matrix.[33] Progress in the discovery of new support materials for the heterogenization of homogeneous catalysts has been periodically reviewed.[34]

In this Review, we highlight the application of magnetic nanoparticles (MNPs) as catalysts and as catalyst supports. The advantages of these systems over conventional nonmagnetic porous solids with high specific surface areas are summarized. Prior to this, methods for the synthesis, stabilization, and characterization of MNPs will be addressed briefly.

2. Heterogenization of Homogeneous Catalysts: Why Magnetic Nanoparticles?

The main focus of catalysis research in the past was to enhance catalytic activity and selectivity. Recovery of the catalyst was not really a serious concern. However, in "green chemistry" approaches for catalytic reactions, the recovery and reuse of catalysts becomes an important factor because of stringent ecological and economical demands for sustainability.[35,36] Homogeneous catalysts have the advantage that they are well defined on a molecular level and readily soluble in the reaction medium. Such single-site catalysts are highly accessible to the substrates and often show high catalytic activity and selectivity, even under mild conditions. However, removing them from the reaction mixture to avoid contamination of the product requires expensive and tedious purification steps.[36] Moreover, the catalyst often consists of a high-priced noble metal and/or ligand. Thus, despite their intrinsic advantages, homogeneous catalysts are used in less than 20% of the industrially relevant processes.[37] On the other hand, there are often different catalytically active sites with differing activities and selectivities in the bulk material of a heterogeneous catalyst, which are challenging to probe on a molecular level.[38]

Recycling of homogeneous catalysts is thus an important issue in the sustainable and large-scale production of fine chemicals. It is of special importance for enantioselective transformations, in which the cost of sophisticated ligands often exceeds that of the noble metal employed.[39] The catalyst can be recycled under liquid–liquid and solid–liquid conditions. Liquid–liquid techniques rely on dissolving the catalyst and the product in different nonmiscible solvents, which allows recovery by simple phase separation. However, the process is limited by the solubility of reactants in the catalyst medium (usually water) and by the mass transfer through the interface. The high interfacial tension between water and nonpolar organic solvents results in the interface area being small, which leads to the total activity of the system being lower.[40] Solid–liquid techniques are based on the immobilization of catalytically active metal particles or compounds on solid supports (for example, organic polymers/resins or inorganic oxides). In the case of solid particles suspended in a liquid, the rate of transfer of reactants within the liquid to the catalyst is inversely proportional to the particle diameter. Thus, the activity (and the selectivity) of the suspended catalyst will benefit from decreasing the particle size.[41] It is worth mentioning at this point that the dispersion of most conventional heterogeneous catalysts in liquid media is poor and in most cases distinct solid–liquid separation occurs, even after vigorous stirring.

One way to overcome this drawback is to keep the size of the particles as small as possible.[23,42] Nanoparticles have recently emerged as efficient alternatives for the immobilization of homogeneous catalysts and as catalysts themselves.[6,32,43] The large specific surface area of nonporous nanoparticles means that high loadings of catalytically active sites are guaranteed and diffusion in the pores will no longer limit the kinetics. For example, spherical nanoparticles with a diameter of about 10 nm have a calculated surface area of $600\ m^2 cm^{-3}$, which is comparable to many porous supports used for the immobilization of homogeneous catalysts.[44] Thus, one could say that there is plenty of room on the surface of these nanoparticles for the heterogenization of

Sankaranarayanapillai Shylesh was born in 1978 in Kerala (India), and completed his BSc in chemistry at the University of Kerala, in 1998. For his master of science in polymer chemistry (2000), he moved to the University of Calicut (Kerala), and for an MPhil in chemistry to the Cochin University of Science and Technology (CUSAT; Kerala). In 2006 he completed his PhD at the National Chemical Laboratory (NCL), Pune (India) with A. P. Singh. Since 2008 he has been working as a research fellow of the Alexander von Humboldt-Foundation in the group of Prof. W. R. Thiel at the TU Kaiserslautern.

Volker Schünemann was born in 1963 in Lübeck (Germany). After graduating in physics at the University of Hamburg, he completed his PhD in 1993 with A. X. Trautwein at the Medical University of Lübeck. After postdoctoral research with Prof. W. M. H. Sachtler at Northwestern University (Evanston, USA) he returned to the Trautwein group. In 2004 he became professor for biophysics and medical physics at the University of Kaiserslautern. His current interests are the role of iron in biology, bioinorganic chemistry, as well as nanoparticles and spin cross-over systems. A further core area is Mössbauer spectroscopy.

various homogeneous catalysts. Investigating such small-sized particles will also assist in understanding the relationships between homogeneous and heterogeneous catalysis, and could efficiently bridge the gap between these two traditional disciplines. Unlike conventional micrometer-sized particles, nanoparticles can be easily dispersed in a liquid medium to form stable suspensions. However, particles with diameters of less than 100 nm are difficult to separate by filtration techniques. In such cases, expensive ultracentrifugation is often the only way to separate the product and catalyst. This drawback can be overcome by using magnetic nanoparticles (MNPs), which can be easily removed from the reaction mixture by magnetic separation.

At this point, the unique magnetic features of ferromagnetic materials of a certain size (10–20 nm) will be discussed. They often exhibit a special form of magnetism called superparamagnetism.[45] Magnetic solids possess magnetic domains with well-defined magnetic sublattices which are separated by domain walls. The magnetic moments of these domains are oriented randomly if the solid has not been magnetized by the application of an external magnetic field. Below a critical size, an MNP possesses only a single magnetic domain and has a net magnetic moment that results from the sum of all uncompensated spins in the nanoparticle. Such particles are named single-domain particles. Thermal excitation enables the magnetization of the single-domain particles to relax between the axes of easy magnetization. Such magnetic behavior of small single-domain particles is called superparamagnetism. In the simplest case of uniaxial relaxation, a relaxation process where the magnetization flips around an angle of 180°, the relaxation rate of a single domain particle with volume V at a temperature T is given by the Néel Equation [Eq. (1)].[46]

$$\nu = \nu_0 \exp\left(-\frac{KV}{k_B T}\right) \quad (1)$$

The energy barrier $E = KV$ is called the anisotropy energy and describes the strength of the "pinning" of the single-domain particle magnetization; ν_0 is a pre-exponential factor on the order of 10^9 to 10^{12} s^{-1}. Every magnetic material has its own characteristic anisotropy constant K, but in the case of single-domain particles, K may be considerably increased by almost one order of magnitude from the solid state value because of surface and form anisotropy contributions. Although superparamagnetic particles possess a a fluctuating magnetic moment $\vec{\mu}$ rather than a permanent one, they will respond to an external magnetic field $\vec{B}$. However, it is important to note that the resulting force $\vec{F}_m$ will be—just as in the case of a paramagnetic material—proportional to the magnetic field gradient, according to [Eq. (2)].[47]

$$\vec{F}_m = (\vec{\mu}\nabla)\vec{B} \quad (2)$$

If the particle size increases above a critical size, multi-domain magnetism predominates. In this case each magnetic domain possesses independent directionality, which results in a decrease in the magnetic coercivity (Figure 2).[48] For example, when the diameter of cobalt nanoparticles increases from 4 to 8 nm, the magnetic coercivity at 5 K increases from 370 to 1680 Oe, while a further increase to 13 nm decreases the magnetic coercivity to 250 Oe.[49] Some of the interesting magnetic features of superparamagnetic particles can be summarized as follows:

- Superparamagnetic particles can be manipulated by external magnetic field gradients.
- The field required to fully align all the particle moments is generally high; therefore, saturation will not be observed at lower Tesla values.
- When the field is removed, thermal energy allows reorientation of the spins of the particles in a way that no external energy is required to demagnetize the system.[45]

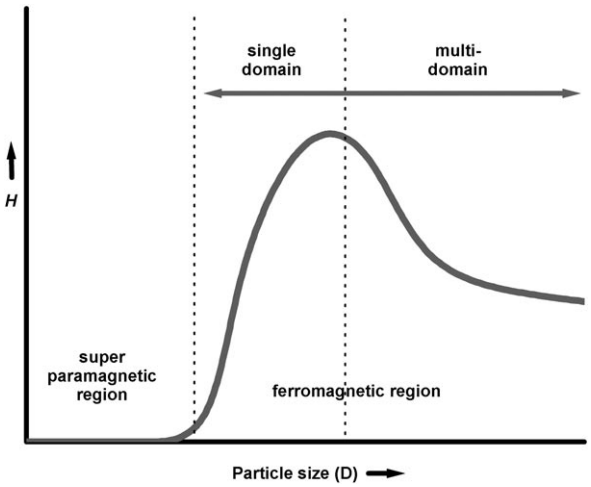

Figure 2. Plot of magnetic coercivity versus particle size.[45]

This peculiar nature has resulted in different methods having recently been developed for the synthesis of superparamagnetic nanoparticles with a defined size and shape. Such particles have found application, for example, in contrast enhancement in magnetic resonance imaging (MRI), in drug-delivery systems, in bioseparation, and in catalysis.[26,50] The specific advantages of magnetic nanomaterials in catalysis can be summarized as follows:

- The particles possess high external surfaces.

Werner R. Thiel was born in 1961 in Munich (Germany), studied chemistry at the TU München, and completed his PhD in 1990 with W. A. Herrmann. After postdoctoral research with D. Astruc in Bordeaux (France), supported by a Feodor Lynen grant, he returned to the TU München and finished his habilitation in 1997. In 2000 he moved to TU Chemnitz and in 2004 became full professor of inorganic chemistry at the TU Kaiserslautern. His research concerns homogeneous and heterogeneous catalysis, particularly structure–reactivity relationships for catalytic transformations and the immobilization of catalysts on inorganic supports.

- The catalytically active sites can be distributed on the outer surface of the support; thus pore diffusion constraints are avoided.
- The small size of the particles (typically < 50 nm) means they are highly dispersable in solvents; thus the external active sites are readily accessible to the incoming reactants.
- The application of an external magnetic field allows the particles to be removed in a simple and efficient way (typically $> 99\,\%$).

However, MNPs tend to aggregate in clusters or clumps when treated without any protection agents, thus canceling out their unique properties derived from their small size.[51] Protocols for coating such reactive nanoparticles with surfactants were developed to circumvent this problem.[52] Alternatively, coating these particles with inorganic layers such as silica is considered as an efficient approach. This treatment not only stabilizes the MNPs, but also allows further modification of the surface with other functional groups.

3. Synthesis of Superparamagnetic Nanoparticles

Intensive studies on the conditions—the use of different precursors, solvents, and capping agents—for the synthesis of colloidal particles recently led to the development of various sized/shaped superparamagnetic nanoparticles.[26,53] Such magnetic colloids can be metals (Fe, Co, Ni), alloys (FePt, $FePt_3$), metal oxides (FeO, Fe_2O_3, Fe_3O_4), or ferrites ($CoFe_2O_4$, $MnFe_2O_4$). Iron chloride, acetate, acetylacetonate, and carbonyls are commonly used precursors for the synthesis of iron oxide nanoparticles.[54] Iron pentacarbonyl ($[Fe(CO)_5]$) is a widely used precursor for the synthesis of Fe nanoparticles.[55] The synthesis of pure metal nanoparticles is considered a difficult task, since metals such as iron are readily oxidized under ambient conditions. This means that at least the surface of such particles is covered by various native oxides. Among the iron oxides, γ-Fe_2O_3 (maghemite) and Fe_3O_4 (magnetite) have received more attention than FeO since smaller FeO nanoparticles are again quite sensitive towards oxygen.[56] In maghemite, the iron ions are distributed in the octahedral (O_h) and tetrahedral (T_d) sites of the spinel structure, with cationic vacancies within the octahedral sites.[57]

Ferrites of the spinel type with the general formula MFe_2O_4 (M = Co, Mn, Ni) are probably the most widely used and studied magnetic materials in heterogeneous catalysis.[58] The magnetic moments of ferrite nanoparticles are intrinsically related to the composition of the ferrite particles.[59] For example, the incorporation of Co^{2+} ions into an iron oxide matrix to give $CoFe_2O_4$ enhances the magnetic anisotropy relative to a pure Fe_3O_4 nanoparticle of similar size, whereas the insertion of Mn^{2+} ions ($MnFe_2O_4$) decreases it.[60] Alternatively, the magnetic and chemical properties of monometallic elements can be significantly altered by the development of alloy particles.[61] A particularly successful example of this class are the face-centered tetragonal (fct) alloys MPt (M = Fe, Co). In their crystalline form they have the highest magnetic anisotropy and they are particularly less sensitive towards oxidation than pure iron or other platinum-free magnetic metals. Sun et al. reported the first synthesis of monodisperse FePt alloy nanoparticles by a simultaneous reduction of platinum acetylacetonate ($[Pt(acac)_2]$) and thermal decomposition of $[Fe(CO)_5]$ in a mixture of oleic acid and oleylamine. The composition of these particles was adjusted by simply varying the molar ratio between the two metal precursors.[62]

A wide variety of methods including co-precipitation, thermal decomposition, synthesis in microemulsions or under hydrothermal conditions, and laser pyrolysis techniques were employed for the synthesis of magnetic materials.[26,63] Among these methods, co-precipitation is considered to be the most facile way to generate iron oxides. It is typically carried out with an aqueous solution containing Fe^{2+}/Fe^{3+} salts and base added under inert conditions at ambient temperatures. The surfaces of the iron oxide nanocrystals formed are stabilized by surfactants or associated ions. Notably, the phase purity as well as the size and the shape of these particles will depend, for example, on the nature of the iron precursor used, the pH value of the reaction mixture, the reaction temperature, and time. The advantages of this method lie in its simplicity, the use of readily available metal precursors, the use of aqueous solutions, and high overall yields. However, a major limitation is the difficulty in controling the size of the particles, in other words polydisperse products are obtained. Therefore, size-selection procedures, such as the addition of electrolytes, are applied to stabilize the colloid solution. This will precipitate larger particles, thereby leaving smaller monodisperse particles in the supernatant, which can be isolated.[53,64]

When a high degree of stability and accurate control over the particle size is desired, nonhydrolytic thermal decomposition methods are generally used. Monodisperse MNPs can easily be developed through this approach by using (organo)metallic precursors (mainly metal–cupferron complexes, metal acetylacetonates, or metal carbonyls) in high-boiling solvents containing surfactant stabilizers.[65] Alivisatos and co-workers, for example, developed a thermal decomposition method for producing monodispersed γ-Fe_2O_3 nanocrystals by pyrolyzing an iron–cupferron complex (cupferron = *N*-nitrosophenylhydroxylamine, $C_6H_5N(NO)O^-$) in trioctylamine at 200–300 °C. Uniform γ-Fe_2O_3 nanocrystals of about 6–7 nm were obtained by a "hot-injection" method at 300 °C.[66] Hyeon et al. and Sun et al. later developed very successful methods to produce monodisperse Fe_3O_4 nanoparticles, without a size-selection procedure, based on thermal decomposition at high temperatures in the presence of oleic acid and oleylamine as stabilizers.[67] This method not only produces highly crystalline and monodispersed magnetic particles it also assists in the fabrication of more complex heterostructured nanoparticles.[45,68]

MNPs have also been prepared by microemulsion methods. However, this process is difficult to control and thus the particles were polydispersed;[69] furthermore, the yields are low. Laser pyrolysis of carbonyl precursors was recently shown to also be effective in the synthesis of uniform iron nanoparticles with narrow particle size distributions, without aggregation.[70] For example, passivated iron nanoparticles

could be synthesized by laser pyrolysis of a mixture of iron pentacarbonyl and ethylene followed by controlled oxidation. The developed nanoparticles had an iron/iron oxide core–shell structure, in which the thickness of the shell was independent of the initial conditions.[71]

4. Stabilization/Surface Modification of MNPs

As mentioned above, pristine iron oxide MNPs will aggregate rapidly into large clusters and thus will lose their unique properties associated with the presence of single domains. The nanoparticles have to be coated with organic surfactants to prevent irreversible aggregation, and so retain their nanoscale properties. It is well known from catalysis that metal nanoparticles of high surface energy will aggregate into large particles in the absence of stabilizing agents. This in turn results in a loss of active reaction sites and specific surface areas, and thus enhances deactivation.[9,10] Since most of the MNPs derived from metals or metal alloys are susceptible to easy oxidation upon exposure to air, or even solvated oxygen species, core–shell structures have usually been employed to protect these materials and retain their nanoscale properties.[72] The term "particle engineering" is used to describe the synthesis of core–shell particles with defined morphology. This strategy is of broad interest since it also allows the integration of multiple functionalities to a single nanoparticle system.[73]

4.1. Stabilization by Organic Coatings

Coating the surface with amphiphilic capping molecules such as long-chain fatty acids, diols, or alkyl amines is the common way to prevent aggregation of individual particles, and also to regulate the size and the size distribution of MNPs.[74] The surfactants used as stabilizing agents play a vital role in the nucleation and growth of the developing nanoparticles in the solution. This means that, according to the nature of the stabilization agent, the size, shape, magnetic, and chemical properties of the nanoparticle can be controlled by the dynamic adsorption and desorption properties of the surfactant molecules.[75] However, the exchange properties of these ligands during further modification of the nanoparticle depend on the strength and nature of the bond between the ligands and the nanoparticles. For example, oleic acid (CH_3-$(CH_2)_7CH{=}CH(CH_2)_7COOH$), which possesses a double bond at the 9,10-position, is a widely used compound for passivating iron oxides because of its ability to produce highly uniform and nearly monodisperse nanocrystals.[76] O'Brien and co-workers studied the properties of oleic acid as a surfactant in detail, and noted that the degradation of oleic acid during the thermal decomposition used for the synthesis of iron oxide nanocrystals promoted the formation of high-quality γ-Fe_2O_3 nanocrystals.[77] The authors postulated that the mixture of organic species formed under these high-temperature conditions has the unique ability to form γ-Fe_2O_3 nanocrystals of high uniformity. Surfactants with shorter alkyl chains can also assist surface modifications, but alkyl chains with at least six carbon atoms are in general necessary to provide sufficient stabilization by steric repulsion.

Coating the surface of nanoparticles with polymers is an alternative approach to stabilizing the surface.[78] The synthetic routes employed to generate polymer coatings on nanoparticles are generally classified in to two major groups: direct polymerization on the particle surface or adsorption on the nanoparticles.[73,79] Among all the methods reported in this context, atom-transfer radical polymerization (ATRP) is widely used to generate highly monodispersed particles without the need to apply challenging conditions to form the desired core (Fe, Fe_2O_3) and shell (polymer) structures.[80] Furthermore, a variety of polymeric materials such as polypyrrole, poly(*N*-vinyl-2-pyrrolidone), poly(vinyl alcohol), and poly(glycerol monoacrylate) as well as di- and triblock copolymers containing carboxylate, phosphate, or sulfate groups were used for the formation of stable polymeric shells on iron oxide nanoparticle cores.[53,79,81] Since the polymer coatings are relatively thin, they can not prevent oxidation of highly reactive metal nanoparticles. Often the coatings are not stable at high temperatures, unless the polymer possesses a functional group that binds strongly to the particle.[82] These properties are critical for metal nanoparticles because of their highly reactive nature as well as their intrinsic catalytic behavior.

4.2. Stabilization by Inorganic Coatings

Compared to MNPs stabilized or protected by organic surfactants, inorganic oxide coatings such as silica offer unique advantages for applications, paticularly in biomedecine and catalysis. The presence of a large amount of surfactant on the surface of the nanoparticle will interfere with applications in biomedicine, and the inherent reactivity of pristine iron oxide nanoparticles leads to degradation of the bioactive components.[83] Iron oxides are themselves well known to act as catalysts. It is necessary to build up a strong barrier between the magnetic core and the molecular catalysts to circumvent unwanted interactions with molecular catalysts bound to the surface of the nanoparticle. Coating MNPs with silica avoids unfavorable contacts with the core and prevents particle aggregation. Furthermore, the presence of surface silanol groups allows simple surface derivatization with a variety of functional groups. The silica coating makes the MNPs more hydrophilic and thus more biocompatible than those stabilized by oleic acid.

Coating iron oxides with silica to form core–shell structures is quite simple because of the presence of surface FeOH groups. The deposition of silica on pure metals is more complicated because of the lack of hydroxy groups. It is, therefore, necessary to apply processes which make the metal surface vitreophilic before starting the coating process.[84] The sol–gel process is the preferred method for the coating of MNPs with silica.[85,86] This process basically relies on the well-known Stöber method in which silica is formed over the nanoparticles through the hydrolysis and subsequent condensation of silicon alkoxides (typically, tetraethyl orthosilicate, TEOS) in alcohol/water mixtures under basic reaction

conditions. Interestingly, the thickness of the silica shell can easily be manipulated by the reaction conditions. Xia and co-workers elegantly showed that the thickness of the silica shell can simply be tuned by varying the concentration of TEOS added to a mixture of commercially available ferrofluids (magnetic fluids) in water, 2-propanol, and 30% aqueous ammonia.[87] Thus, good control over the thickness of the silica shell (2–100 nm) could be achieved without homogeneous nucleation of silica. High-resolution transmission electron microscopy (HR-TEM) images demonstrate the efficiency of this approach and also prove the crystalline nature of the iron oxide core and the amorphous nature of the silica shell, with uniform particle size and shape.

Philipse et al. illustrated that Fe_3O_4@SiO_2 MNPs with a mean diameter of 60–120 nm could be obtained by the Stöber method when the bare Fe_3O_4 MNPs were pretreated with a layer of silicate in aqueous solution.[88] Without this primary silica coating process, coating with TEOS in ethanol/ammonia mixtures yielded magnetic clusters embedded in large silica aggregates. The authors proposed that the primary thin silica layer on the Fe_3O_4 MNP surface reduces the isoelectric point (IEP) of the magnetite and maintains its colloidal stability during the second coating step.

In another study, Deng et al. reported in detail the affect of alcohols (methanol, ethanol, 2-propanol, *n*-propanol), the ratio of alcohol to water, and the amount of aqueous ammonia added during the synthesis on the formation of silica-coated magnetic nanoparticles.[89] It was shown that a pH value between 8–10 is ideal for the coating reaction, as it reduces the solubility of the silicate species in solution and also results in a homogeneous coating on the nanoparticle surface without the formation of new silica nuclei. Furthermore, low concentrations of MNPs and appropriate treatment with sonication to separate individual magnetic particles before the coating steps is preferred to obtain typical core–shell nanostructures, otherwise multinuclei iron oxide cores embedded inside silica shells will be produced (Figure 3).[87,90]

Coating magnetic nanoparticles with precious metals such as gold is another approach. The presence of gold assists further functionalization reactions with various sulfur-containing ligands.[91] However, this approach is difficult due to the different natures of the core and shell. A particularly successful example is the synthesis of platinum-coated cobalt by mixing cobalt nanoparticles (ca. 6 nm) and $[Pt(hfac)_2]$ (hfac = hexafluroacetylacetonate) in a nonane solution containing $C_{12}H_{25}NC$ as the stabilizer. The formation of bimetallic core–shell CoPt nanoparticles is proposed to arise by a redox transmetalation reaction between Co^0 and Pt^{2+} because of the presence of $[Co(hfac)_2]$ as a by-product after the reaction.[92] Such bimetallic nanoparticles are especially interesting for catalysis since magnetic and catalytically active components are integrated in the same system, and the precious noble metal can be conserved by replacing the interior of the nanoparticles with inexpensive core metals. Recently, carbon-coated magnetic nanoparticles also gained attention as catalyst supports because of their high chemical and thermal stability.[93] Stark and co-workers reported the synthesis of carbon-coated magnetic nanobeads with a rate of more than 30 $g\,h^{-1}$ by the addition of acetylene to a nanoparticle-forming flame (reducing flame synthesis). The beads consisting of a carbon shell and a cobalt core exhibited excellent magnetic properties and high stabilities in air at temperatures up to 190 °C and are viable for functionalization by diazonium chemistry to yield Cl-, NO_2-, and NH_2-functionalized magnetic nanobeads for applications in organic synthesis.[94]

At this juncture, it is worth pointing out that the formation of typical core–shell architectures was generally observed in small batch experiments. It turned out to be difficult to reproduce the architecture on a large scale. However, a stringent core–shell architecture is not a prerequisite for applications in catalysis. The presence of multinuclei iron oxide cores embedded in various shells (Figure 3) also allows simple separation of the particles. An alternative way to enhance the magnetism is to produce composite particles by immobilization of magnetic colloids in or on a nonmagnetic support.[95] This will also assist in the simple and rapid separation because of the high number of superparamagnetic particles. Two strategies have in general been applied for the synthesis of such composites: the superparamagnetic particles can be introduced on the surface of a preformed nonmagnetic support (for example, a polymer or silica beads) or the superparamagnetic particles can be encapsulated inside a nonmagnetic matrix such as mesoporous silica (Figure 3).

The synthesis of magnetic porous-structured materials has attracted particular attention because of their ordered pore channels. They are available in a tuneable size range (2–50 nm) for hosting a variety of bio/catalytic compounds. Reactive silica sites (Si-OH) inside the pores can easily be modified by well-known reactions of silicon. Such materials are typically obtained by introducing magnetic particles into the as-synthesized porous matrix or by the synthesis of a porous layer on the surface of premade magnetic nanoparticles.[96–100] Weisner and co-workers reported a self-assembly approach based on a block copolymer for the synthesis of thermally stable, mesoporous alumosilicates with a large number of superparamagnetic nanoparticles embedded in their pore walls. This occurred without blockage of the pores—an important requirement for catalytic applications.[97] A sol prepared from (3-glycidoxypropyl)trimethoxysilane

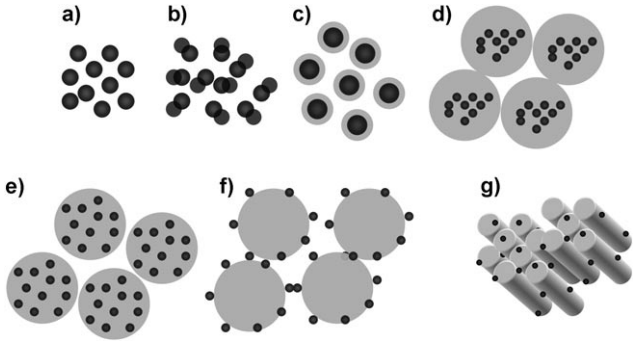

Figure 3. Different morphologies of MNPs/nanocomposites: a) spherical MNPs, b) bimetallic MNPs, c) typical core–shell MNPs, d) multinuclei MNPs embeded in core–shell particles, e) MNP-silica nanocomposites, f) MNP-decorated silica spheres, g) MNP encapsulated in mesoporous materials.

and aluminum *sec*-butanoxide was mixed with a solution of the amphiphilic diblock copolymer poly(isoprene-*block*-ethylene oxide) and iron(III) ethoxide to form a polymer–inorganic nanocomposite with 25 mol% iron. Mesoporous silicas containing bimetallic PtCo nanoparticles were recently generated by a liquid-crystal templating method by using neutral surfactants. Superparamagnetic CoO-MCM-41 mesoporous nanocomposites with variable amounts of cobalt were developed by a one-step procedure by co-hydrolysis and co-condensation of inorganic precursors in a water/triethanolamine medium.[98,99] A further example of this approach includes the synthesis of a mesoporous silica shell on a magnetic core by sol–gel polymerization of a mixture of TEOS and *n*-octadecyltrimethoxysilane (C_{18}-TMS), as reported by Zhao et al.[100]

Besides mesoporous silica, porous carbonaceous materials such as mesoporous carbon or carbon nanotubes have been modified with magnetic nanoparticles for applications in catalysis.[93,101–103] Li et al. reported, for example, the synthesis of magnetic iron nanoparticles with a diameter of about 1 nm inside single-walled carbon nanotubes (SWCNT) by using ferrocene as the starting material. TEM imaging showed the decoration of the inner channels with dotlike iron particles, while magnetic data proved that the encapsulated iron nanoparticles are present in the metallic phase and exhibit superparamagnetic behavior.[102] Stoffelbach et al. functionalized the surface of multiwalled carbon nanotubes (MWCNTs) by chemically grafting carboxylic acid groups through radical polymerization of azo compounds.[103] The MWCNTs were then decorated with magnetic nanoparticles by the addition of positively charged Fe_3O_4 nanoparticles to the negatively charged MWCNTs.

5. Characterization of Superparamagnetic Nanoparticles/Nanocomposites

Various physicochemical characterization techniques can be employed to probe the crystalline nature, the phase purity, the magnetic behavior, and the morphology of magnetic nanoparticles/nanocomposites. Common characterization techniques, such as X-ray diffraction (XRD), are used to prove the crystalline structure and the phase purity of the particles.

5.1. X-ray Diffraction and Small-Angle Scattering

The diffraction pattern can be used to quantify the proportion of iron oxide formed in a mixture by comparing the peak intensities in the experimental and reference diffractograms. This method was used to show that iron oxide–silica nanocomposites prepared from iron(II) *tert*-butoxide and tetraethyl orthosilicate (TEOS) have magnetite cores if the silica concentration is low, but exhibit maghemite cores when the silica content is high (for example, 30 mol%).[104] In addition, XRD can be used to calculate the crystal sizes d through evaluation of the line broadening β (in units of radians) and the corresponding Bragg angle θ, by using the Scherrer Equation [Eq. (3)].[105,106] K is the shape

$$d = \frac{K\lambda}{\beta \cos\theta} \quad (3)$$

factor which depends on the particle shape, and is approximately 0.9, and λ is the wavelength of the X-rays.

Analysis of the line broadening of the (311) peak according to Eq. (3) yields a mean particle size of 230–270 nm for the average size of the magnetite phases in Fe-Co/magnetite nanocomposites.[107] Below a particle size of about 3 nm, other scattering techniques such as small-angle X-ray scattering (SAXS) or small-angle neutron scattering (SANS) can be used to obtain mean particle sizes as well as size distributions.[108] Small-angle scattering is scattering which occurs for small values of the scattering vector $\vec{s}$, the magnitude of which is defined by Equation (4). The scattering of radial symmetric objects with electron density $\rho(r)$ can be described in terms of the radius of gyration R_g, which is defined by Equation (5). The scattered intensity $I(s)$ of an ensemble of diluted objects i (for example, nanoparticles) with homogeneous electron density, and the corresponding radii of gyration R_{gi} can be written as Equation (6),[109] where $I_i(0)$ is the scattering intensity in the direction of the incoming X-ray beam.[110] These equations were first derived by Guinier, by assuming $sR_g \leq 2$.[109] If one assumes homogeneous spherelike particles, their diameter d and the radius of gyration are related through Equation (7).

$$s = \frac{4\pi \sin\theta}{\lambda} \quad (4)$$

$$R_g^2 = \frac{\int r^4 \rho(r) dr}{\int r^2 \rho(r) dr} \quad (5)$$

$$I(s) = \sum_i I_i(0) \exp\left(-\frac{(R_{gi}s)^2}{3}\right) \quad (6)$$

$$d = 2\sqrt{\frac{5}{3}} R_g \quad (7)$$

More sophisticated data analysis has also been used to identify particle shapes.[111] Determination of the mean coordination number by X-ray absorption techniques such as EXAFS also provides information about systems with particles greater than 2 nm and a corresponding large surface contribution.[112]

5.2. Electron Microscopy

Transmission electron microscopy images correlated with energy-dispersive X-ray analysis (EDX) are used to measure the size uniformity, the shape of the nanoparticles, as well as the elemental composition of the core–shell structures. Alternatively, high-resolution TEM (HR-TEM) images provide electron diffraction patterns from single nanoparticles and thereby allow the crystal lattice to be probed with atomic resolution. This method is also used to analyze the thickness of the core and shell.[113] Conventional TEM also provides the

opportunity to measure the electron diffraction from single particles, which allows identification of local particle phases. However, sample preparation is a crucial step in TEM characterizations, as it can effect aggregation of colloids. The data may consequently not reflect the actual size and distribution present in solution.

5.3. Light Scattering

The measurement of dynamic light scattering (DLS) is another technique for obtaining information about the size of the particle. The determination of the diffusion coefficient of the nanoparticles in solution gives access to the hydrodynamic radius of a corresponding sphere and to the polydispersity of the colloidal solution. This technique is especially suited to follow aggregation processes, and has recently been used to study the long-term stability of MNPs with an iron oxide core and a gold shell, with particle distributions ranging from 10 to 200 nm.[114] However the method is not reliable if the nanoparticles are fluorescent.

5.4. DC and AC Susceptibility

Measurements of magnetization can also be used to obtain information about particle sizes and particle distributions within a sample. SQUID magnetometry and vibrating sample magnetometry (VSM) are the techniques commonly used to determine the net magnetization of magnetic nanoparticles. In general, a plot of the magnetization curve (magnetization M against the magnetic field strength H) enables the saturation magnetization M_s, the residual magnetization at $H=0$ (remanence magnetization, M_r), and the coercivity (H_c)—the external field required to reduce the magnetization back to zero—to be determined.[115]

The magnetization of a sample of non-interacting superparamagnetic particles with magnetic moments μ as a function of temperature T and external field B can be described by the Langevin function $L(x)=\coth(x)-1/x$ with $x=\mu B/k_B T$. Thus, the magnetization of a distribution of non-interacting particles with magnetic moments μ_i and relative volume contributions v_i can be written as Equation (8).[116]

$$M(T,B)=M_s\sum_i v_i L\left(\frac{\mu_i B}{k_B T}\right) \tag{8}$$

Determination of the particle moments μ_i is possible by fitting temperature- and/or field-dependent DC susceptibility measurements obtained, for example, from SQUID data to Equation (8) by assuming a given particle size distribution v_i. If the saturation magnetization M_s and the particle phase are known, it is possible to calculate the number of atoms within a particle and also the size of the particles by assuming a certain particle shape. For example, the diameter d (in nm) of spherical α-Fe particles with bcc structure is related to the number of atoms within the particle L by $d=0.282\,L^{1/3}$.[117]

The superparamagnetic blocking temperature is usually defined as the temperature at which half of the particles have relaxation times that are larger than the window of the spectroscopic method used for their characterization. Blocking temperatures within a typical time window of some minutes can be obtained by comparing field-cooled and zero-field-cooled DC susceptibility measurements. Another possibility for measuring the relaxation rates of the superparamagnetic particle moments within time windows of seconds to microseconds is AC susceptibility.[118] A small magnetic field $\hat{H}(t)$, which oscillates with frequency ω, induces magnetization $\hat{M}(t)$ in a sample according to the complex description given in Equation (9).

$$\hat{M}(t)=\chi_{AC}\hat{H}(t) \quad \text{with} \quad \chi_{AC}=\chi'(\omega,T)-i\chi''(\omega,T) \tag{9}$$

χ_{AC} is termed the alternating field or the AC susceptibility. Relaxation times can be determined from Cole–Cole plots obtained from frequency-dependent AC-susceptibility measurements. Alternatively, if one assumes the validity of the Curie law, by fitting the real part of the temperature and frequency-dependent susceptibility, the relaxation times can be determined according to Equation (10).

$$\chi'(\omega,T)\sim\frac{1}{T(1+\omega^2\tau^2)} \tag{10}$$

Fitting Equation (10) to temperature-dependent AC-susceptibility data allows determination of the relaxation times $\tau(T)$, and through the Neel Equation the determination of the anisotropy energies KV.[111] Another straightforward method for the determination of relaxation rates, irrespective of superparamagnetic blocking temperatures $T_B(\omega)$, is the determination of the maximum of $\chi'(\omega,T)$.[119] This method has also been applied very recently to nickel/zinc ferrite nanoparticles generated from a reverse micelle process.[120]

5.5. Mössbauer Spectroscopy

A typical problem associated with the characterization of magnetite and maghemite iron oxide nanoparticles is that both systems possess an inverse spinel structure and are thus difficult to distinguish by X-ray diffraction techniques. Nuclear resonance absorption of γ rays, better known as Mössbauer spectroscopy, can be used to identify iron (oxide) phases of iron-containing MNPs.[104,115a,120,121] If the relaxation of a superparamagnetic MNP is shorter than the lifetime of the excited state of the ^{57}Fe nucleus (ca. 10^{-7} s), the nucleus "sees" on average no magnetic field, and only a quadrupole doublet is observed. This is often the case if small nanoparticles of metallic iron or iron oxides are measured at room temperature. Measurements at cryogenic temperatures are needed to identify unambiguously the magnetic phase of these systems. Lowering the temperature results in the relaxation rate of the superparamagnetic particles being slowed down and the observation of a magnetically split pattern.[122] This technique can be applied to identify and distinguish metallic iron from iron carbide phases, even in particle systems with diameters as small as about 1 nm, on the

basis of their different hyperfine fields ($B_{hf} = -34$ versus -28 T at 4.2 K). This is especially interesting if the MNPs to be characterized have been prepared by thermal decomposition of iron carbonyl compounds. Mössbauer measurements in high external fields are needed to differentiate between magnetite and maghemite iron oxide nanoparticles by identifying the corresponding magnetic sublattices of the particles.

A simple approach to determining the superparamagnetic blocking temperature T_B of the particles within the characteristic time window of Mössbauer spectroscopy (10^{-7} s) is to measure the temperature at which half of the spectral area of the Mössbauer spectrum shows magnetic splitting and the other half of the spectrum shows a doublet or a single line depending on the size of the quadrupole splitting. For this temperature, one assumes $k_B T_B \approx K V$. Thus, by taking the anisotropy constant K from the literature, it is possible to estimate the mean particle volume V.

Another very elegant method to determine the magnetic moment μ of superparamagnetic particles is Mössbauer spectroscopic measurements at temperatures above T_B in various external magnetic fields.[123] In this case, the energy of the particles in a magnetic field μB is much larger than the anisotropy energy, so $\mu B \gg K V$ holds. The observed magnetic hyperfine field B_{obs} is calculated from Equation (11), where B_0 is the saturation hyperfine field, L the Langevin function, and k_B the Boltzmann constant. If the condition $\mu B/k_B T \gg 1$ is fulfilled, for example, for particles having particle magnetizations of 1000–10000 μ_B and external fields B on the order of 1 T as well as temperatures around 80 K Equation (11) simplifies to Equation (12).

$$B_{obs} = B_0 L\left(\frac{\mu B}{k_B T}\right) + B \tag{11}$$

$$|B_{obs} - B_0| = B_0\left(1 - \frac{k_B T}{\mu B}\right) \tag{12}$$

This method was first used to determine the size of 6 nm Fe_3O_4 particles[122] and later to measure 2.5 nm α-Fe particles on carbon black.[124] It has also been used to determine α-Fe particles with sizes of (1–2 nm) in zeolite NaX[125] and recently to 1–2 nm sized Fe grains in silver films.[126]

5.6. Ferromagnetic Resonance

Ferromagnetic resonance (FMR) can be conveniently performed on X-Band EPR spectrometers, and has been used to determine very low concentrations of magnetite particles (ca. 4×10^{-12} cm^{-3}) in mammalian blood vessels.[127] It can also be used to determine the magnetization of superparamagnetic particles through double integration of the experimental data. As this method may be inaccurate, an alternative is the analysis of the FMR line width $\delta H_{pp}(T)$, which is related to the effective anisotropy field $H_{eff}(T)$ through the equation $H_{eff}(T) = {}^1/_2\, \delta H_{pp}(T)$.[128] For the case of non-interacting particles, the anisotropy field H_a is calculated at the superparamagnetic blocking temperature T_B within the FMR time window (ca. 10^{-10} s) by using Equation (13).[129,130] Here, K denotes the anisotropy constant, as given in Equation (1); Equation (13) also holds if the anisotropy field H_{eff} shows no temperature dependence.

$$H_{eff}(T_B) = H_a = \frac{2K}{M_s} \tag{13}$$

For the case of uniaxial relaxing particles with volume V and moment μ, the temperature dependence of the effective anisotropy field is given by the Langevin function [see Eq. (8)] according to Equation (14). Thus, the particle moments μ can also be determined by fitting the temperature dependence of the FMR line width to Equation (14). For the case of interacting particles, Equation (14) has to be slightly modified and a mean-field approach can be used.[131]

$$H_{eff} = \frac{2K}{M_s} L\left(\frac{\mu B}{k_B T}\right). \tag{14}$$

5.7. Miscellaneous Methods

Other physicochemical techniques, such as atomic force microscopy (AFM), thermogravimetric analysis (TGA), differential scanning calorimetry (DSC), X-ray photoelectron spectroscopy (XPS), Raman spectroscopy, Fourier-transform infrared spectroscopy (FT-IR), time of flight/secondary ion mass spectrometry (TOF-SIMS), and potentiometric techniques are also used to investigate the surface properties of functionalized iron oxide nanoparticles. In most cases, a combination of the above-mentioned characterization techniques is required for an exact determination of the nanoparticle composition. A critical evaluation of the particle features is of particular importance for magnetic resonance imaging (MRI) applications. However, one should not forget that the characterization of, for example, organic functional groups on the support surfaces generally provides information on the nature of these functional groups. Most techniques are unable to provide information on the accessibility or the chemical environment of the organic groups.

Wet chemical analysis methods (ATR-IR, UV/Vis, NMR, conductometric titrations, etc) have attracted much attention for the characterization of organic–inorganic hybrid materials. Such techniques can provide a quantitative analysis of the organic functional groups. They also assist in elucidating the reactivity of the functional sites.[132] For example, Moon et al. utilized optical ellipsometry and UV/Vis spectroscopy to analyze the relative surface density of aminosilane layers grafted on fused silica and silicon wafers.[132a] For a quantitative analysis, the primary amines on the surface were treated with 4-nitrobenzaldehyde followed by hydrolysis, and the amount of generated 4-nitrobenzaldehyde determined. In another approach, Polito et al. reported the first application of high-resolution magic-angle spinning (HR-MAS) for the spectroscopic analysis of complex organic molecules bound to paramagnetic iron oxide nanoparticles.[132d] NMR spectroscopic measurements on ligands immobilized on MNPs is difficult due to pronounced line broadening caused by the absence of ligand mobility and the paramagnetic support. The

authors also showed that combining HR-MAS NMR with MALDI-TOF MS provides a useful platform for an accurate, detailed characterization of organic molecules bound to magnetic nanomaterials, and thus gives access to structural information on grafted organic functional groups in suspension.

Very recently, Baiker and co-workers were able to show that in situ ATR-IR (ATR = attenuated total reflection) spectroscopy can be used for the quantification of organic functional groups present on MNP surfaces. It can also be used to follow the transformation of immobilized organic groups for an accurate comparison between homogeneous and heterogeneous reactions.[132e] The formation of a new bond directly at the functional group of interest as well as the disappearance of the reactant in solution could be easily monitored at the same time. All these examples suggest that a combination of classical solid-state analytical methods and wet analysis techniques can enhance the understanding about the reactivity and accessibility of organic functional groups on hybrid nanomaterials, specifically for applications related to catalysis and biomedicine.

6. Applications in Catalysis

In this section, we will discuss the advantages of using superparamagnetic nanoparticles/nanocomposites as catalysts and catalyst supports.

Colloidal nanoparticles with a diameter of less than 50 nm are efficient catalysts for a wide range of industrially relevant organic transformations. For example, palladium and platinum nanoparticles have attracted attention as catalysts for olefin hydrogenation, carbon–carbon coupling reactions, and a series of other reactions. Conventional catalyst separation methods such as filtration and centrifugation become tedious for such small nanoparticles, which hampers the complete separation of the catalyst after the transformation. Magnetic nanoparticles or nanocomposites are considered as ideal supports for the heterogenization of homogeneous catalysts since they efficiently disperse catalytic active sites in the reaction medium. Furthermore, magnetic separation is a "green" process since it avoids the complications of filtration (such as loss of catalyst, oxidation of sensitive metal complexes, and usage of additional solvents for precipitation steps). Thus, waste and costs can be greatly reduced. Figure 4 shows a laboratory scale example, where a simple clamp magnet is used to separate the catalyst. For the purpose of discussion, the following topics are classified according to the reaction type.

Figure 4. Magnetic separation of finely dispersed superparamagnetic catalytically active nanoparticles (left: shortly after the application of the magnet; right: 2 min later).

6.1. C–C Bond Formation

Palladium-catalyzed Heck, Suzuki, and Sonogashira coupling reactions are well-studied reactions for the formation of C–C bonds. The resulting products have found numerous applications as intermediates in the synthesis of natural products and bioactive compounds. The difficulties in recycling and reuse of soluble palladium-based catalysts was widely overcome in the past by heterogenization of homogeneous palladium nanoparticles on various solid supports.[133] As an alternative, Gao and co-workers immobilized palladium complexes with N-heterocyclic carbene ligands (NHC-Pd complexes) on the surface of MNPs to generate iron oxide supported palladium complexes for Suzuki, Heck, and Sonogashira cross-coupling reactions.[134] 1-Methylimidazole was first tethered to the surface of iron oxide nanoparticles, and a subsequent deprotonation of the imidazolium group with $Pd(OAc)_2$ in the presence of Na_2CO_3 gave the desired NHC-stabilized palladium complexes (Scheme 1).

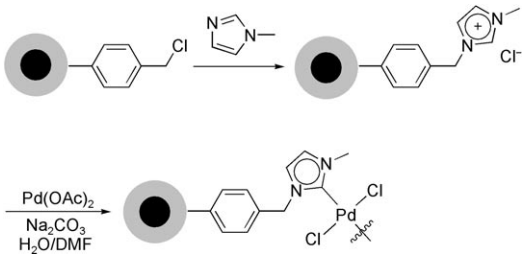

Scheme 1. Synthesis of NHC-Pd complexes on iron oxide nanoparticles.[123]

These supported NHC-Pd catalysts showed high conversions in the cross-coupling reactions mentioned above (Scheme 2). They also retained similar activity over five consecutive reactions. For example, 35% of the Suzuki coupling product was formed after 60 minutes from the reaction of 4-iodoacetophenone in the presence of 7.3 mol% NHC-Pd/iron oxide, while no product formation was observed under identical conditions with Pd/PS (PS = polystyrene), even after 180 minutes. The enhanced catalytic activity of the NHC-Pd/iron oxide compound was attributed to the easy access of the reactants to the active sites. This avoids problems of conventional heterogeneous supports, where a high proportion of the active sites are buried deep inside the materials. The catalysts can simply be recovered by magnetofiltration. The same authors also described on an emulsion polymerization technique for the formation of superparamagnetic core–shell nanoparticles consisting of γ-Fe_2O_3 cores and polymer shells with a diameter of about 2 nm that were used as soluble supports for immobilizing NHC-Pd catalysts for Suzuki coupling reactions. These heterogenized palladium catalysts exhibited superior activity (> 80%) in the

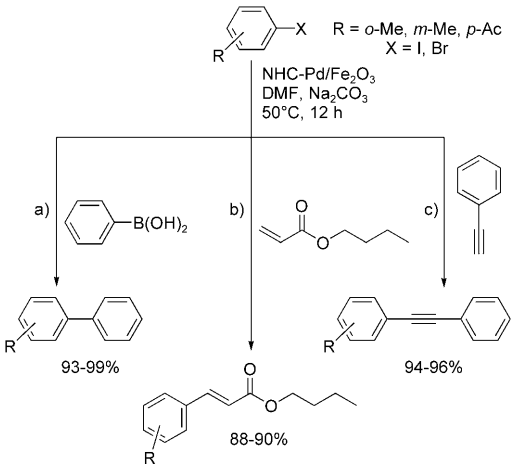

Scheme 2. Catalytic activity of NHC-Pd/iron oxide catalysts in a) Suzuki, b) Heck, and c) Sonogashira coupling reactions.[134]

Suzuki cross-coupling of aryl halides and aryl boronic acids, and could be recycled five times without any loss in activity.[135]

Gao and co-workers also reported that MNPs could be used as novel matrices for supported solid-phase organic synthesis on polymeric resins.[136] This is a synthetic challenge, since most of the catalytically active sites attached to solid-phase resins are not situated on the surface, but are buried in the interior of the polymer beads. Thus, a chemical reagent and its carrier (orthogonal support) need to penetrate inside the polymer bead, which is swollen in an organic medium, for further reaction. The authors used the above-mentioned NHC-Pd/iron oxide catalyst for solid-phase Suzuki cross-coupling reactions. As a consequence of their small size, magnetic nanoparticles are able to penetrate the resin pores and bring the attached catalytically active groups in proximity to the immobilized reagent inside the beads. The authors also evaluated the relationship between the core size of the particles and the reaction yields by using iron oxide cores of 4, 12, and 22 nm functionalized with similar molar amount of palladium. They noted that the reaction yield depends strongly on the size of the iron oxide cores: Pd/4 nm iron oxide produces the maximum yield (87%), followed by the 12 nm and 22 nm species. However, more than six days were required to complete the reaction because of the slow diffusion of the particles in and out of the resin pores. Furthermore, catalyst separation is difficult: It required repeated magnetic separation to completely remove the catalyst from the resin.

Surface modification of MNPs with appropriate ligands will assist the stabilization of colloidal metal nanoparticles (Pd, Rh, Ru). Wang et al. used Fe_3O_4 MNPs functionalized with (3-aminopropyl)trimethoxysilane for binding Pd^0 nanoparticles.[137] HR-TEM data proved that the Pd^0 produced during the first reduction of the Pd^{II} precursers binds to the amine-coated Fe_3O_4 MNPs and grows into bigger clusters during the course of the reaction. The catalytic activity of the Pd/Fe_3O_4 nanoparticles was investigated for the Heck coupling of acrylic acid with iodobenzene. The product yield decreased from 81% in the first run to 53% in the fifth run. This decrease was related to an aggregation of magnetic catalyst bodies, which resulted in a reduced active surface area and difficulties in redispersing the catalyst for reuse. This finding again highlights the need for more efficient stabilization or protecting agents.

Palladium nanoparticles with diameters of about 1 nm supported on phosphate-functionalized MNPs were reported to be stable, recyclable, and efficient catalysts for Suzuki and Heck reactions.[138] They were active in the Suzuki cross-coupling of bromobenzene with phenylboronic acid in a three-phase system and gave a yield of 83% in the Heck coupling of bromobenzene and styrene (56%). The authors noted that the MNP-supported Pd^0 catalyst was more active than a MNP-supported NHC-Pd complex in the Suzuki cross-coupling reaction, and also more active than Pd^0 heterogenized on different supports (MgO, TiO_2, and ZrO_2) in the Heck reactions. Recently, Lu et al. reported the immobilization of dipyridylpalladium complexes on MNPs through a click reaction (Scheme 3). This catalyst showed high conversions of 82–99% in Suzuki cross-coupling reactions, with better recyclability when DMF was used as the solvent and K_2CO_3 as the base.[139]

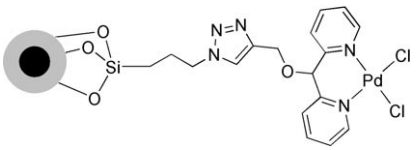

Scheme 3. Dipyridylpalladium complexes heterogenized on MNPs.[139]

Dopamine (DA) has turned out to be a robust anchor to graft Pd nanoparticles on ferrites (Pd/DA-$NiFe_2O_4$). This catalyst system can again be separated magnetically from Suzuki and Heck coupling reactions of aromatic halides.[140] The heterogenized ligand is rapidly accessible from inexpensive precursors in a one-step reaction, and the catalyst gives high yields even for aryl chlorides. Furthermore, the catalyst is completely recoverable, and the catalytic activity remains unaltered after three reactions in DMF when K_3PO_4 (Suzuki reactions) or K_2CO_3 (Heck reactions) is used as the base (Scheme 4). The authors postulated that the high degree of dispersion of the materials in DMF, and thus the presence many active Pd particles, is responsible for the high activity.

Varma and co-workers reported the synthesis of nanostructured metal oxides (Fe, Co, Mn, Cr, Mo) under microwave irradiation in aqueous solution without any reducing or capping agents.[141] Various 3D architectures such as octahedrons, spheres, rods, needles, and hexagonal "snowflakes" were obtained when hexacyano complexes were used as the

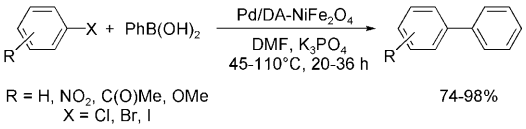

Scheme 4. Suzuki cross-coupling reactions with palladium supported on nanoferrites.[140]

precursors. Among these morphologies, needle-structured nano iron oxides were studied as novel supports for catalysis. The needle tips of the nanoferrite support were functionalized with dopamine to anchor the palladium. The resulting palladium catalysts displayed excellent activity for Suzuki, Heck, and Sonogashira coupling reactions, and could be recycled five times, with consistent yields (Scheme 5).

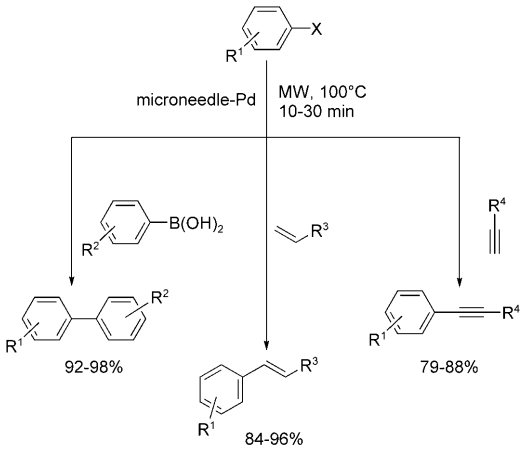

Scheme 5. Coupling reactions carried out with microneedle-palladium catalysts. MW = microwaves.[141]

More recently, a magnetically separable Pd/Fe_3O_4 catalyst obtained by a wet impregnation method was found to be a highly efficient catalyst for the carbonylative Sonogashira coupling reaction of aryl iodides and terminal alkynes under phosphine-free conditions.[142] Catalyst screening showed that the best yields were obtained with Et_3N as the base, toluene as the solvent, and a CO pressure of 2 MPa at 130 °C. A series of aryl iodides and terminal alkynes were tested to explore the generality and scope of the reaction. Aryl iodides bearing electron-withdrawing or electron-donating groups in the *para*, *meta*, and *ortho* positions afforded the corresponding α,β-alkynyl ketones in good yields (Scheme 6). However, the authors noted that palladium leaches out from the iron oxide support during the reactions and becomes redeposited on the support at the end of the reaction. The support thereby assists in recycling the palladium: The catalyst could be used seven times without any significant decrease in activity.

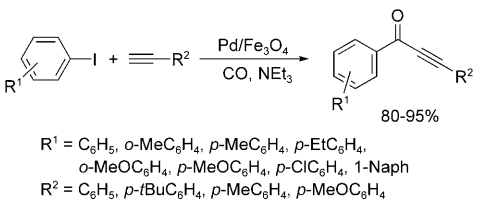

Scheme 6. Carbonylative Sonogashira coupling of aryl iodides and alkynes in the presence of a magnetic Pd/Fe_3O_4 catalyst. Naph = naphthyl.[142]

Hyeon and co-workers reported a generalized procedure for the assembly of multifunctional nanoparticles on silica nanospheres.[143] Uniform silica spheres (ca. 500 nm) synthesized by the Stöber method were first functionalized with amino groups by reaction with 3-aminopropyltrimethoxysilane. To assemble the magnetic nanoparticles on the silica spheres, Fe_3O_4 nanoparticles were treated with 2-bromo-2-methylpropionic acid and coupled with the amino groups. The subsequent functionalization of the remaining amino groups with Au, CdSe/ZnS, and Pd afforded multifunctionalized silica spheres. Among them, the Pd/SiO_2-Fe_3O_4 combination showed high catalytic activity in the Sonogashira coupling of aryl iodides and bromides (Scheme 7). However, the catalyst showed a constant decrease in activity (98→17 % conversion) over four recycling processes because of the loss of Pd nanoparticles from the silica nanospheres.

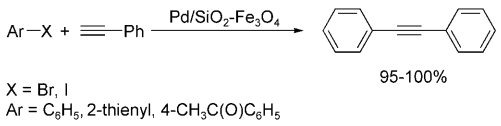

Scheme 7. Sonogashira couping reactions with magnetic Pd/SiO_2-Fe_3O_4 catalysts.[132]

Recently, interest arose in using carbon nanotubes as catalyst supports. However, the introduction of functional groups usually deteriorate their mechanic and electronic properties, and the functional group may be unstable under the conditions of a certain catalytic transformation.[93,144] Hence, doping the carbon nanotubes with heteroatoms, especially nitrogenated sites, was used as a method to provide strong interactions between the catalyst and the support without further functionalization. By using this concept, Yoon et al. demonstrated that nitrogen-doped magnetic carbon nanoparticles, prepared by using iron-doped polypyrole precursors at a carbonization temperature of 800 °C, can be used for the efficient deposition of Pd nanoparticles with a high degree of dispersion and high stability.[145] A unique feature of these materials is that the Pd nanoparticles do not agglomerate even at high loadings (40 %), and the synthesis does not require the presence of expensive ligands for the stabilization of the MNPs. The palladium-containing nitrogen-doped magnetic carbon nanoparticles (Pd/N-MCNPs) showed high catalytic activity (> 90 % yield) in Heck, Suzuki, and Sonogoshira reactions. This was attributed to a good dispersion of Pd over the nitrogenated sites as well to the porous structure of the carbon particles (Scheme 8).

Similarly, Ko and Jang reported that palladium nanoparticles grafted on magnetic polymer nanotubes, prepared by vapor-deposition polymerization (VDP), were highly efficient catalysts for coupling reactions.[146] Carboxylated pyrrole monomers were chemically polymerized in the presence of iron(III) chloride as the oxidizing agent. The magnetic phases were introduced into the carbon nanotubes by precipitation of residual iron complexes. The magnetic, carboxylated polypyrrole nanotubes provide stable anchoring sites for metal salts and thereby assist in generating palladium nanocatalysts. The activity of the Pd catalysts was examined in

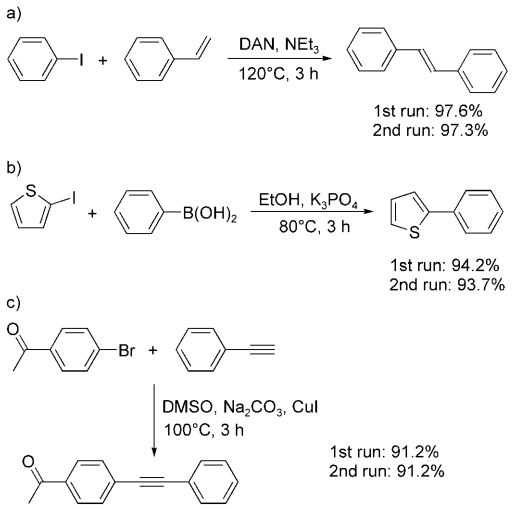

Scheme 8. a) Heck, b) Suzuki, and c) Sonogashira reactions catalyzed by palladium-containing nitrogen-doped magnetic carbon nanoparticles. DAN = dimethylacrylonitrile.[145]

the olefination of activated/non-activated aryl halides and butyl acrylate. The yields were greater than 97%, whereas a conventional carbon-supported Pd catalyst gave distinctly lower yields. The remarkable high yields are attributed to the high specific surface area of the palladium nanoparticles having abundant edge and vertex sites.

Quinuclidine heterogenized on MNPs protected with polyvinylpyrrolidone (PVP) was reported to be an efficient, recoverable catalyst for the Morita–Baylis–Hillman (MBH) reaction. This system showed no loss of catalytic activity even after seven recycles.[147] The MBH reaction occurs without any catalytically active metal, with high atom economy, and under mild reaction conditions.[148] The quinuclidine-supported MNPs exhibited activity comparable to 1,4-diazabicyclo-[2.2.2]octane (DABCO), a classical catalyst for the MBH reaction, and showed better activity than a silica-bound quinuclidine. This again highlights the importance of nanosized supports for catalysis. The catalyst showed enhanced activity towards a wide range of Michael donors and aldehydes, and the reaction proceded equally well in the absence of methanol, and is thus the most effective heterogeneous MBH catalyst reported to date (Scheme 9).

In 2007 Chouhan et al. reported the grafting of proline on MNPs and its use for a CuI-catalyzed Ullmann coupling reactions of aryl or heteroaryl bromides with different

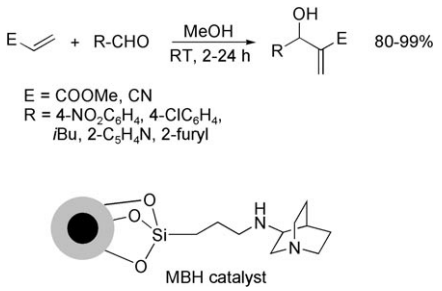

Scheme 9. Morita–Baylis–Hillman reaction with a quinuclidine catalyst supported on MNPs.[147]

nitrogen-containing heterocycles to give the corresponding *N*-aryl compounds.[149] High catalytic activities were observed with N heterocycles such as pyrazole, indole, and benzimidazole (Scheme 10). The catalyst could be reused after magnetic

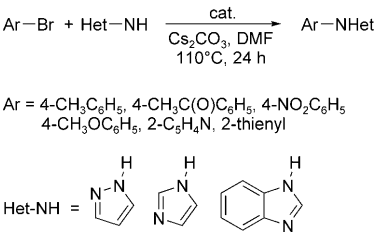

Scheme 10. Ullmann coupling with CuI coordinated to proline-functionalized MNPs.[149]

separation, with yields only reducing slightly (from 98% in the first to 93% in the fourth run). Bedford et al. reported that iron MNPs stabilized with poly(ethylene glycol) (PEG), and either preformed or formed in situ, are excellent catalysts for the cross-coupling of (aryl)MgX with primary and secondary alkyl halides with a β-hydrogen atom. These iron nanoparticles were also used for the first time in a tandem ring-closing/cross-coupling sequence.[150] Table 1 summarizes some material aspects of these MNP catalysts for C–C coupling reactions.

6.2. Hydrogenation

Transition-metal-catalyzed hydrogenation of alkynes or alkenes and transfer hydrogenation of ketones are highly relevant organic transformations because of their immense applications in the synthesis of fine chemicals. Noble metals

Table 1: C–C coupling reactions catalyzed by magnetic nanosupports.

Reaction studied	Morphology and particle composition	Magn. nature[a]	Reusability no. of cycles	Ref.
Suzuki	NHC-Pd/polymer coated γ-Fe_2O_3, core–shell	sp	5	[120]
Heck	Pd/NH_2-Fe_3O_4, core–shell	sp	8	[122]
Suzuki, Heck	Pd/DA-$NiFe_2O_4$, spherical	sp	3	[125]
Suzuki, Heck, Sonogashira	Pd/DA-α-Fe_2O_3, needlelike	n.m.	5	[126]
carbonylative Sonogashira	Pd/Fe_3O_4, spherical	n.m.	7	[127]
Sonogashira	Pd/SiO_2-Fe_3O_4, spherical	sp	4	[128]
Suzuki, Heck, Sonogashira	Pd/N-MCNPs, spherical	sp	3	[130]
Heck	Pd/polypyrrole nanotubes	fm	5	[131]
MBH	γ-Fe_2O_3, spherical	n.m.	7	[132]

[a] sp = superparamagnetic, n.m. = not mentioned, fm = ferromagnetic.

generally catalyze these reactions with high turnover numbers (TON). Nanoparticles of these metals were immobilized on porous solid supports with high specific surface areas so that the nobel metals could be recycled and reused.[151]

However, coating noble metals on the surface of metal nanoparticles is quite difficult. Thus, transmetalation reactions were recently used for the generation of bimetallic core–shell nanoparticles. Jun et al. demonstrated this approach with the synthesis of core–shell Co@Pt nanoparticles obtained by a redox transmetalation reaction between [Pt(hfac)$_2$] and cobalt nanoparticles, and investigated the catalytic activity of the platinum shells in different hydrogenation reactions.[92,152] This catalyst has advantages over single platinum-based catalysts since a large number of noble metal atoms are located on the surface of the particles and thus are accessible to the reactants, while the magnetic core assists in the separation and recycling. The authors demonstrated that the hydrogenation of 1-decene is complete within 4 h at room temperature and that the catalysts can be recycled seven times without any loss of activity. In comparison, a classical Pt/C catalyst showed a decrease in activity from 100% to 76% after only two cycles. Furthermore, the Co@Pt catalyst resulted in 100% hydrogenation of different substrates, such as styrene, nitrobenzene, and cinnamaldehyde, under mild conditions. The structure of the olefin had no effect on the reactivity. TEM data confirm that the high activity and stability of the Co@Pt catalysts arise from their unchanged composition—without aggregation—because of the presence of dodecyl isocyanide.

Amine- or thiol-stabilized MNPs were also used for the stabilization of Pd, Ru, and Ni nanoparticles. Ying et al. described palladium supported on magnetic silica nanoparticles for the catalytic hydrogenation of nitrobenzene.[153] Monodisperse silica-coated Fe_2O_3 particles obtained from water in cyclohexane reverse microemulsions were functionalized with thiols or amines for interaction with the palladium. TEM investigations showed that amine-based silylating agents such as *N*-(2-aminoethyl)-3-aminopropyltrimethoxysilane produce smaller Pd nanoclusters (2.2 ± 1.7 nm) and more narrow cluster size distributions than mercaptopropyl-functionalized samples (2.9 ± 1.7 nm). The Pd/NH_2-SiO_2-Fe_2O_3 catalyst displayed a higher rate of conversion (0.39 μmol s^{-1}) for the hydrogenation of nitrobenzene to aniline than did Pd/SH-SiO_2-Fe_2O_3 and a commercial Pd/C catalyst (0.12 and 0.08 μmol s^{-1}, respectively). Recycling by magnetic separation indicated that amines are stronger ligands for Pd nanoparticles than thiols and thereby lead to less aggregation and growth of Pd nanoclusters during the hydrogenation reactions.

Similarly, the immobilization of palladium on the dopamine-terminated surface of Fe_3O_4 and $NiFe_2O_4$ nanoparticles was reported. These systems were used for the hydrogenation of aromatic nitro and azide derivatives to their respective amines, as well as in the hydrogenation of other unsaturated compounds.[154] The activity of this catalyst was higher in ethanol than in ethyl acetate, which was explained by a better dispersion of the catalyst in ethanol. The catalysts were also completely recoverable and the activity remained unaltered even after ten successive cycles.

In a similar approach, Varma and co-workers grafted nickel nanoparticles on to dopamine-functionalized MNPs and examined the activities of these catalysts in hydrogenation reactions.[155] Here, a solvent effect was also noticed: the hydrogenation of alkynes to alkanes in methanol occurred in greater than 90% yield, while in dichloromethane the formation of alkenes predominated. The reduction of carbonyl derivatives to alcohols also proceeded smoothly with these systems (Scheme 11). A variety of ketones could be reduced within 30 minutes in high yields and high chemoselectivity; the reduction of nitro groups to amines is dominant for nitro-functionalized ketones.

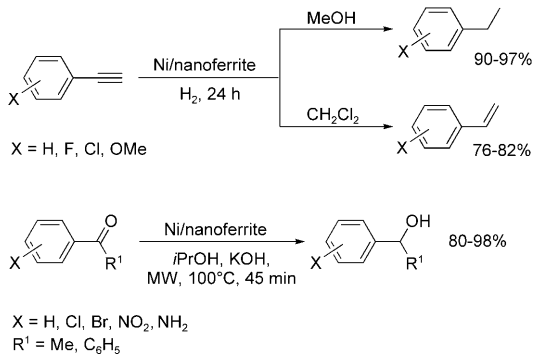

Scheme 11. Hydrogenation and transfer hydrogenation reactions with Ni/nanoferrite catalysts.[155]

Ruthenium supported on dopamine-modified MNPs ($Ru(OH)_x$/DA-$NiFe_2O_4$) were used as recyclable catalysts for the hydrogenation of alkynes (yield: >95%) under microwave irradiation.[156] These systems were also active in the transfer hydrogenation of carbonyl compounds. Substrates such as acetophenone or bromoacetophenone were converted into the corresponding alcohols in 30 minutes with greater than 98% selectivity. The high activity and selectivity remained even after five reaction cycles. These conversions could also be carried out under conventional heating conditions by using longer reaction times.

In 2007, a magnetically separable palladium catalyst for olefin hydrogenation under solvent-free conditions was reported by Rossi et al.[157] Silica-coated superparamagnetic iron oxide nanoparticles were first modified with thiol groups. A thermal curing step produced a stable cross-linked silica layer. Palladium nanoparticles were then grafted on to the thiol groups. The catalytic activity of the samples in the hydrogenation of cyclohexene ($p(H_2) = 6$ bar; $T = 75$ °C) under solvent-free conditions was high (turnover frequency (TOF) = 11 500 h^{-1}) and comparable to a commercially available Pd/C catalyst. The catalyst could be reused 20 times without loss of activity. Recently, these authors reported the immobilization of Rh and Ru nanoparticles on amine-functionalized silica-coated MNPs (NH_2-SiO_2-Fe_3O_4) for hydrogenation reactions.[158,159] The hydrogenation of cyclohexene under mild reaction conditions in the presence of a Ru/NH_2-SiO_2-Fe_3O_4 catalyst occurred with more than 99% of the cyclohexene converted after 5 h (TOF = 420 h^{-1}).

Similar supported Rh systems even showed a 18 times higher TOF.

Palladium nanoparticles supported in multilayered polyelectrolyte films formed by layer-by-layer (LbL) self-assembly of poly(acrylic acid) and a polyethylenimine–palladium(II) complex on $CoFe_2O_4$ MNPs were examined in the hydrogenation of olefinic alcohols.[160] Notably, the hydrogenation was catalyzed by palladium(0) generated in the outermost layer of the hybrid nanocomposite. The reason for this is the restricted diffusion of alcohols into the ionically cross-linked multilayered films. This finding indeed highlights that formation of a multilayer in such systems is not really necessary for applications in catalysis. Olefinic alcohols with different substituents at the carbon atom in the α position to the double bond, for example, allylic alcohol (TOF = 854 h^{-1}), 3-buten-2-ol (TOF = 328 h^{-1}), and 1-penten-3-ol (TOF = 126 h^{-1}), were hydrogenated in the presence of the nanocomposite catalyst. The size-dependant activities observed in these hydrogenations imply that the polyelectrolyte film restricts access of bulky substrates to the active palladium nanoparticles. The catalysts could be recycled ten times by magnetic separation without any decrease in the catalytic activity.

Platinum nanoparticles supported on MNPs modified with ionic liquids (ILs) were found to be efficient and reusable catalysts for the chemoselective hydrogenation of α,β-unsaturated aldehydes and alkynes.[161] The adsorption of Pt nanoparticles on the IL-functionalized MNPs was achieved by ion exchange with K_2PtCl_4 followed by reduction with hydrazine (Scheme 12). These catalysts were used for the

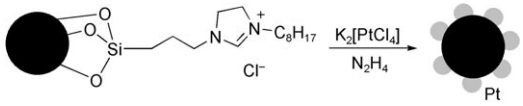

Scheme 12. Synthesis of platinum nanoparticles on ionic liquid modified MNPs.[161]

hydrogenation of diphenylacetylene, 1-ethynyl-4-methylbenzene, 3-phenylprop-2-yn-1-ol, and methyl-3-phenylpropiolate in methanol at 90 °C and under 14 bar H_2. *cis*-Alkenes were formed selectively; allylic alcohols were formed exclusively in the hydrogenation of α,β-unsaturated aldehydes. Zhang et al. recently reported a Pt/γ-Fe_2O_3 magnetic nanocomposite which showed high activity and selectivity in the catalytic hydrogenation of *o*-chloronitrobenzene.[162] Interestingly, the catalytic dehydrochlorination usually observed with this substrate was not evident, even after complete conversion.

Sulfonated triphenylphosphines were used to support rhodium on iron oxide MNPs. These catalysts were used in the hydrogenation of alkenes and for the 1,4-addition of aryl boronic acids to dimethyl itaconate ($ItMe_2$). They could be reused in water up to ten times. The immobilization procedure is quite simple, since no modification of either the MNP support or the organometallic rhodium precursur is required.[163] Two different methods were used for the immobilization: first [RhCl(tppts)$_3$] (tppts = trisodium triphenylphosphine-3,3′,3″-trisulfonate) was used directly without any ligand modification. In a second approach, [{RhCl(cod)}$_2$] (cod = 1,5-cyclooctadiene) was treated with sodium triphenylphosphino-3-monosulfonate to produce [RhCl(cod)(tppms)], which was then attached to the magnetic nanoparticles. The activity of the catalysts was investigated under single-phase (1,4-addition of boronic acid) and two-phase (hydrogenation) conditions in water, with $ItMe_2$ as the substrate. The nanoparticle-supported [RhCl(TPPTS)$_3$] catalyst resulted in complete conversion of the substrate (4 h, $p(H_2) = 3.5$ bar, $T = 50$ °C). This catalyst was also active (conversion > 99 %) in the hydrogenation of *n*-hexene and *n*-dodecene, without isomerization of the C=C bonds.

Magnetic nanoalloys encapsulated in quasispherical carbon shells were prepared in large amounts by sequential spraying, chemical precipitation, and controlled pyrolysis.[164] As discussed earlier, graphite shells are ideal coatings for the isolation of MNPs and prevention of particle aggregation, since the closely packed graphitic networks are chemically inert and impermeable. Various crystalline nanoalloys, such as FeNi, FeCu, and FeCo, were synthesized and coated with a layer of graphite. Pyrolysis of the iron precursor $Na_2[Fe(CN)_5NO]\cdot 2H_2O$ results in nitrogen atoms in the graphitic carbon, which makes these particles structurally different from those obtained by traditional carbon deposition, where the carbon shells are composed only of carbon atoms. Palladium nanoparticles were deposited on the carbon support by impregnation with [Pd(acac)$_2$] (acac = acetylacetonate) in acetone. These systems exhibited higher initial rates (1.529 μmol s^{-1}) than a commercial Pd/C catalyst (0.835 μmol s^{-1}) in the hydrogenation of nitrobenzene.

Lu et al. developed a magnetically recoverable mesoporous catalyst based on carbon-coated cobalt MNPs.[165] Ordered mesoporous SBA-15 was impregnated with furfuryl alcohol, which was subsequently polymerized to block the pores of the silica template. The external surface of the mesoporous silica/polymer nanocomposite was then covered with cobalt nanoparticles, which were protected with a thin layer (ca. 1 nm) of graphitic carbon. The polyfurfural residue inside the pores was subsequently converted into carbon, and the silica template was removed with HF to develop a superparamagnetic carbon material with an open pore system. Even though a multistep synthesis procedure is required for these materials, these magnetic, mesoporous carbon materials are interesting for applications related to catalysis since the cobalt nanoparticles do not block the pores of the material. Functionalization of the inner pores of the mesoporous carbon with Pd gave a catalyst with high activity and stability, as well as excellent reusability for the hydrogenation of octene.

6.3. Hydroformylation

Yoon et al. used the strong interaction between carboxylic acids and ferrite-type MNPs to graft the cationic complex [Rh(η^6-benzoicacid)(cod)]BF_4 onto $CoFe_2O_4$ MNPs and used this system for olefin hydroformylation.[166] The rhodium-functionalized $CoFe_2O_4$ MNPs showed, similar to the homogeneous catalyst, high catalytic activity in combination with

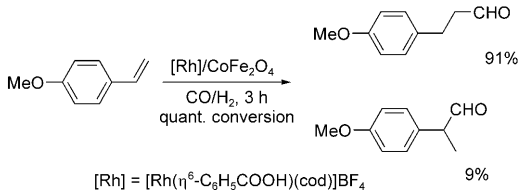

Scheme 13. Hydroformylation catalyzed by rhodium supported on MNPs.[166]

excellent regioselectivity in the hydroformylation of 4-vinylanisole (Scheme 13). The authors assigned the high activity to the "quasihomogeneous" nature of the material.

Dendrimers can be used to support nanoparticles so as to enhance the solubility in organic solvents.[167] Based on this concept, in 2006 Abu-Reziq et al. used an interesting approach for the heterogenization of a homogeneous rhodium catalyst:[168] Polyaminoamido (PAMAM) dendrons of up to the third generation were generated on amino-functionalized silica-coated MNPs by Michael addition of methylacrylate to give aminopropionate ester groups which were subsequently converted into aminoamides with ethylenediamine. The teminal amino groups on the dendrons covalently tethered on the MNPs were finally converted into phosphine groups by tratment with diphenylphosphinomethanol. Treatment with $[\{Rh(cod)Cl\}_2]$ gave the catalytically active dendronic MNPs. The catalysts were tested in the hydroformylation of different olefin substrates (50 °C, $p(CO) = 34.5$ bar, $p(H_2) = 34.5$ bar). Nonpolar solvents led to a higher selectivity for the branched aldehydes. No significant electronic influence could be noted with substituted styrenes. Among the catalysts tested, the first generation samples (G1) showed the best activity (Scheme 14). However, the catalysts were not selective in the hydroformylation of linear aliphatic olefins: for example, 1-octene gave the isomeric aldehydes in a 2.2:1 ratio (linear/branched).

6.4. Oxidation and Epoxidation

The oxidation of alcohols and olefins is synthetically useful because the reaction products are important materials in the production of fine chemicals. Beller and co-workers

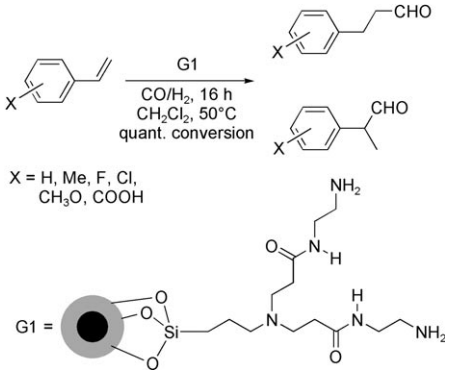

Scheme 14. Rhodium-catalyzed hydroformylation with dendronic magnetic silica nanoparticles.[168]

examined the catalytic performance of magnetically recyclable "unfunctionalized"' nano-Fe_2O_3 catalysts in oxidation reactions under mild conditions, with hydrogen peroxide used as the oxidizing agent.[169] The liquid-phase oxidation of benzyl alcohol to benzaldehyde proceeded with excellent activity (85% conversion) and a selectivity of 35% in the presence of nano-γ-Fe_2O_3 particles with diameters of 3–5 nm. Increasing the size of the particles to 20–50 nm decreased the conversion to 33%, with a benzaldehyde selectivity of 97%, whereas Fe_2O_3 particles with a diameter of more than 100 nm showed very low catalytic activities. Aromatic olefins were also oxidized to the corresponding aldehydes under similar conditions (Scheme 15). The high activity of the nano-γ-Fe_2O_3

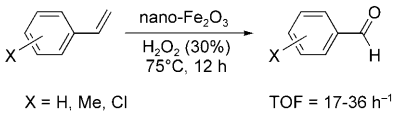

Scheme 15. Nano-Fe_2O_3-catalyzed oxidation of olefins to aldehydes.[169]

was attributed to the high surface area of the particles, which have coordinatively unsaturated iron sites and vacancies for substrate activation. These results highlight that catalytic activity close to that of homogeneous Fe^{3+} catalysts can be attained by reducing the size of the heterogeneous Fe_2O_3 catalysts.

The TONs observed in the oxidation reactions with the simple nano-γ-Fe_2O_3 catalysts were not very high. Polshettiwar and Varma elegantly overcame this drawback by supporting palladium nanoparticles on dopamine-modified nanoferrites.[170] The oxidation of benzyl alcohol proceeded with a TON of 720 and greater than 99% selectivity. Furthermore, the catalyst exhibited excellent activity for a variety of other aromatic, aliphatic, and heterocyclic alcohols, and was also found equally active in the oxidation of a series of substituted aromatic olefins (TON = 600–680; Scheme 16).

Catalytic oxidation with molecular oxygen instead of (organic) peroxides is attractive for environmental and economic reasons. Mizuno and co-workers investigated the aerobic oxidation of alcohols and amines by using ruthenium hydroxide supported on magnetite ($Ru(OH)_x/Fe_3O_4$).[171] Primary and secondary benzylic alcohols were converted into the corresponding aldehydes and ketones in high yields. Primary alcohols, however, reacted significantly faster, which was attributed to the formation of ruthenium alkoxides. The catalysts were also active in the oxidation of sulfur-containing alcohols and of primary benzylic, aliphatic, and heterocyclic amines. The reactions with amines resulted in the formation of the corresponding nitriles in high yields (Scheme 17).

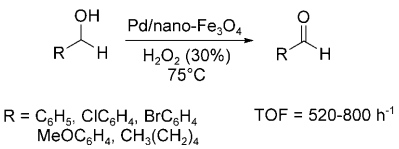

Scheme 16. Pd/Nano-Fe_3O_4-catalyzed oxidation of alcohols.[170]

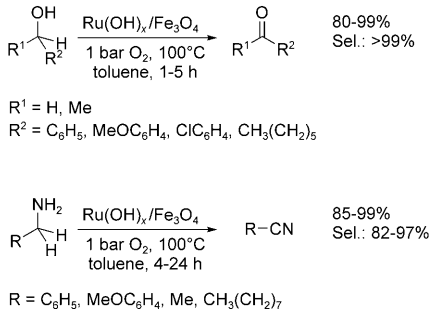

Scheme 17. Aerobic oxidation of alcohols and amines catalyzed by $Ru(OH)_x/Fe_3O_4$.[171]

Aerobic oxidation of cyclohexane gives a mixture of cyclohexanone and cyclohexanol (K/A oil), which are starting compounds for the synthesis of adipic acid and caprolactame—precursors for nylon 6 and nylon 66 polymers.[172] Tong et al. used magnetic $CoFe_2O_4$ nanocrystals prepared by a sol–gel autocombustion method as efficient and recyclable heterogeneous catalysts for the aerobic oxidation of cyclohexane in the absence of solvents and reducing agents.[173] Catalyst screening studies showed that the pure stoichiometric $CoFe_2O_4$ nanocrystals showed excellent catalytic activity (16.2% conversion, $p(O_2) = 16$ bar, 145 °C) and greater than 90% selectivity for the cyclohexanone and cyclohexanol products. These results are significantly better than those of homogeneous cobalt acetate, nanosized cobalt and iron oxides, or their mixtures. Additionally, the $CoFe_2O_4$ nanocrystals showed moderate activity (3–9% conversion) in the oxidation of linear olefins.

In 2009, Rossi et al. reported magnetically recoverable Ru^{III}-functionalized NH_2-SiO_2-Fe_3O_4 supports for the oxidation of aryl and alkyl alcohols under 3 bar of molecular oxygen at 100 °C.[159] The oxidation of non-activated alcohols (such as octanol) as well as the oxidation of diols to diketones proceeds smoothly with high rates of conversion and selectivities (no carboxylic acids formed). Very recently, Baiker and co-workers investigated gold nanoparticles deposited on superparamagnetic iron oxide–ceria nanocomposites (Au/CeO_2-Fe_2O_3) by the addition of $Au(OAc)_3$ to the preformed mixed oxide. These systems are active in the aerobic oxidation of amines.[174] A series of amines, including benzylamine, dibenzylamine, *N*-*tert*-butylbenzylamine, and indoline, were oxidized to the corresponding imines with good conversions and excellent selectivities (87–100%). Compared to the recycling properties of several supported gold catalysts, the Au/CeO_2-Fe_2O_3 catalyst iron oxide–ceria nanocomposite showed just a minimum loss of activity.

Hydroxyapatite (HAP, $Ca_{10}(PO_4)_6(OH)_2$) is a useful support for high-performance heterogeneous catalysts because of its structural stability, its ability to undergo ionic substitution, and its adsorption capacity,.[175] Kaneda et al. reported the synthesis of MNPs with encapsulated hydroxyapatite nanocomposites by the simultaneous crystallization of HAP and γ-Fe_2O_3 under basic conditions. The ion-exchange ability of the external hydroxyapatite surface was used to substitute calcium with ruthenium. The resulting RuHAP-γ-Fe_2O_3 is a recyclable catalyst for the aerobic oxidation of alcohols.[176] It allows the oxidation of different benzylic, allylic, aliphatic, and heterocyclic alcohols at room temperature and under atmospheric pressure (Scheme 18). Remarkably, the catalyst does not require any additive or co-catalyst, even works under mild reaction conditions, and is compatible with the oxidation of sterically bulky alcohols. For example, 3,5-dibenzyloxybenzyl alcohol and cholestanol were successfully converted quantitatively into the corresponding carbonyl compounds.

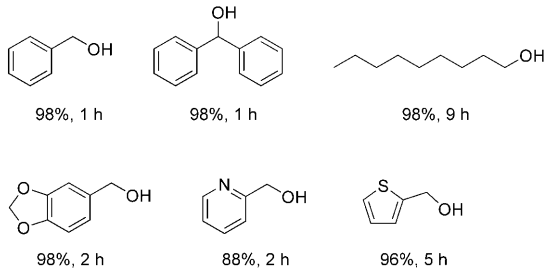

Scheme 18. Substrate scope for the aerobic oxidation of alcohols with the Ru/HAP-γ-Fe_2O_3 catalyst.[176]

In a recent publication, Arai et al. described the formation of an organic–inorganic hybrid polymer on the surface of magnetic beads derived from iron oxide by employing an in situ self-assembly process.[177] The hybrid polymer consists of $[\{[Cu(bpy)(BF_4)_2](bpy)\}_n]$ (bpy = 4,4′-bipyridine) and forms directly on the surface of amino-functionalized magnetic beads from $Cu(BF_4)_2$ and 4,4′-bipyridine. The material Cu(bpy)/HPMB (HPMB = hybrid polymer encapsulated magnetic beads) was used as a catalyst for the oxidation of silyl enolates to give the corresponding α-hydroxylcarbonyl compounds. It showed a catalytic activity that was even higher than the activity of a homogeneous $[\{[Cu(bpy)(BF_4)_2(H_2O)_2]$-$(bpy)\}_n]$ catalyst under identical reaction conditions (Scheme 19). More interestingly, the use of commercially available aminomethylated polystyrene as the support led to the catalytic activity of the hybrid polymer decreasing sharply.

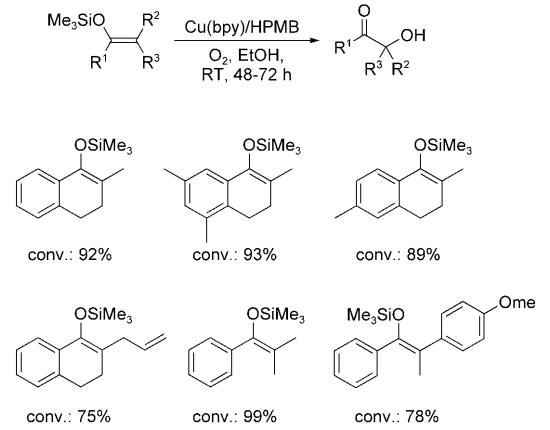

Scheme 19. Synthesis of α-hydroxy ketones by using the Cu(bpy)/HPMB catalyst.[177]

Graphene-coated cobalt nanobeads, which were functionalized with propargyl ether–TEMPO (TEMPO = 2,2,6,6-tetramethylpiperidine-1-oxyl) by a copper-catalyzed click reaction, were recently used for the chemoselective oxidation of benzylic and aliphatic alcohols. In this case, hypochlorite was used as the oxidant (Scheme 20). No overoxidation to the corresponding carboxylic acid was observed, and the catalysts could be recycled by magnetic separation six times without any loss of activity. Similar to other TEMPO-mediated oxidation reactions, secondary alcohols are oxidized significantly slower than primary alcohols.[178]

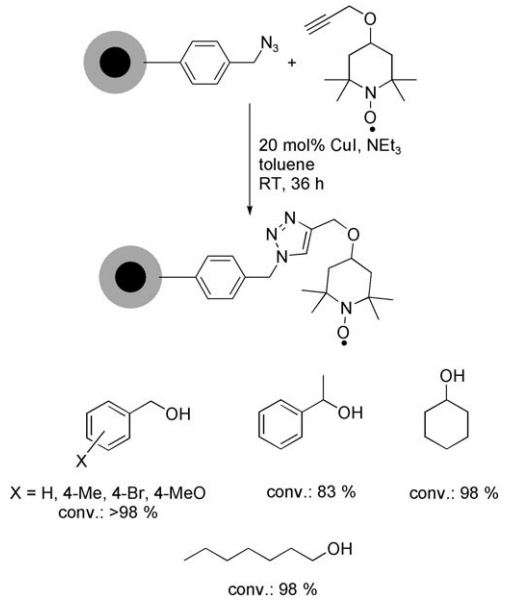

Scheme 20. Synthesis of TEMPO-functionalized MNPs; substrates for TEMPO-catalyzed oxidations.[178]

A magnetically recoverable epoxidation catalyst based on molybdenum dioxide nanoparticles incorporated in a mesoporous silica shell on silica-coated MNPs was recently reported by Hyeon and co-workers.[179] Haematite (α-Fe_2O_3) particles of about 400 nm in diameter obtained from a hydrothermal reaction were first protected with a dense silica coating ($d = 50$ nm). An additional mesoporous silica shell was then generated on the surface of these particles by condensation of TEOS and *n*-octadecyltrimethoxysilane (C_{18}-TMS). MoO_2 was then introduced into the mesoporous silica shell by impregnation with ammonium molybdate followed by reduction with H_2 (catalyst: MoO_2/SiO_2-Fe_2O_3).

The activity of this catalyst depends on the solvent and the oxidant (best combination: CCl_4/*t*BuOOH). High yields of epoxides (> 80 %) were found for substrates such as cyclododecene, cycloheptene, cyclohexene, and indene (Scheme 21). The catalyst could be recycled six times without major loss in activity (1st run: 99 % conversion, 6th run: 94 % conversion). Remarkably, nonporous silica MNPs impregnated with molybdenum dioxide nanoparticles showed poorer conversions (37 % conversion) than MNPs covered with mesoporous silica (99 % conversion), which reveals the importance of high specific surface areas.

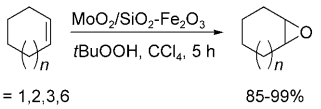

Scheme 21. Olefin epoxidation catalyzed by MoO_2/Fe_2O_3-SiO_2.

Organic–inorganic hybrid nanocatalysts obtained by covalently anchoring $[(L\text{-}L)MoO(O_2)_2]$ (L-L = (3-triethoxysilylpropyl)[3-(2-pyridyl)-1-pyrazolyl]acetamide) on silica MNPs were reported by Thiel and co-workers to be robust magnetically separable epoxidation catalysts (Scheme 22).[180]

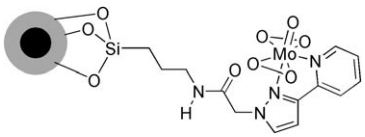

Scheme 22. Heterogenized molybdenumperoxo catalyst for olefin epoxidation on silica-coated MNPs.[180]

In this case, the combination of $CHCl_3$ as solvent and *t*BuOOH as oxidant gave the best results for a series of substrates (for example, cyclooctene, cycloheptene, cyclohexene, styrene, and 1-octene). This catalyst showed a significantly enhanced catalytic activity and recyclability (six times) compared to similar molybdenum catalysts supported on neat mesoporous MCM-41 or silica nanospheres. The authors attributed this finding to the better isolation and a uniform dispersion of the catalytically active sites on the surface. The relatively strong interaction between the chelating ligand and the molybdenum center as well as the covalent grafting between the organic ligand and the magnetic silica support prevent leaching of the active sites.

Recently, Tang et al. investigated titanium-functionalized SiO_2-FePt MNPs, developed by a layer-by-layer bottom-up approach, for diverse oxidation reactions.[181,182] Different amounts of tetrabutyl orthotitanate (TBOT) were used to cover the outer shell of silica-coated FePt MNPs. The authors postulated a substitution of Si sites by Ti, since TBOT diffuses into the silica layer. Among all the catalysts investigated, materials with 18.9 wt % TiO_2 showed the best catalytic performance for the epoxidation of *trans*-stilbene in the presence of *t*BuOOH (15 % conversion, > 90 % selectivity). A further increase in the titanium concentration in the outer shell decreased the catalytic activity, which was related to the formation of unreactive Ti-O-Ti units instead of catalytically active Ti-O-Si units.

In an alternative approach, Mori et al. described a two-step coating process including a ligand-exchange step with (3-mercaptopropyl)triethoxysilane and a sol–gel process using tetraethyl orthosilicate and tetrapropyl orthotitanate for the preparation of TiO_2/SiO_2-FePt catalysts. Various characterization methods proved that isolated and tetrahedrally coordinated titanium species are located in the external layer of the nanocomposite. This catalyst was used four times with consistent activity (TON = 48) for the epoxidation of cyclooctene. 30 % H_2O_2 was used as the oxidant.[183]

Zhang et al. reported a magnetically recoverable Ag/Fe_3O_4 nanocomposite for the catalytic epoxidation of styrene, with *tert*-butylhydroperoxide (TBHP) used as the oxidant.[184] The synthesis takes place by the addition of $AgNO_3$ and $FeCl_3$ to a solution of ethylene glycol and polyvinylpyrolidine (PVP) to form a suspension of AgCl with adsorbed Fe^{III} ions. The Ag^+ ions are then reduced to Ag by ethylene glycol; PVP-assisted aggregation causes crystallization of the Fe_3O_4 and the generation of the Ag/Fe_3O_4 nanocomposite. HR-TEM images show the coexistence of both Ag and Fe_3O_4 in the composite. When the reaction is performed in the absence of PVP, Ag particles become separated from the Fe_3O_4. The catalytic properties of this catalyst were evaluated in the epoxidation of styrene: styrene oxide was formed in 84% yield after 13 h with a TOF of 1473 h^{-1}, and the activity remained almost constant over five cycles. The high catalytic activity compared to other systems was explained by a synergetic interaction between the Fe_3O_4 nanoparticles and the Ag nanocrystals (Scheme 23). Table 2 summarizes some material aspects of the MNP catalysts in hydrogenation and oxidation reactions.

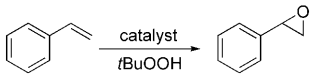

Ag/Fe_3O_4: 84%, TOF = 1473 h^{-1}
Ag: 64%, TOF = 539 h^{-1}
Ag + Fe_3O_4: 43%, TOF = 761 h^{-1}

Scheme 23. Epoxidation of styrene catalyzed by a Ag/Fe_3O_4 nanocomposite and a series of other nanocatalysts.[184]

Table 2: Hydrogenation and oxidation reactions catalyzed by magnetic nanosupports.

Reaction studied	Morphology and particle composition	Magn. nature[a]	Reusability no. of cycles	Ref.
hydrogenation of 1-decene	Co@Pt, core–shell	sp	7	[137]
hydrogenation of nitrobenzene	Pd/SH-SiO_2-Fe_2O_3 and Pd/NH_2-SiO_2-Fe_2O_3	n.m.	14	[138]
transfer hydrogenation of carbonyl compounds	Ru(OH)$_x$/DA-$NiFe_2O_4$, spherical	sp	5	[141]
hydrogenation of cyclohexene	Pd/SH-SiO_2-Fe_3O_4, core–shell	sp	20	[142]
hydrogenation of alkynes/α,β-unsaturated aldehydes	Pt/IL-MNP, spherical	n.m.	4	[146]
hydrogenation of nitrobenzene	Pd/carbon encapsulated nanoalloys	n.m.	n.m.	[149]
hydrogenation of octene	Pd/magnetic mesoporous carbon	n.m.	2	[150]
oxidation of alcohols and olefins	γ-Fe_2O_3, spherical	fm	5	[154]
oxidation of amines	Au/CeO_2-FeO_x	sp	2	[159]
oxidation of alcohols	Ru/HAP-γ-Fe_2O_3	sp	n.m.	[161]
epoxidation of alkenes	MoO_2/mesoporous coated MNPs	fm	6	[164]
oxidation of *trans*-stilbene	TiO_2/SiO_2-FePt	sp	n.m.	[166]

[a] sp = superparamagnetic, n.m. = not mentioned, fm = ferromagnetic.

6.5. Organocatalysis

Metal-free catalysts for the synthesis of organic molecules have recently attracted widespread attention.[185] Polshettiwar et al. reported the synthesis of glutathione-functionalized MNPs for a catalytic Paal–Knorr reaction.[186] The glutathione (GT) molecules were anchored on magnetic nanoferrite through their thiol groups. The catalyst (nano-FGT) displayed high activity for a wide variety of alkyl, aryl, and heterocyclic amines (Scheme 24). Remarkably, functionalized amines were selectively converted into the corresponding pyrroles, while preserving their functional groups (esters, ketones, alcohols, C=C bonds, etc.). Chiral (*R*)-α- and (*S*)-α-methylbenzylamine yielded the corresponding pyrroles without racemezation. The catalysts could be recycled by magnetic separation five times without loss of catalytic activity.

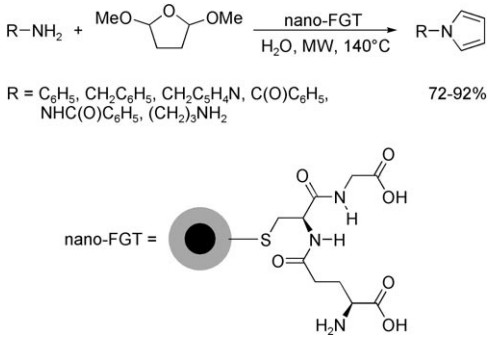

Scheme 24. Nano-FGT-catalyzed Paal–Knorr reactions.[186]

The use of phase-transfer catalysts (PTC) is an environmentally benign alternative to homogeneous reactions.[187] However, a major drawback associated with PTCs is their separation at the end of the reaction. To exploit the properties of MNP-supported PTCs compared to conventional solid supports (such as polystyrene resins), Kawamura and Sato immobilized a series of quaternary ammonium and phosphonium salts on the surface of MNPs and evaluated their activity in the O-alkylation of PhONa with *n*BuBr. The authors noted that the immobilization of quaternary salts on MNPs did not affect the activity of the PTC, while systems anchored to polystyrene resins are less efficient.[188] The MNP catalysts can be easily recovered after the reaction and can be reused four times with only a minimal loss of activity (1st run 94% yield, 4th run 89% yield).

In an identical approach, Kawamura and Sato immobilized crown ethers on MNPs and evaluated their activity as catalysts in solid–liquid phase-transfer reactions.[189] Crown ethers are versatile PTCs in a series of organic syntheses, but they are highly toxic, expensive, and difficult to reuse.[190] The catalytic activity of crown ethers supported on MNPs (MNP-crown) was evaluated in the halogen exchange of 1-bromooc-

tane with KI under solid–liquid PTC conditions. The catalytic activity of the MNP-crown was almost identical to that of free crown ethers (Scheme 25), and still depends strongly on the ring size. Furthermore, the catalysts can be reused eight times without any loss in activity.

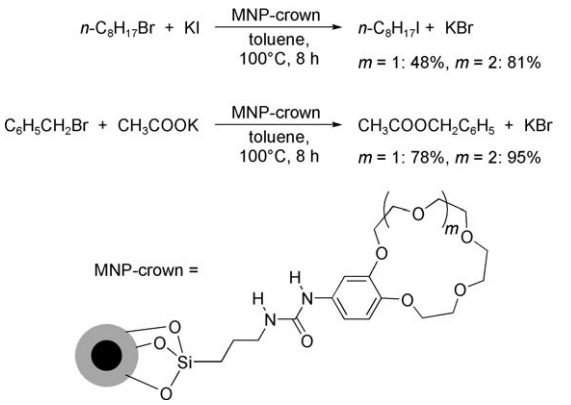

Scheme 25. Crown ethers supported on MNPs for halogen exchange and substitution reactions.[189]

6.6. Enantioselective Catalysis

Asymmetric catalysis is one of the most powerful methods to produce enantiomerically pure compounds.[191] Despite huge efforts devoted to this subject, the contribution of asymmetric catalysis in the overall production of chiral chemicals is lower than originally expected. There are severe problems arising from the typical drawbacks of homogeneous catalysis, including catalyst recycling. This fact is of special importance since the price of sophisticated chiral ligands often exceeds that of the noble metal employed.[192] Heterogenization of chiral catalysts on high surface area, solid organic–inorganic hybrid mesoporous supports was employed as an approach to aid catalyst recovery. However, chiral catalysts immobilized on porous supports were often found to be less efficient than their homogeneous counterparts.[34h]

As an alternative approach, Lin and co-workers demonstrated an elegant way to immobilize chiral [Ru(binap-PO_3H_2)Cl_2(dpen)] (binap = 2,2′-bis(diphenylphosphino)-1,1′-binaphthyl, dpen = 1,2-diphenylethylenediamine) on MNPs through phosphate groups. They reported two different methods: a thermal decomposition method (MNP^1) and a co-precipitation method (MNP^2).[44] These MNP-supported chiral catalysts were used for the enantioselective asymmetric hydrogenation of aromatic ketones and showed high activity and *ee* values of up to 98% (Scheme 26). For example, 1-acetonaphthone was hydrogenated with 100% conversion by using 0.1 mol% of the chiral catalyst on MNP^1 and MNP^2 in 2-propanol to yield α-(1-naphthyl)ethanol with 98.0% and 97.6% *ee*, respectively. The immobilized catalysts could be recycled by magnetic separation (MNP^1: 5 times, MNP^2: 14 times) without any loss of activity or enantioselectivity. Thus, the heterogenization of chiral metal complexes is a promising alternative to classical homogeneous catalysis.

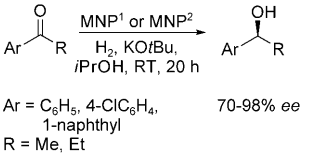

Scheme 26. Hydrogenation of aromatic ketones with chiral Ru complexes supported on MNPs.[44]

The functionalization of MNPs with chiral primary/tertiary diamines (loading: 0.39 mmol g^{-1}) leads to a catalyst for the aldol reaction of acetone or cyclohexanone with a series of aldehydes.[193] The catalyst (MNP-amine*) shows similar activity and stereoselectivity as the amine in a homogeneous phase (Scheme 27). Aromatic aldehydes generally give better results than aliphatic aldehydes.

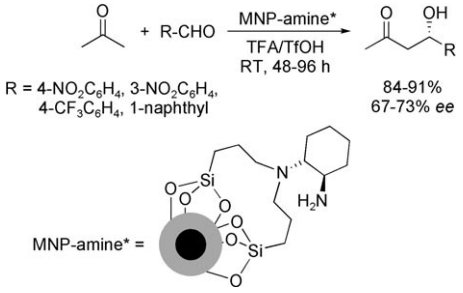

Scheme 27. Asymmetric aldol reaction of acetone catalyzed by amine catalysts supported on MNPs. TFA = trifluoroacetic acid, TfOH = trifluoromethanesulfonic acid.[193]

The first chiral 4-*N*,*N*′-dimethylaminopyridine (DMAP) derivatives supported on MNPs used for enantioselective acylations were recently reported by Gleeson et al.[194] The catalyst was prepared by anchoring *N*-methyldopamine hydrochloride onto MNPs, followed by a S_NAr reaction with a chiral chloropyridine in toluene. The catalysts were evaluated as promotors in the acylative kinetic resolution of monoprotected *cis*-diols. The use of 5 mol% of catalyst enabled the *sec*-alcohols to be resolved with 99% *ee* (for the resolved alcohols) at 72% conversions. The catalysts were also able to promote the kinetic resolution of a range of *sec*-alcohols with various steric and electronic features by using acetic anhydride as the acylating agent. They could be recycled up to a remarkable 20 times with consistent activity and enantioselectivity (Scheme 28).

The modification of a surface with chiral pockets by the adsorption of chiral ligands is an interesting approach to generate chiral heterogeneous catalysts. Parvalescu and co-workers reported the synthesis of Fe_3O_4 colloids modified with cinchonidine embedded in silica,[195] and used these MNPs for the hydrogenolysis of bicyclo[2.2.2.]oct-7-enes (Scheme 29). The modification process had no influence on the catalytic properties of the materials, while the nature of substituents on the substrate severely influenced the activity. Small substituents such as hydrogen, for example, favor interaction with the catalytically active sites (ca. 84% conversion), whereas bulky substituents such as phenyl groups

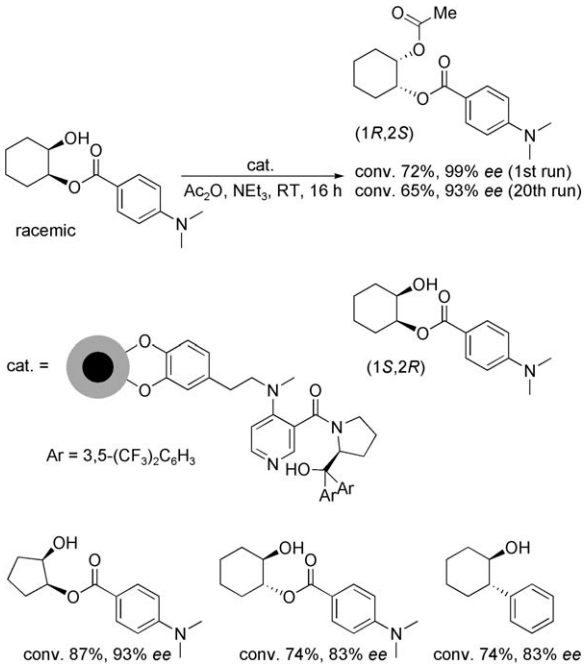

Scheme 28. Synthesis of chiral DMAP derivatives supported on MNPs and their evaluation as asymmetric acylation catalysts.[194]

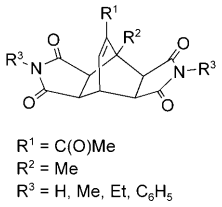

Scheme 29. Bicyclo[2.2.2]oct-7-enes evaluated in asymmetric hydrogenolysis.[195]

lead to a drastic decrease in the activity (ca. 10%). However, no enantioselectivity was found for this reaction, irrespective of the substrate. Embedding the cinchonidine-modified Fe_3O_4 colloids directly in silica resulted in a decrease in the activity (about 40% conversion). The authors attributed this effect to the mass-transfer limitations of large substrates in the solid matrix as well as to the inaccessibility of colloids that were buried deep inside the silica matrix.

In a similar strategy, cinchonidine (CD) modified Pt was immobilized on silica MNPs (CD-Pt/SiO_2-Fe_3O_4) for the enantioselective hydrogenation of activated ketones.[196] The cinchonidine-modified catalyst showed a catalytic performance (in terms of activity, enantioselectivity) that was the same as that of the best known commercial Pt/Al_2O_3 catalyst for the enantioselective hydrogenation of α-ketoesters and α,α,α,-trifluoroacetophenone (Scheme 30). The catalysts could be recycled up to eight times with just a minimum decrease in the enantioselectivity (1st run: 57% *ee*, 8th run: 52% *ee*).

Very recently, Reiser and co-workers reported two different azide-functionalized magnetic silica nanoparticles for the

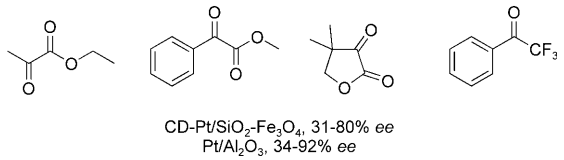

Scheme 30. Substrate scope for the enantioselective hydrogenation using a cinchonidine-modified CD-Pt/Fe_3O_4-SiO_2 catalyst.[196]

immobilization of azabis(oxazoline)copper(II) complexes (Scheme 31).[197] Azabis(oxazoline) ligands are particularly attractive candidates for heterogenization since they are known to bind strongly to metal sites.[198] These heterogenized catalysts showed high yields and selectivities in the asymmetric benzoylation of 1,2-diols.

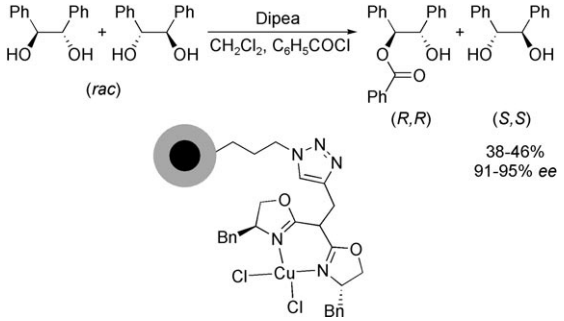

Scheme 31. Asymmetric benzoylation with azabis(oxazoline)copper(II) catalysts heterogenized on MNPs. Bn = benzyl, dipea = diisopropylethylarginine.[197]

Lee et al. developed a magnetic mesocellular mesoporous silica support with a 3D open-pore structure for the filtration-free recycling of chiral ligands for catalytic asymmetric dihydroxylation (AD).[199] The inner pore walls of a mesocellular silica (MCF) were grafted with MNPs by thermal decomposition of iron propionate. A cinchona alkaloid was then functionalized inside the pore channels. The MCF catalyst exhibited similar reaction rates and enantioselectivity as those reported for the homogeneous ligand (Scheme 32).

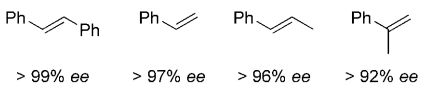

Scheme 32. Evaluation of the substrate spectrum for the asymmetric dihydroxylation with a cinchona alkaloid modified magnetic MCF catalyst.[199]

The results were comparable to those of a high surface area, nonmagnetic SBA-15 support for a series of olefin substrates. The high *ee* values obtained with these catalysts were attributed to the 3D pore structure and to the small particle sizes, which make all the active sites highly dispersed and accessible. The catalysts could be recycled eight times; however, a new batch of toxic OsO_4 had to be added for every recycle to obtain reasonable reaction rates. The

leaching of osmium seems to be a general drawback for heterogeneous AD reactions.[200]

In 2009, Li and co-workers immobilized Ru-TsDPEN (TsDPEN = *N*-(*p*-toluenesulfonyl)-1,2-diphenylethylenediamine) on a magnetic siliceous mesocellular foam material.[201] The authors noted that the heterogenized system gave high catalytic activities and *ee* values as well as excellent reusability (nine times) in the asymmetric transfer hydrogenation of imines with $HCOOH/NEt_3$ and aromatic ketones with aqueous HCOONa (Scheme 33).

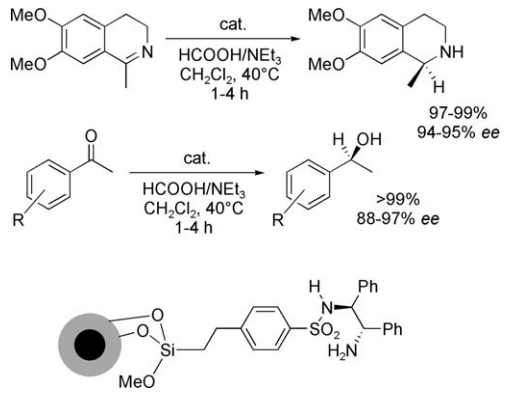

Scheme 33. Asymmetric transfer hydrogenation of imines and ketones with TsDPEN-Ru supported on a magnetic mesocellular foam.[201]

6.7. Acid–Base Reactions

Jones and co-workers reported the first synthesis of acid- and base-functionalized MNPs, which they applied in different catalytic transformations. Sulfonic acids with increasing acidity (alkyl sulfonic acids, phenylsulfonic acid, perfluoroalkylsulfonic acids, perfluoroarylsulfonic acids) were immobilized on silica-coated cobalt ferrite ($CoFe_2O_4$) MNPs by employing appropriate thiol precursors to produce magnetically recyclable acid catalysts.[202] The authors noted that the silica coating is required to avoid unwanted decomposition of the peroxide during the oxidation of alkyl thiols to alkyl sulfonic acids. The magnetic, solid acid catalysts exhibited similar or enhanced activity in the deprotection of benzaldehyde dimethylacetal compared to the corresponding homogeneous systems. The authors subsequently noted that the perfluoroalkylsulfonic acid catalyst is leached out during the reactions and that the activity is due to leached sulfonic acid groups. Furthermore, a comparison between MNP- and SBA-15-supported sulfonic acids proved that the latter exhibit higher activities because of their high surface area and a better dispersion of the acid species inside the pore channels.

The hydrolysis of nitriles is a very efficient method for the synthesis of amides and especially useful for various chemical and pharmaceutical applications.[203] Conventional homogeneous acids/bases are used in stoichiometric amounts in this reaction. Polshettiwar and Varma used ruthenium hydroxide ($Ru(OH)_x$) supported on MNP as an efficient recyclable catalyst for the hydrolysis of nitriles under microwave heating in aqueous solution.[204] The reaction proceeded smoothly with activated, non-activated, and heterocyclic nitriles (Scheme 34). The hydrolysis of 3-/4-nitrobenzonitrile and of 3-/4-cyanopyridine proceed almost as fast, thus indicating that the steric bulk of the substrate only has a minor impact on the reaction rate.

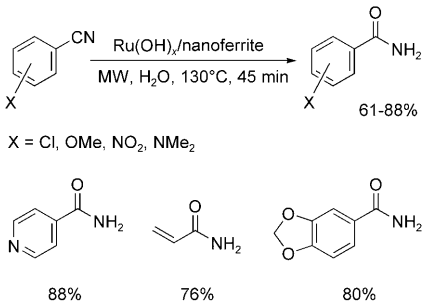

Scheme 34. Nitrile hydrolysis catalyzed by $Ru(OH)_x$/nanoferrite.[204]

Dálaigh et al. investigated the catalytic activity of the "hypernucleophilic" acylation catalyst DMAP supported on MNPs for a series of acylations at ambient temperatures and at very low catalyst loadings. These systems can be recycled an unprecedented 30 times without any discernable loss in catalytic activity.[205] Treatment of silica-coated MNPs with an excess of trimethoxysilane derivatives of DMAP resulted in an organocatalyst loading of 0.20 mmol g^{-1}. The remaining acidic surface Si-OH groups were protected with *n*-propyltrimethoxysilane. The supported DMAP catalyst promoted a further series of synthetically useful reactions which were not possible with the conventional homogeneous catalyst systems.[206] For example, the MNP-supported DMAP showed high activity (> 98% conversion) in the acetylation of 1-phenylethanol with acetic anhydride (Scheme 35), in the peracetylation of D-glucose at room temperature, in the protection of indole with *tert*-butoxycarbonyl (Boc), and in the rearrangement of a quaternary *O*-acyl enolate to form an azlactone with a stereogenic center.

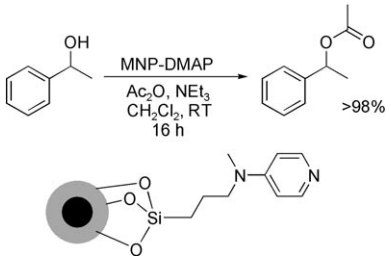

Scheme 35. Acetylation of 1-phenylethanol with a DMAP derivative supported on MNPs.[205]

Cobalt ferrite nanoparticles synthesized by the microemulsion method were functionalized with *N*-[3-(trimethoxysilyl)propyl]ethylenediamine to create basic sites. These systems were used for the Knoevenagel condensation of aromatic and heteroaromatic aldehydes with malonic acid dinitrile.[207] Complete conversion was achieved for benzaldehyde within 5 minutes in the presence of 2.5 mol% catalyst in refluxing benzene. Aromatic aldehydes with electron-with-

drawing groups (for example, -NO_2, -Cl) and electron-donating groups (for example, -OH, -Me, -OMe) resulted in quantitative conversion in different solvents such as benzene, THF, and ethyl acetate (Scheme 36). However, a sharp decrease in activity was noted when the acidic Si-OH

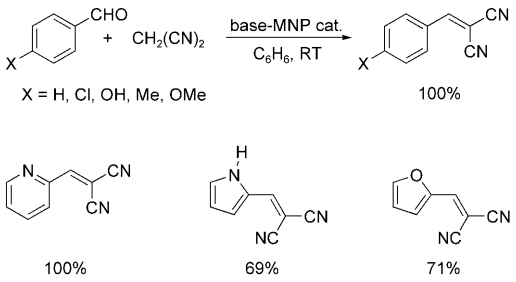

Scheme 36. Knoevenagel condensation catalyzed by diamino-functionalized SiO_2-$CoFe_2O_4$.[207]

groups residing on the external surface of the catalyst were removed by methylation. This finding is similar to other reports on hydrophobic amine-functionalized silica catalysts.[208] The activity of MNP-anchored basic catalysts was comparable to that of a large-pore, amine-functionalized SBA-15 (pore diameter ca. 101 Å) and higher than that of a MCM-48 material (pore diameter ca. 22 Å), which was attributed to mass-transfer problems.

Ionic liquids recently emerged as promising media for homogeneous catalysis and even as catalysts themselves.[209] Imidazole-based ILs with various alkyl-chain lengths grafted on MNPs encapsulated in a hydroxyapatite (HAP) support were recently reported as efficient and recyclable heterogeneous catalysts for the Knoevenagel condensation between aldehydes and malonic acid dinitrile under mild conditions in an aqueous environment.[210] The presence of 1-3 nm γ-Fe_2O_3 particles in the HAP matrix was confirmed by XRD, XPS, and TEM images. The successful functionalization of the material with ionic liquids was confirmed by typical absorptions of the imidazolium groups in the IR spectrum. Supported basic ILs (SBIL) showed higher catalytic activity than the carrier HAP-γ-Fe_2O_3 and the homogeneous basic IL [Bmim]OH (Bmim = 1-*n*-butyl-3-methylimidazolium). The authors attributed this effect to a cooperative activation by the support and the basic ILs. Furthermore, SBILs with different alkyl chains attached to the imidazolium moiety showed a size-dependent activity ($CH_3 > C_4H_9 > C_8H_{17} > C_{16}H_{33}$), which arose from the lower accessibility of the cation with increasing steric hindrance as well as a lower loading of basic centers. Various aromatic, aliphatic, and heteroaromatic aldehydes could be converted into the corresponding products in high yields with these SBIL catalysts (Scheme 37).

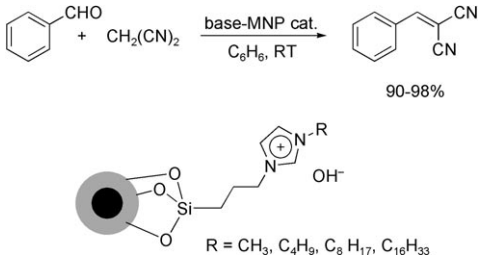

Scheme 37. Knoevenagel condensation catalyzed by basic ionic liquids grafted on a magnetic HAP support.[210]

6.8. Micellaneous Reactions

The degradation of halogenated organic pollutants is a serious environmental concern. Conventional thermal or chemical oxidation processes are often inefficient and do not result in complete decomposition of such compounds, which may result in the formation of even more toxic halogenated compounds. An alternative approach is catalytic dechlorination with molecular hydrogen.[211] Kaneda and co-workers, for example, reported the dechlorination of organohalogenides with molecular hydrogen in the presence of a Pd nanocluster catalyst supported on magnetically separable hydroxyapatite (Pd/HAP-γ-Fe_2O_3).[212] A variety of aromatic chlorides and bromides could be dehalogenated to their corresponding arenes in high yields (> 99 %, Scheme 38). The

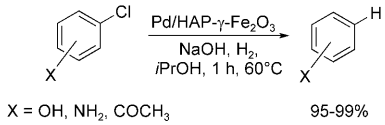

Scheme 38. Dehalogenation catalyzed by Pd nanoclusters immobilized on a magnetically separable hydroxyapatite.[212]

dechlorination of chlorobenzene produces benzene with an excellent TOF of 2500 h^{-1} in the presence of only 1 bar H_2. Catalyst screening studies further revealed that the most promising results were obtained with 2-propanol as the solvent and NaOH as the base. The catalytic activity of Pd/HAP-γ-Fe_2O_3 was found to be significantly higher than that of HAP-Pd and Pd/γ-Fe_2O_3 because of the presence of very small Pd nanoclusters on the surface of the HAP-γ-Fe_2O_3 support.

Kwon et al. investigated a magnetically separable palladium catalyst that was synthesized by a sol–gel process. Palladium nanoparticles and superparamagnetic iron oxide nanoparticles were incorporated in an aluminum oxyhydroxide matrix.[213] The catalyst showed high activity and regioselectivity for the hydrogenolysis of epoxides at room temperature under an H_2 pressure of 1 bar, and could be reused 25 times without loss of activity. For example, quantitative conversion and complete regioselectivity could be found for the hydrodechlorination of epichlorohydrin, which makes this catalyst outstanding with respect to commercial catalysts such as Pd/C, Pd/Al_2O_3, Pd/$CaCO_3$, Pd/$BaCO_3$, and PdEnCat. Furthermore, this catalyst accepts a broad spectrum of substrates (Scheme 39). It transforms *trans*-stilbene oxide exclusively into 1,2-diphenylethanol, while a commercially available Pd/C catalyst (5 mol %) produces a mixture of 1,2-diphenylethanol and dibenzyl (85:15) under similar reaction conditions. Furthermore, the configuration is retained in

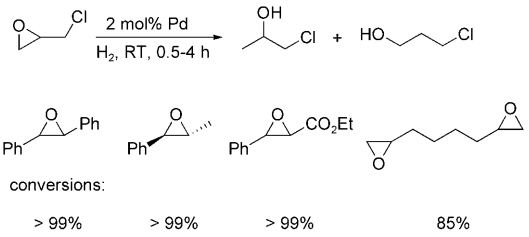

Scheme 39. Hydrogenolysis of epoxides catalyzed by Pd nanoparticles immobilized on a superparamagnetic iron oxide/aluminum oxyhydroxide matrix.[213]

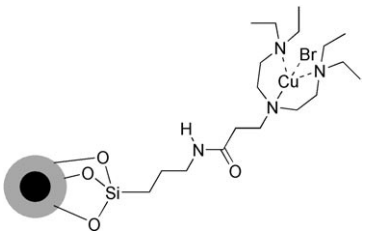

Scheme 41. Molecular structure of a tedta-Cu ATRP catalyst supported on MNPs.[215]

the hydrogenolytic ring opening of (*R*,*R*)-2-methyl-3-phenyloxirane, with only (*R*)-1-phenyl-2-propanol (99% *ee*) formed.

In 2009, an ionic liquid immobilized on MNPs was used as a recyclable catalyst (up to 11 times) for the cycloaddition of CO_2 and epoxides to produce cyclic carbonates under a low CO_2 pressure (10 bar).[214] The ionic liquid precursors were synthesized by quarternization of *N*-alkyl imidazoles with 3-chloropropyltrimethoxysilane, and could be grafted on silica-coated MNPs with a loading of 0.60 mmol g^{-1}. MNP-supported ionic liquids (MNP-ILs) with longer alkyl side chains (MNP-2, MNP-3) showed poorer catalytic activities, while the short-chain MNP-1 gave activities comparable to the unsupported [Bmim]Br. Different substrates such as styrene oxide, epichlorohydrin, propyleneoxide, glycidyl phenyl ether, and cyclohexeneoxide were converted quantitatively into the cyclic carbonates at 140 °C and 10 bar CO_2 in the presence of 1 mol% catalyst (Scheme 40).

Ding et al. reported that MNPs can be used to support catalysts for the atom-transfer radical polymerization (ATRP) of methyl methacrylate (MMA).[215] In this approach, Fe_3O_4 MNPs were first functionalized with 3-aminopropyltrimethoxysilane to anchor the amine groups on the surface of the MNPs. The generation of acrylamides by reaction of the amine groups with acryloyl chloride was followed by addition of tetraethyldiethylenetriamine (TEDETA) and subsequent complexation with CuBr (Scheme 41). In contrast to catalysts supported on micrometer-sized particles, which gave polymers with high polydispersity, the catalyst supported on MNP resulted in ATRP similar to homogeneous systems. The recycled catalyst maintained a similar activity and also gave the same excellent control over the polymerization. This finding again proves the advantages of those quasihomogeneous catalytic systems for specific reactions.

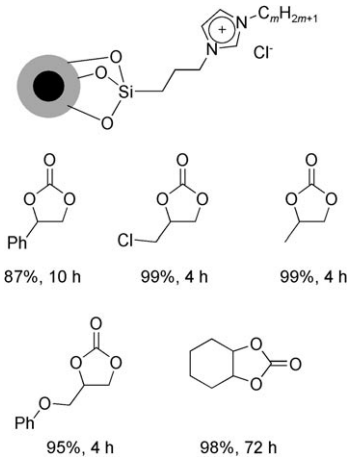

Scheme 40. Ionic liquid catalysts immobilized on MNPs for the synthesis of cyclic carbonates.[203]

The separation of different catalysts in an essentially pure form after one-pot multistep reaction cascades, and thus allowing the reuse of the recovered catalysts in various other catalytic reactions, is a synthetic challenge. Jones and co-workers elegantly demonstrated that the combination of functionalized MNPs with traditional catalysts that could be recovered by gravimetric techniques allows the promotion of one-pot multistep catalytic reactions with complete recovery of the catalysts in their pure form.[216] Superparamagnetic iron oxide MNPs functionalized with *N*-[3-(trimethoxysilyl)propyl]ethylenediamine as basic sites were used with a sulfonic acid polymer resin in a tandem deacetalization/Knoevenagel reaction. Complete conversion was noted, with TOFs of 3 h^{-1} for the acid resin catalyst and 75 h^{-1} for the basic catalyst (Scheme 42). The basic MNP catalyst could be simply recovered after the reactions by magnetic separation, while the nonmagnetic resin catalyst was recovered by gravimetric separation. The reaction sequence was further extended to a subsequent hydrogenation by combination of the MNP-supported basic catalyst and the sulfonic acid polymer resin together with a new solid catalyst (Pt/Al_2O_3) enclosed in a membrane. The reaction proceeds smoothly with an overall yield of 78%.

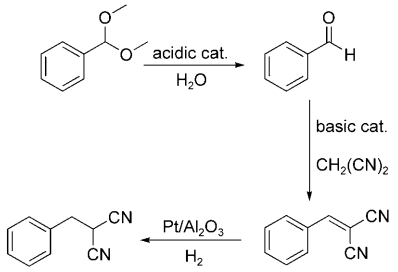

Scheme 42. Reaction cascades catalyzed by the combination of three different catalyst systems.[216]

In an almost identical approach, Abu-Reziq et al. used a one-pot multistep reaction catalyzed by a magnetically separable solid, wherein a palladium catalyst is encapsulated in a silica–polyethylenimine (SG-PEI) composite in the

presence of MNP grafted ionic liquids (Pd/SG-MNP-PEI).[217] The authors applied this catalyst together with polystyrene sulfonic acid to the one-pot dehydration/hydrogenation of benzylic alcohols. The PS-SO_3H catalyst promotes the dehydration of benzyl alcohols, whereas the Pd/SG-MNP-PEI nanocomposite catalyzes the hydrogenation of the double bond formed during the first step to give alkylated arenes as the final products (Scheme 43). The Pd catalyst could be easily recovered by magnetic separation after the reactions and could be reused for other catalytic reactions, such as the carbonylation of iodoarenes or Heck and Suzuki cross-coupling reactions.

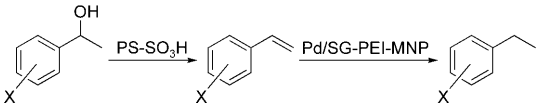

Scheme 43. One-pot reaction cascade catalyzed by a polystyrene supported sulfonic acid and a magnetically recyclable palladium system.[217]

The photocatalytic activity of nanostructured TiO_2 is well documented. The combination with MNPs allows a simple removal of such finely dispersed TiO_2 particles.[218] Immobilization of nanostructured TiO_2 in different magnetic supports (such as magnetite, ferrites, Fe_3O_4-SiO_2, or γ-Fe_2O_3-SiO_2) was recently used for a series of photodegradation reactions.[219] Wang et al. reported the synthesis of TiO_2/γ-Fe_2O_3-SiO_2 for the photodegradation of methylene blue under UV irradiation.[220] The silica coating acts as a barrier between the magnetic cores and the titania shells. Xuan et al. very recently investigated a hollow spherical TiO_2/Fe_3O_4 hybrid photocatalyst, developed through a poly(styrene-acrylic acid) (PSA) template method, for the photocatalytic degradation of rhodamine B.[221]

At the end of this Review it should be noted that small functionalized superparamagnetic iron oxide particles possess weak magnetic responses, which sometimes makes it difficult to separate them efficiently from solutions by moderate magnetic field strengths. Embedding large numbers of iron oxide cores can tackle this problem. However, Yin and coworkers put forward another method: they synthesized a composite nanostructure with two different functional substructures, which combines a high specific surface area with simple magnetic separation.[222] For this purpose, silica-encapsulated multinuclei Fe_2O_3 MNPs were first grafted with a thick layer of poly(*N*-isopropylacrylamide). The composite particles were then formed by the assembly of sterically confined small silica spheres (satellites) on the polymer network. The satellite silica particles provide high surface areas for the efficient loading of other nanocatalysts through silylation reactions. For example, the surfaces of the satellite silica spheres were functionalized with 3-aminopropyltrimethoxysilane and then gold immobilized at the amine groups for the reduction of 4-nitrophenol with $NaBH_4$. A complete conversion of 4-nitrophenol was noted within 1 h, and the catalysts could be recycled eight times with identical reaction rates. In contrast, Au nanoparticles loaded on supports without any silica colloids displayed a continuous decrease in activity after each cycle.

The same authors also immobilized gold on core–shell silica magnetic nanoparticles for the catalytic reduction of 4-nitrophenol to 4-aminophenol, with $NaBH_4$ used as the reducing agent. They noted a 14% decrease in activity after the second cycle because of the detachment of Au particles from the support and their subsequent aggregation. By employing an "encapsulation and etching strategy" they were able to overcome this drawback by protecting the gold particles with another silica shell and making the external silica shell mesoporous by controlled etching with NaOH.[223] By this approach, the nanoparticles were isolated and protected in porous silica shells, thereby avoiding mass-transfer problems and preventing coagulation of the nanoparticles during reactions. Hence, the nanocomposite maintains its high catalytic activity over six successive reaction cycles.

7. Summary and Outlook

A whole series of MNP-functionalized catalysts have been synthesized during the last few years which give identical or even higher reactivity than the corresponding homogeneous catalysts. Simple modification of the MNP surface with organic ligands enhances the adsorption of catalytically active colloidal metal nanoparticles, as highlighted with palladium-mediated C–C coupling as well as Ru-, Rh-, and Pd-catalyzed hydrogenation reactions. The excellent dispersity of the MNPs in different solvents is an additional advantage, since it exposes the surface-bound active reaction sites for the reactants in an optimal way. This allows diffusion limitation to be overcome, which is often found for systems heterogenized in microporous or mesoporous solids. Remarkably, MNP heterogenized catalysts can be recycled many times by simple magnetic filtration without any loss of activity thanks to the unique magnetic properties of the superparamagnetic particles.

Moreno-Mañas and Pleixats stated that the reproducibility in the properties of nanoparticles such as size, dispersion, catalytic performance, recoverability, and reuse without loss of activity are of paramount importance for application.[133d] The majority of these problems have been overcome during the last few years. Future directions of research should focus on enhancing the stability of colloidal metal nanoparticles supported on MNPs and the critical evaluation of the presence of homogeneous active metal species during the catalytic reactions. Moreover, for reactions catalyzed by metal nanoparticles or supported nanoparticles, detailed examination of morphological changes of nanoparticles during the catalytic transformations have to be carried out. Since metal nanoparticles are highly reactive and possess high surface to volume ratios and high surface energies, the stabilization of such materials during or after catalytic reactions is without doubt an important issue. A detailed examination of such issues assists a detailed understanding of the mechanism of nanocatalysis and also provides valuable hints for the generation of stable nanoparticles to enhance or

retain their catalytic activity. The sustainable synthesis of (magnetic) metal nanoparticles or nanocomposites using less toxic and readily available precursors as well as environmentally benign solvents or supports under ambient conditions will also make this field of chemical research more "green". We foresee that the existing methods of catalyst heterogenization will be extended to magnetic nanoparticles and nanocomposites, especially when an expensive chiral ligand or a noble metal is involved.

The Alexander von Humboldt-Foundation is gratefully acknowledged for a research grant to S.S. Our work was further supported by the joint research project "NanoKat" at the TU Kaiserslautern.

Received: October 9, 2009

[1] a) *Metal Nanoparticles. Synthesis Characterization and Applications* (Eds.: D. L. Feldheim, C. A. Fross, Jr.), Marcel Dekker, New York, **2002**; b) J. Grunes, J. Zhu, G. A. Somorjai, *Chem. Commun.* **2003**, 2257 – 2260; c) S. Reculusa, C. Poncet-Legrend, A. Perro, E. Duguet, E. Bourgeat-Lami, C. Mingotaud, S. Ravaine, *Chem. Mater.* **2005**, *17*, 3338 – 3344; d) C. J. Murphy, *J. Mater. Chem.* **2008**, *18*, 2173 – 2176; e) R. J. P. Corriu, A. Mehdi, C. Reye, *J. Mater. Chem.* **2005**, *15*, 4285 – 4294.

[2] a) A. L. Rogach, D. V. Talapin, E. V. Shevchenko, A. Kornowski, M. Haase, H. Weller, *Adv. Funct. Mater.* **2002**, *12*, 653 – 664; b) C. B. Murray, D. J. Norris, M. G. Bawendi, *J. Am. Chem. Soc.* **1993**, *115*, 8706 – 8715.

[3] J.-W. Jun, J.-S. Choi, J. Cheon, *Angew. Chem.* **2006**, *118*, 3492 – 3517; *Angew. Chem. Int. Ed.* **2006**, *45*, 3414 – 3439.

[4] M. A. El-Sayed, *Acc. Chem. Res.* **2001**, *34*, 257 – 264.

[5] a) *Nanoparticles and Catalysis* (Ed.: D. Astruc), Wiley-VCH, Weinheim, **2008**; b) H. Bonnemann, W. Brijoux, *Active Metals: Preparation, Characterization, Applications* (Ed.: A. Fürstner), Wiley-VCH, Weinheim, **1996**; c) H. Bönnemann, W. Brijoux, R. Brinkmann, T. Joussen, B. Korall, E. Dinjus, *Angew. Chem.* **1991**, *103*, 1344 – 1346; *Angew. Chem. Int. Ed. Engl.* **1991**, *30*, 1312 – 1314.

[6] R. Narayanan, M. A. El-Sayed, *J. Phys. Chem. B* **2005**, *109*, 12663 – 12676.

[7] H. Bonnemann, G. Braun, G. B. Brijoux, R. Brinkman, A. S. Tilling, S. K. Schulze, K. Siepen, *J. Organomet. Chem.* **1996**, *520*, 143 – 162.

[8] a) S.-W. Kim, S. U. Son, S. S. Lee, T. Hyeon, Y. K. Chung, *Chem. Commun.* **2001**, 2212 – 2213; b) S. U. Son, S. I. Lee, Y. K. Chung, S.-W. Kim, T. Hyeon, *Org. Lett.* **2002**, *4*, 277 – 279.

[9] G. Schmid, *Chem. Rev.* **1992**, *92*, 1709 – 1727.

[10] L. N. Lewis, *Chem. Rev.* **1993**, *93*, 2693 – 2730.

[11] a) M. C. Daniel, D. Astruc, *Chem. Rev.* **2004**, *104*, 293 – 346; b) D. Astruc, F. Lu, J. R. Aranzaes, *Angew. Chem.* **2005**, *117*, 8062 – 8083; *Angew. Chem. Int. Ed.* **2005**, *44*, 7852 – 7872; c) J. A. Dahl, B. L. S. Maddux, J. E. Hutchinson, *Chem. Rev.* **2007**, *107*, 2228 – 2269; d) A. Roucoux, J. Schulz, H. Patin, *Chem. Rev.* **2002**, *102*, 3757 – 3778.

[12] a) T. S. Ahmadi, Z. L. Wang, T. C. Green, A. Henglein, M. A. El-Sayed, *Science* **1996**, *272*, 1924 – 1925; b) R. Narayanan, M. A. El-Sayed, *Nano Lett.* **2004**, *4*, 1343 – 1348; c) R. Narayanan, M. A. El-Sayed, *Langmuir* **2005**, *21*, 2027 – 2033.

[13] a) T. Teranishi, M. Miyake, *Chem. Mater.* **1998**, *10*, 594 – 600; b) Y. Li, M. A. El-Sayed, *J. Phys. Chem. B* **2001**, *105*, 8938 – 8943.

[14] a) R. Narayanan, M. A. El-Sayed, *J. Phys. Chem. B* **2004**, *108*, 8572 – 8580; b) T. K. Sau, A. Pal, T. Pal, *J. Phys. Chem. B* **2001**, *105*, 9266 – 9272.

[15] a) R. Narayanan, M. A. El-Sayed, *J. Am. Chem. Soc.* **2003**, *125*, 8340 – 8347; b) S. Kidambi, J.-H. Dai, J. Lin, M. L. Bruening, *J. Am. Chem. Soc.* **2004**, *126*, 8493 – 8500; c) L. R. Gröschel, A. Haidar, K.-H. Beyer, R. Reichert, R. Schomacker, *Catal. Lett.* **2004**, *95*, 67 – 75.

[16] a) J. Schulz, A. Rovcoux, H. Patin, *Chem. Eur. J.* **2000**, *6*, 618 – 624; b) V. Mévellec, A. Roucoux, E. Ramirez, K. Philippot, B. Chaudert, *Adv. Synth. Catal.* **2004**, *346*, 72 – 76; c) C. C. Yang, C. C. Wan, Y. Y. Wang, *J. Colloid Interface Sci.* **2004**, *279*, 433 – 437.

[17] a) M. Zhao, L. Sun, R. M. Crooks, *J. Am. Chem. Soc.* **1998**, *120*, 4877 – 4878; b) R. M. Crooks, M. Zhao, L. Sun, V. Chechik, L. K. Yeung, *Acc. Chem. Res.* **2001**, *34*, 181 – 190; c) M. Zhao, R. M. Crooks, *Angew. Chem.* **1999**, *111*, 375 – 377; *Angew. Chem. Int. Ed.* **1999**, *38*, 364 – 366; d) L. Balogh, D. A. Tomalia, *J. Am. Chem. Soc.* **1998**, *120*, 7355 – 7356; e) K. Esumi, A. Suzuki, N. Aihara, K. Usui, K. Torigoe, *Langmuir* **1998**, *14*, 3157 – 3159; f) K. Esumi, R. Isono, T. Yoshimura, *Langmuir* **2004**, *20*, 237 – 243; g) L. Wu, B.-L. Li, Y.-Y. Huang, H.-F. Zhou, Y.-M. He, Q.-H. Fan, *Org. Lett.* **2006**, *8*, 3605 – 3608.

[18] a) V. Caló, A. Nacci, A. Monopoli, S. Laera, N. Cioffi, *J. Org. Chem.* **2003**, *68*, 2929 – 2933; b) R. R. Deshmukh, R. Rajagopal, K. V. Srinivasan, *Chem. Commun.* **2001**, 1544 – 1545.

[19] a) G. A. Somorjai, J. Y. Park, *Angew. Chem.* **2008**, *120*, 9352 – 9368; *Angew. Chem. Int. Ed.* **2008**, *47*, 9212 – 9228; b) J. Park, E. Kang, S. U. Son, H. M. Park, M. K. Lee, J. Kim, K. W. Kim, H.-J. Noh, J.-H. Park, C. J. Bae, J.-G. Park, T. Hyeon, *Adv. Mater.* **2005**, *17*, 429 – 434.

[20] a) C. Burda, X. Chen, R. Narayanan, M. A. El-Sayed, *Chem. Rev.* **2005**, *105*, 1025 – 1102; b) A. Doyle, S. K. Shaikhutdinov, S. D. Jackson, H. J. Freund, *Angew. Chem.* **2003**, *115*, 5398 – 5401; *Angew. Chem. Int. Ed.* **2003**, *42*, 5240 – 5243; c) L.-S. Li, J. Hu, W. Yang, A. P. Alivisatos, *Nano Lett.* **2001**, *1*, 349 – 351; d) M. Steigerwald, L. E. Brus, *Acc. Chem. Res.* **1990**, *23*, 183 – 188; e) F. Porta, M. Rossi, *J. Mol. Catal. A* **2003**, *204*, 553 – 559; f) A. R. Tao, S. Habas, P. D. Yang, *Small* **2008**, *4*, 310 – 325.

[21] S. M. Davis, F. Zaera, G. A. Somorjai, *J. Catal.* **1984**, *85*, 206 – 223.

[22] H. Lee, S. E. Habas, S. Kweskin, D. Butcher, G. A. Somorjai, P. Yang, *Angew. Chem.* **2006**, *118*, 7988 – 7992; *Angew. Chem. Int. Ed.* **2006**, *45*, 7824 – 7828.

[23] a) J. M. Campelo, D. Luna, R. Luque, J. M. Marinas, A. A. Romero, *ChemSusChem* **2009**, *2*, 18 – 45; b) G. Glaspell, H. M. A. Hassan, A. Elzatahry, V. Abdalsayed, M. S. El-Shall, *Top. Catal.* **2008**, *47*, 22 – 31; c) P. Claus, A. Bruckner, C. Mohr, H. Hofmeister, *J. Am. Chem. Soc.* **2000**, *122*, 11430 – 11439; d) A. Martino, S. A. Yamanaka, J. S. Kawola, D. A. Ly, *Chem. Mater.* **1997**, *9*, 423 – 429; e) X. D. Mu, D. G. Evans, Y. Kou, *Catal. Lett.* **2004**, *97*, 151 – 154; f) C. B. Hwang, Y. S. Fu, Y.-L. Lu, S.-W. Jang, P.-T. Chou, C.-R. Wang, S.-J. Yu, *J. Catal.* **2000**, *195*, 336 – 341; g) J. A. Dahl, B. L. S. Maddux, J. E. Hutchinson, *Chem. Rev.* **2007**, *107*, 2228 – 2269.

[24] a) T. K. Sau, C. J. Murphy, *J. Am. Chem. Soc.* **2004**, *126*, 8648 – 8649; b) F. Kim, J. H. Song, P. Yang, *J. Am. Chem. Soc.* **2002**, *124*, 14316 – 14317.

[25] a) C. N. R. Rao, A. Muller, A. K. Cheetham, *The Chemistry of Nanomaterials: Synthesis and Applications*, *Vol. 1*, Wiley-VCH, Weinheim, **2004**; b) P. T. Anastas, M. M. Kirchkoff, *Acc. Chem. Res.* **2002**, *35*, 686 – 694; c) G. Schmid, V. Maihack, F. Lantermann, S. Peschel, *J. Chem. Soc. Dalton Trans.* **1996**, 589 – 595; d) W. Yan, S. Mahurin, S. Overbury, S. Dai, *Top. Catal.* **2006**, *39*, 199 – 212; e) R. M. Rioux, H. Song, J. D. Hofelmeyer, P. Yang, G. A. Somorjai, *J. Phys. Chem. B* **2005**, *109*, 2192 – 2202; f) G.

Budroni, A. Corma, *Angew. Chem.* **2006**, *118*, 3406 – 3409; *Angew. Chem. Int. Ed.* **2006**, *45*, 3328 – 3331.

[26] a) A. H. Lu, E. L. Salabas, F. Schüth, *Angew. Chem.* **2007**, *119*, 1242 – 1266; *Angew. Chem. Int. Ed.* **2007**, *46*, 1222 – 1244; b) U. Jeong, X. Teng, Y. Wang, H. Yang, Y. Xia, *Adv. Mater.* **2007**, *19*, 33 – 60; c) Y. W. Jun, J. W. Seo, J. Cheon, *Acc. Chem. Res.* **2008**, *41*, 179 – 189.

[27] a) Y. Borodko, S. E. Habas, M. Koebel, P. Yang, H. Frei, G. A. Somorjai, *J. Phys. Chem. B* **2006**, *110*, 23052 – 23059; b) I. Washio, Y. Xiong, Y. Yin, Y. Xia, *Adv. Mater.* **2006**, *18*, 1745 – 1749.

[28] L. D. Rampino, F. F. Nord, *J. Am. Chem. Soc.* **1941**, *63*, 2745 – 2749.

[29] a) G. J. Hutchings, *J. Mater. Chem.* **2009**, *19*, 1222 – 1235; b) G. C. Bond, P. A. Sermon, *Gold Bull.* **1973**, *6*, 102 – 105; c) H. Hirai, Y. Nakao, N. J. Toshima, *Macromol. Sci. Chem. A* **1978**, *12*, 1117 – 1119; d) B. F. G. Johnson, *Top. Catal.* **2003**, *24*, 147 – 159; e) M. Haruta, T. Kobayashi, H. Sano, N. Yamada, *Chem. Lett.* **1987**, 405 – 407; f) M. Haruta, *Chem. Rec.* **2003**, *3*, 75 – 87.

[30] a) M. T. Reetz, W. Helbig, *J. Am. Chem. Soc.* **1994**, *116*, 7401 – 7402; b) M. T. Reetz, G. Lohmer, *Chem. Commun.* **1996**, 1921 – 1922; c) M. T. Reetz, E. Westermann, *Angew. Chem.* **2000**, *112*, 170 – 173; *Angew. Chem. Int. Ed.* **2000**, *39*, 165 – 168; d) Y. Li, X. M. Hong, D. M. Collard, M. A. El-Sayed, *Org. Lett.* **2000**, *2*, 2385 – 2388; e) M. T. Reetz, J. G. deVries, *Chem. Commun.* **2004**, 1559 – 1563.

[31] L. N. Lewis, N. Lewis, *J. Am. Chem. Soc.* **1986**, *108*, 7228 – 7231.

[32] a) M. Valden, X. Lai, D. W. Goodman, *Science* **1998**, *281*, 1647 – 1650; b) R. J. White, R. Luque, V. Budarin, J. H. Clark, D. J. Macquarrie, *Chem. Soc. Rev.* **2009**, *38*, 481 – 494; c) D. J. Cole-Hamilton, *Science* **2003**, *299*, 1702 – 1706; d) X. Pan, X. Bao, *Chem. Commun.* **2008**, 6271 – 6281.

[33] C. A. Mirkin, *Small* **2005**, *1*, 14 – 16.

[34] a) A. Taguchi, F. Schüth, *Microporous Mesoporous Mater.* **2005**, *77*, 1 – 45; b) J. A. Melero, R. V. Grieken, G. Morales, *Chem. Rev.* **2006**, *106*, 3790 – 3812; c) D. E. De Vos, M. Dams, B. F. Sels, P. A. Jacobs, *Chem. Rev.* **2002**, *102*, 3615 – 3640; d) F. Schüth, W. Schmidt, *Adv. Mater.* **2002**, *14*, 629 – 638; e) A. Corma, H. Garcia, *Adv. Synth. Catal.* **2006**, *348*, 1391 – 1412; f) M. Gruttadauria, F. Giacalone, R. Noto, *Chem. Soc. Rev.* **2008**, *37*, 1666 – 1688; g) M. Benaglia, A. Puglisi, F. Cozzi, *Chem. Rev.* **2003**, *103*, 3401 – 3430; h) C. E. Song, S. G. Lee, *Chem. Rev.* **2002**, *102*, 3495 – 3524; i) D. E. DeVos, M. Dams, B. F. Sels, P. A. Jacobs, *Chem. Rev.* **2002**, *102*, 3615 – 3640; j) S. Fujita, S. Inagaki, *Chem. Mater.* **2008**, *20*, 891 – 908; k) A. P. Wight, M. E. Davis, *Chem. Rev.* **2002**, *102*, 3589 – 3614; l) J. Y. Ying, C. P. Mehnert, M. S. Wong, *Angew. Chem.* **1999**, *111*, 58 – 82; *Angew. Chem. Int. Ed.* **1999**, *38*, 56 – 77; m) F. Hoffmann, M. Cornelius, J. Morell, M. Fröba, *Angew. Chem.* **2006**, *118*, 3290 – 3328; *Angew. Chem. Int. Ed.* **2006**, *45*, 3216 – 3251; n) S. Shylesh, P. P. Samuel, S. Sisodiya, A. P. Singh, *Catal. Surv. Asia* **2008**, *12*, 266 – 282.

[35] a) J. Gladysz, *Chem. Rev.* **2002**, *102*, 3215 – 3216; b) J. Gladysz, *Pure Appl. Chem.* **2001**, *73*, 1319 – 1324.

[36] a) J. Grunes, J. Zhu, G. A. Somorjai, *Chem. Commun.* **2003**, 2257 – 2260; b) A. T. Bell, *Science* **2003**, *299*, 1688 – 1691; c) R. Schlögl, S. B. Abd Hamid, *Angew. Chem.* **2004**, *116*, 1656 – 1667; *Angew. Chem. Int. Ed.* **2004**, *43*, 1628 – 1637.

[37] a) R. A. Sheldon, H. van Bekkum, *Fine Chemicals through Heterogeneous Catalysis*, Wiley-VCH, Weinheim, **2001**; b) R. A. Sheldon, *Chem. Commun.* **2008**, 3352 – 3365; c) R. A. Sheldon, *J. Environ. Monit.* **2008**, *10*, 406 – 407.

[38] a) J. M. Thomas, W. J. Thomas, *Principles and Practice of Heterogenous Catalysis*, Wiley-VCH, Weinheim, **1997**; b) G. A. Somorjai, R. M. Rioux, *Catal. Today* **2005**, *100*, 201 – 215.

[39] a) F. Cozzi, *Adv. Synth. Catal.* **2006**, *348*, 1367 – 1390; b) B. M. L. Dioos, I. F. J. Vankelecom, P. A. Jacobs, *Adv. Synth. Catal.* **2006**, *348*, 1413 – 1446.

[40] a) A. Behr, G. Henze, R. Schomacker, *Adv. Synth. Catal.* **2006**, *348*, 1485 – 1495; b) D. E. Bergbreiter, S. D. Sung, *Adv. Synth. Catal.* **2006**, *348*, 1352 – 1366.

[41] W. Teunissen, A. A. Bol, J. W. Geus, *Catal. Today* **1999**, *48*, 329 – 336.

[42] R. Narayanan, M. A. El-Sayed, *J. Phys. Chem. B* **2005**, *109*, 12663 – 12676.

[43] a) A. C. Templeton, M. J. Hostetler, E. K. Warmoth, S. Chen, C. M. Hartshorn, V. M. Krishnamurthy, M. D. E. Forber, R. W. Murray, *J. Am. Chem. Soc.* **1998**, *120*, 4845 – 4849; b) J. Fan, S. Chen, Y. Gao, *Colloids Surf. B* **2003**, *28*, 199 – 202; c) K. Marubayashi, S. Takizawa, T. Kawakusu, T. Arai, H. Sasai, *Org. Lett.* **2003**, *5*, 4409 – 4412; d) G. Budroni, A. Corma, *Angew. Chem.* **2006**, *118*, 3406 – 3409; *Angew. Chem. Int. Ed.* **2006**, *45*, 3328 – 3331.

[44] A. Hu, G. T. Yee, W. Lin, *J. Am. Chem. Soc.* **2005**, *127*, 12486 – 12487.

[45] a) C. M. Sorensen, *Nanomaterials in Chemistry* (Ed. K. J. Klabunde), Wiley, New York, **2001**; b) D. L. Leslie-Pelecky, R. D. Rieke, *Chem. Mater.* **1996**, *8*, 1770 – 1883; c) D. L. Huber, *Small* **2005**, *1*, 482 – 501; d) Y.-W. Jun, J. S. Choi, J. Cheon, *Chem. Commun.* **2007**, 1203 – 1214; e) N. A. Frey, S. Peng, K. Cheng, S. Sun, *Chem. Soc. Rev.* **2009**, *38*, 2532 – 2542.

[46] L. Neel, *Ann. Geophys. Ser. B* **1949**, *5*, 99 – 136.

[47] Q. A. Pankhurst, J. Connolly, S. K. Jones, J. Dobson, *J. Phys. D* **2003**, *36*, R167 – R181.

[48] a) G. C. Hadjipanayis, G. A. Prinz, *Science and Technology of Nano-structured Magnetic Materials*, Plenum, New York, **1991**; b) B. D. Cullity, *Introduction to Magnetic Materials* (Ed.: M. Cohen), Addison-Wesley, New York, **1972**.

[49] J.-I. Park, N.-J. Kang, Y.-W. Jun, S. J. Oh, H.-C. Ri, J. Cheon, *ChemPhysChem* **2002**, *3*, 543 – 547.

[50] a) G. M. Whitesides, R. J. Kazlauskas, L. Josephson, *Trends Biotechnol.* **1983**, *1*, 144 – 148; b) A. K. Gupta, M. Gupta, *Biomaterials* **2005**, *26*, 3995 – 4021; c) J. Fan, Y. Gao, *J. Exp. Nanosci.* **2006**, *1*, 457; d) N. Zhao, W. Ma, Z. Cui, W. Song, C. Xu, M. Gao, *ACS Nano* **2009**, *3*, 1775 – 1780; e) Y. H. Zheng, Y. Cheng, Y. S. Wang, F. Bao, L. H. Zhou, X. F. Wei, Y. Y. Zhang, Q. Zheng, *J. Phys. Chem. B* **2006**, *110*, 3093 – 3097; f) J. Manuel Perez, *Nat. Nanotechnol.* **2007**, *2*, 535 – 536.

[51] a) L. Shen, P. E. Laibinis, T. A. Hatton, *Langmuir* **1999**, *15*, 447 – 453; b) X.-C. Shen, X.-Z. Fang, Y.-H. Zhou, H. Liang, *Chem. Lett.* **2004**, *33*, 1468 – 1469.

[52] a) M.-H. Liao, K.-Y. Wu, D.-H. Chen, *Chem. Lett.* **2003**, *32*, 488 – 490; b) R. Matsuno, K. Yamamoto, H. Otsuka, A. Takahara, *Chem. Mater.* **2003**, *15*, 3 – 5; c) X. Liu, Y. Guan, Z. Ma, H. Liu, *Langmuir* **2004**, *20*, 10278 – 10282; d) X. Huang, A. Schmucker, J. Dyke, S. M. Hall, J. Retrum, B. Stein, V. Remmer, D. V. Baxter, B. Dragnea, L. M. Bronstein, *J. Mater. Chem.* **2009**, *19*, 4231 – 4239; e) J.-Y. Kim, J.-T. Kim, E.-A. Song, Y.-K. Min, H. Hamaguchi, *Macromolecules* **2008**, *41*, 2886 – 2889.

[53] a) R. M. Cornell, U. Schwartmann, *The Iron Oxide: Structure, Properties, Reactions, Occurrences and Uses*, Wiley-VCH, Weinheim, **2003**; b) T. Hyeon, *Chem. Commun.* **2003**, 927 – 934.

[54] a) S. H. Sun, H. Zeng, *J. Am. Chem. Soc.* **2002**, *124*, 8204 – 8205; b) X. Wang, J. Zhuang, Q. Peng, Y. D. Li, *Nature* **2005**, *437*, 121 – 123; c) F. X. Redl, C. T. Black, G. C. Papaefthymiou, R. L. Sandstrom, M. Yin, H. Zeng, C. B. Murray, S. P. O'Brien, *J. Am. Chem. Soc.* **2004**, *126*, 14583 – 14599.

[55] a) C. H. Griffiths, M. P. Ohoro, T. W. Smith, *J. Appl. Phys.* **1979**, *50*, 7108 – 7115; b) K. S. Suslick, M. M. Fang, T. Hyeon, *J. Am. Chem. Soc.* **1996**, *118*, 11960 – 11961.

[56] S. Laurent, D. Forge, M. Port, A. Roch, C. Robic, L. V. Elst, R. N. Muller, *Chem. Rev.* **2008**, *108*, 2064 – 2110.

[57] a) J. R. Jeong, S. J. Lee, J. D. Kim, S.-C. Shin, *Phys. Status Solidi* **2004**, *241*, 1593 – 1596; b) I. Rabias, M. Fardis, E. Devlin, N. Boukos, D. Tgitrouli, G. Papavassiliou, *ACS Nano* **2008**, *2*, 977 – 983.

[58] Z. J. Zhang, Z. L. Wang, B. C. Chakoumakos, J. S. Yin, *J. Am. Chem. Soc.* **1998**, *120*, 1800 – 1804.

[59] a) T. Mathew, N. R. Shiju, K. Sreekumar, B. S. Rao, C. S. Gopinath, *J. Catal.* **2002**, *210*, 405 – 417; b) T. Mathew, S. Shylesh, S. N. Reddy, C. P. Sebastian, S. K. Date, B. S. Rao, S. D. Kulkarni, *Catal. Lett.* **2004**, *93*, 155 – 163.

[60] a) C. R. Vestal, Z. J. Zhang, *Nano Lett.* **2003**, *3*, 1739 – 1743; b) G. V. M. Jacintho, A. G. Brolo, P. Corio, P. A. Z. Suarez, J. C. Rubin, *J. Phys. Chem. B* **2009**, *113*, 7684 – 7691.

[61] a) C. T. Black, C. B. Murray, R. L. Sandstorm, S. Sun, *Science* **2000**, *290*, 1131 – 1134; b) S. Sun, *Adv. Mater.* **2006**, *18*, 393 – 403; c) J. I. Park, M. G. Kim, Y. W. Jun, J. S. Lee, W. R. Lee, J. Cheon, *J. Am. Chem. Soc.* **2004**, *126*, 9072 – 9078; d) H. Zeng, J. Li, Z. L. Wang, J. P. Liu, S. Sun, *Nano Lett.* **2004**, *4*, 187 – 190; e) X. W. Teng, H. Yang, *J. Am. Chem. Soc.* **2003**, *125*, 14559 – 14563; f) J. Luo, M. M. Maye, V. Petkov, N. N. Kariuki, L. Wang, P. Njoki, D. Mott, Y. Lin, C.-J. Zhong, *Chem. Mater.* **2005**, *17*, 3086 – 3091; g) M. Chen, J. P. Liu, S. Sun, *J. Am. Chem. Soc.* **2004**, *126*, 8394 – 8395.

[62] S. Sun, C. B. Murray, D. Weller, L. Folks, A. Moser, *Science* **2000**, *287*, 1989 – 1992.

[63] Y. Lee, J. Lee, C. J. Bae, J.-G. Park, H.-J. Noh, J.-H. Park, T. Hyeon, *Adv. Funct. Mater.* **2005**, *15*, 503 – 506.

[64] J. A. López Pérez, M. A. Lopez Quintela, J. Mira, J. Rivas, S. W. Charles, *J. Phys. Chem. B* **1997**, *101*, 8045 – 8047.

[65] P. Tartaj, M. P. Morales, S. V. Verdaguer, T. G. Carreno, C. J. Serna, *Synthesis Properties and Biomedical Application of Magnetic Nanoparticle: Handbook of Magnetic Materials*, Elsevier, The Netherlands, **2006**.

[66] J. Rockenberger, E. C. Scher, A. P. Alivisatos, *J. Am. Chem. Soc.* **1999**, *121*, 11595 – 11596.

[67] a) T. Hyeon, S. S. Lee, J. Park, Y. Chung, H. B. Na, *J. Am. Chem. Soc.* **2001**, *123*, 12798 – 12801; b) S. Sun, H. Zeng, D. B. Robinson, S. Raoux, P. M. Rice, S. X. Wang, G. Li, *J. Am. Chem. Soc.* **2004**, *126*, 273 – 279; c) S. Sun, H. Zeng, *J. Am. Chem. Soc.* **2002**, *124*, 8204 – 8205.

[68] a) J. Cheon, N. J. Kang, S-M. Lee, J.-H. Lee, J. H. Yoon, S. J. Oh, *J. Am. Chem. Soc.* **2004**, *126*, 1950 – 1951; b) Y. Chu, J. Hu, W. Yang, C. Wang, Z. Z. Zhang, *J. Phys. Chem. B* **2006**, *110*, 3135 – 3139.

[69] a) N. Moumen, M. P. Pileni, *Chem. Mater.* **1996**, *8*, 1128 – 1134; b) N. Moumen, M. P. Pileni, *J. Phys. Chem.* **1996**, *100*, 1867 – 1873; c) C. Liu, B. Zou, A. J. Rondinone, Z. J. Zhang, *J. Phys. Chem. B* **2000**, *104*, 1141 – 1145; d) K. Woo, H. J. Lee, J.-P. Ahn, Y. S. Park, *Adv. Mater.* **2003**, *15*, 1761 – 1764.

[70] a) H. Hofmeister, F. Huisken, B. Kohn, R. Alexandrescu, S. Cojocru, A. Crunteanu, L. Morjan, L. Diamandescu, *Appl. Phys. A* **2001**, *72*, 7 – 11; b) Y. He, X. Li, M. T. Swihart, *Chem. Mater.* **2005**, *17*, 1017 – 1026.

[71] O. Bomatí-Miguel, P. Tartaj, M. P. Morales, P. Bonville, U. G. Schindler, X. Q. Zhao, S. V. Verdaguer, *Small* **2006**, *2*, 1476 – 1483.

[72] a) H. Bonnemann, W. Brijoux, R. Brinkmann, N. Matoussevitch, N. Waldoefner, N. Palina, H. Modrow, *Inorg. Chim. Acta* **2003**, *350*, 617 – 624; b) J. Nogues, J. Sort, V. Langlas, V. Skumryev, S. Surinach, J. S. Munoz, M. D. Baro, *Phys. Rep.* **2005**, *422*, 65 – 67.

[73] R. Davies, G. A. Schurr, P. Meenan, R. D. Nelson, H. E. Bergna, C. A. S. Brevett, R. H. Goldbaum, *Adv. Mater.* **1998**, *10*, 1264 – 1270.

[74] a) Y. Sahoo, H. Pizen, T. Fried, D. Golodnitsky, L. Burstein, C. N. Sukenik, G. Markovich, *Langmuir* **2001**, *17*, 7907 – 7911; b) R. Massart, *IEEE Trans. Magn.* **1981**, *17*, 1247; c) M. De Cuyper, M. Joniau, *Langmuir* **1991**, *7*, 647 – 652.

[75] P. M. Paulus, H. Bonnemann, A. M. Van der Kraan, F. Luis, J. Sinzig, L. J. De Jongh, *Eur. Phys. J. D* **1999**, *9*, 501 – 504.

[76] a) B. L. Cushing, V. L. Kolesnicheno, C. J. O'Connor, *Chem. Rev.* **2004**, *104*, 3893 – 3946; b) Y. P. H. Sahoo, H. Pizem, T. Fried, D. Golodnitsky, L. Burstein, N. C. Sukenik, G. Markovich, *Langmuir* **2001**, *17*, 7907 – 7911.

[77] A. L. Willis, N. J. Turro, S. O'Brien, *Chem. Mater.* **2005**, *17*, 5970 – 5975.

[78] L. Shen, P. E. Laibinis, T. A. Hatton, *Langmuir* **1999**, *15*, 447 – 453.

[79] F. Caruso, *Adv. Mater.* **2001**, *13*, 11 – 22.

[80] a) Y. Wang, X. W. Teng, J. S. Wang, H. Yang, *Nano Lett.* **2003**, *3*, 789 – 793; b) G. F. Li, J. D. Fan, R. Jiang, Y. Gao, *Chem. Mater.* **2004**, *16*, 1835 – 1837; c) C. R. Vestal, Z. J. Zhang, *J. Am. Chem. Soc.* **2002**, *124*, 14312 – 14313.

[81] a) M. D. Butterworth, S. A. Bell, S. P. Armes, A. W. Simpson, *J. Colloid Interface Sci.* **1996**, *183*, 91 – 94; b) K. A. Harris, J. D. Goff, A. Y. Carmichael, J. S. Riffle, J. J. Harburn, T. G. St. Pierre, M. Saunders, *Chem. Mater.* **2003**, *15*, 1367 – 1377; c) S. R. Wan, Y. Zheng, Y. Q. Liu, H. S. Yan, K. L. Liu, *J. Mater. Chem.* **2005**, *15*, 3424 – 3430.

[82] D. Farrell, S. A. Majetich, J. P. Wilcoxon, *J. Phys. Chem. B* **2003**, *107*, 11022 – 11030.

[83] a) I. J. Bruce, J. Taylor, M. Todd, M. J. Davies, E. Borioni, C. Sangregorio, T. Sen, *J. Magn. Magn. Mater.* **2004**, *284*, 145 – 160; b) P. J. Robinson, P. Dunnill, M. D. Lilly, *Biotechnol. Bioeng.* **1973**, *15*, 603 – 606; c) X. Gao, K. M. K. Yu, K. Tam, S. C. Tsang, *Chem. Commun.* **2003**, 298 – 2999.

[84] L. M. Liz-Marzán, M. Giersig, P. Mulvaney, *Chem. Commun.* **1996**, 731 – 732.

[85] a) W. Stöber, A. Fink, E. J. Bohn, *J. Colloid Interface Sci.* **1968**, *26*, 62 – 65; b) Z. Dai, F. Meiser, H. Möhwald *J. Colloid Interface Sci.* **2005**, *288*, 298 – 302.

[86] a) M. Ohmori, E. Matijevic, *J. Colloid Interface Sci.* **1993**, *160*, 288 – 291; b) P. Tartaj, C. J. Serna, *J. Am. Chem. Soc.* **2003**, *125*, 15754 – 15755; c) P. Tartaj, T. G-Carreno, C. J. Serna, *Adv. Mater.* **2001**, *13*, 1620 – 1624; d) P. Tartaj, T. G. Carreno, C. J. Serna, *Langmuir* **2002**, *18*, 4556 – 4558; e) C. Graf, D. L. J. Vossen, A. Imhof, A. van Blacaderen, *Langmuir* **2003**, *19*, 6693 – 6700.

[87] Y. Lu, Y. Yin, B. T. Mayers, Y. Xia, *Nano Lett.* **2002**, *2*, 183 – 186.

[88] A. P. Philipse, M. P. B. van Bruggen, C. Pathmamanoharan, *Langmuir* **1994**, *10*, 92 – 99.

[89] Y.-H. Deng, C.-C. Wang, J.-H. Hu, W.-L. Yang, S.-K. Fu, *Colloids Surf. A* **2005**, *262*, 87 – 92.

[90] L. M. Liz-Marzán, M. Giersig, P. Mulvaney, *Langmuir* **1996**, *12*, 4329 – 4335.

[91] a) N. L. Rosi, C. A. Mirkin, *Chem. Rev.* **2005**, *105*, 1547 – 1562; b) Z. Ban, Y. A. Barnakov, F. Li, V. O. Golub, C.-J. O'Connor, *J. Mater. Chem.* **2005**, *15*, 4660 – 4662; c) D. Caruntu, B. L. Cushing, G. Caruntu, C. J. O'Connor, *Chem. Mater.* **2005**, *17*, 3398 – 3402; d) S.-J. Cho, J.-C. Idrobo, J. Olomit, K. Liu, N. D. Browning, S. M. Kauzlarich, *Chem. Mater.* **2005**, *17*, 3181 – 3186; e) L. Wang, H.-Y. Park, S. I. Im Lim, M. J. Schadt, D. Mott, J. Luo, X. Wang, C. J. Zhang, *J. Mater. Chem.* **2008**, *18*, 2629 – 2635.

[92] a) J. I. Park, J. Cheon, *J. Am. Chem. Soc.* **2001**, *123*, 5743 – 5746; b) J. I. Park, M. G. Kim, J. W. Jun, J. S. Lee, W. R. Lee, J. Cheon, *J. Am. Chem. Soc.* **2004**, *126*, 9072 – 9078.

[93] a) H. B. S. Chan, B. L. Ellis, H. L. Sharma, W. Frost, V. Caps, R. A. Shields, S. C. Tsang, *Adv. Mater.* **2004**, *16*, 144 – 149; b) J. Geng, D. A. Jefferson, B. F. G. Johnson, *Chem. Commun.* **2004**, 2442 – 2443; c) A. H. Lu, W. Li, E. L. Salabas, B. Spliethoff, F.

Schüth, *Chem. Mater.* **2006**, *18*, 2086 – 2094; d) A. H. Lu, W. Li, A. Kiefer, W. Schmidt, E. Bill, G. Fink, F. Schüth, *J. Am. Chem. Soc.* **2004**, *126*, 8616 – 8617; e) S. I. Nikitenko, Y. Koltypin, O. Palchik, I. Felner, X. N. Xu, A. Gedanken, *Angew. Chem.* **2001**, *113*, 4579 – 4581; *Angew. Chem. Int. Ed.* **2001**, *40*, 4447 – 4449; f) D. Tasis, N. Tagmatarchis, A. Bianco, M. Prato, *Chem. Rev.* **2006**, *106*, 1105 – 1136; g) M. A. Zalich, V. V. Baranauskas, J. S. Riffle, M. Saunders, T. G. St. Pierre, *Chem. Mater.* **2006**, *18*, 2648 – 2655; h) W. S. Seo, J. H. Lee, X. M. Sun, Y. Suzuki, D. Mann, Z. Liu, M. Terashima, P. C. Yang, M. V. McConnell, G. G. Nishimura, H. J. Dai, *Nat. Mater.* **2006**, *5*, 971 – 975.

[94] a) R. N. Grass, E. K. Athanassiou, W. J. Stark, *Angew. Chem.* **2007**, *119*, 4996 – 4999; *Angew. Chem. Int. Ed.* **2007**, *46*, 4909 – 4912; b) R. N. Grass, W. J. Stark, *J. Mater. Chem.* **2006**, *16*, 1825 – 1830; c) F. M. Koehler, N. A. Luechinger, D. Ziegler, E. K. Athanassiou, R. N. Grass, A. Rossi, C. Hierold, A. Stemmer, W. J. Stark, *Angew. Chem.* **2009**, *121*, 230 – 233; *Angew. Chem. Int. Ed.* **2009**, *48*, 224 – 227; d) F. M. Koehler, M. Rossier, M. Waelle, E. K. Athanassiou, L. K. Limbach, R. N. Grass, D. Gunther, W. J. Stark, *Chem. Commun.* **2009**, 4862 – 4864.

[95] a) S. I. Stoeva, F. Huo, J.-S. Lee, C. A. Mirkin, *J. Am. Chem. Soc.* **2005**, *127*, 15362 – 15363; b) F. Caruso, M. Spasova, A. Susha, M. Giersig, R. A. Caruso, *Chem. Mater.* **2001**, *13*, 109 – 116; c) M. Giersig, M. Hilgendorff, *Eur. J. Inorg. Chem.* **2005**, 3571 – 3583.

[96] a) M. Fröba, R. Kohn, G. Bouffaud, O. Richard, G. Tendeloo, *Chem. Mater.* **1999**, *11*, 2858 – 2865; b) A. B. Bourlinos, A. Simopoulos, N. Boukos, D. Petridis, *J. Phys. Chem. B* **2001**, *105*, 7432 – 7437; c) J. Lee, S. Jin, Y. Hwang, J.-G. Park, H. M. Park, T. Hyeon, *Carbon* **2005**, *43*, 2536 – 2539; d) J. Lee, J. Kim, T. Hyeon, *Adv. Mater.* **2006**, *18*, 2073 – 2094; e) D. K. Yi, S. S. Lee, G. C. Papaefthymiou, J. Y. Ying, *Chem. Mater.* **2006**, *18*, 614 – 619; f) C. Graf, D. L. J. Vossen, A. Imhof, A. V. Blaaderen, *Langmuir* **2003**, *19*, 6693 – 6700; g) S. Huang, P. Yang, Z. Cheng, Y. Fan, D. Kong, J. Lin, *J. Phys. Chem. C* **2008**, *112*, 7130 – 7137; h) P. Wu, J. Zhu, Z. Xu, *Adv. Funct. Mater.* **2004**, *14*, 345 – 351; i) T. Sen, A. Sebastianelli, I. J. Bruce, *J. Am. Chem. Soc.* **2006**, *128*, 7130 – 7131; j) J. Zhou, W. Wu, D. Caruntu, M. H. Yu, A. Martin, J. F. Chen, C. J. O'Connor, W. L. Zhou, *J. Phys. Chem. C* **2007**, *111*, 17473 – 17477; k) L. Zhang, G. C. Papaefthymiou, J. Y. Ying, *J. Phys. Chem. B* **2001**, *105*, 7414 – 7423; l) Y. Zhu, L. Zhang, F. M. Schappacher, R. Pöttgen, J. Shi, S. Kaskel, *J. Phys. Chem. C* **2008**, *112*, 8623 – 8628; m) G. Clavel, Y. Guari, J. Larionova, C. Guerin, *New J. Chem.* **2005**, *29*, 275 – 279; n) J. Ge, Y. Hu, M. Biasini, W. P. Beyermann, Y. Yin, *Angew. Chem.* **2007**, *119*, 4420 – 4423; *Angew. Chem. Int. Ed.* **2007**, *46*, 4342 – 4345; o) A. F. Gross, M. R. Diehl, K. C. Beverly, E. K. Richman, S. H. Tolbert, *J. Phys. Chem. B* **2003**, *107*, 5475 – 5482; p) J. Kim, J. E. Lee, J. Lee, Y. H. Yu, B. C. Kim, K. An, Y. Hwang, C. H. Shin, J. G. Park, J. Kim, T. Hyeon, *J. Am. Chem. Soc.* **2006**, *128*, 688 – 689; q) R. P. Hodgkins, A. Ahniyaz, K. Parekh, L. M. Belova, L. Bergstrom, *Langmuir* **2007**, *23*, 8838 – 8844.

[97] C. Garcia, Y. Zhang, F. DiSalvo, V. Weisner, *Angew. Chem.* **2003**, *115*, 1564 – 1568; *Angew. Chem. Int. Ed.* **2003**, *42*, 1526 – 1530.

[98] N. C. King, R. A. Blackley, M. L. Wears, D. M. Newman, W. Zhou, D. W. Bruce, *Chem. Commun.* **2006**, 3414 – 3416.

[99] J. El Haskouri, S. Cabrera, C. Guillern, J. Latorre, A. Beitrán, M. D. Marcos, C. J. Gómez-García, D. Beitrán, P. Amorós, *Eur. J. Inorg. Chem.* **2004**, 1799 – 1803.

[100] W. Zhao, J. Gu, L. Zhang, H. Chen, J. Shi, *J. Am. Chem. Soc.* **2005**, *127*, 8916 – 8917.

[101] a) J. Lee, J. Kim, T. Hyeon, *Adv. Mater.* **2006**, *18*, 2073 – 2094; b) M. A. C. Durate, M. Grzelczak, V. Salguerino-Maceira, M. Giersig, L. M. Liz-Marzán, M. Farle, K. Sierazdki, R. Diaz, *J. Phys. Chem. B* **2005**, *109*, 19060 – 19063; c) J. Jang, H. Yoon, *Adv. Mater.* **2003**, *15*, 2088 – 2091; d) A. H. Lu, W.-C. Li, N. Matoussevitch, B. Spliethoff, H. Bonnemann, F. Schüth, *Chem. Commun.* **2005**, 98 – 100.

[102] Y. Li, T. Kaneko, T. Ogawa, M. Takahashi, R. Hatakeyama, *Chem. Commun.* **2007**, 254 – 256.

[103] F. Stoffelbach, A. Aqil, C. Jerome, R. Jerome, C. Detrembleur, *Chem. Commun.* **2005**, 4532 – 4533.

[104] S. A. Corr, Y. K. Gun′ko, A. P. Douvalis, M. Venkatesan, R. D. Gunning, P. D. Nellist, *J. Phys. Chem. C* **2008**, *112*, 1008 – 1018.

[105] H. P. Klug, L. E. Alexander, *X-Ray Diffraction Procedures For Polycrystalline and Amorphous Materials*, Wiley, New York, **1974**.

[106] M. P. Morales, S. Veintemillas-Verdaguer, M. O. Montero, C. J. Serna, A. Roig, L. Casas, B. Martinez, F. Sadiumenge, *Chem. Mater.* **1999**, *11*, 3058 – 3064.

[107] Q. Wang, A. Wu, L. Yu, Z. Liu, W. Xu, H. Yang, *J. Phys. Chem. C* **2009**, *113*, 19875 – 19882.

[108] P. Lindner, T. Zemb, Neutrons, *X Ray and Light Scattering Methods Applied to Soft Condensed Matter*, Elsevier, Dordrecht, **2002**.

[109] A. Guinier, G. Fournet, *Small-Angle Scattering of X-Rays*, Wiley, New York, **1955**.

[110] O. Glatter, O. Kratky, *Small Angle X-ray Scattering*, Academic Press, London, **1982**.

[111] E. V. Shtykova, X. Huang, X. Gao, J. C. Dyke, A. L. Schmucker, B. Dragnea, N. Remmes, D. V. Baxter, B. Stein, P. V. Konarev, D. I. Svergun, L. M. Bronstein, *J. Phys. Chem. C* **2008**, *112*, 16809 – 16817.

[112] S. Calvin, M. M. Miller, R. Goswami, S.-F. Cheng, S. P. Mulvaney, L. J. Whitman, V. G. Harris, *J. Appl. Phys.* **2003**, *94*, 778 – 783.

[113] a) G. Thomas, A. Hutten, *Nanostruct. Mater.* **1997**, *9*, 271 – 275; b) S. Calvin, M. M. Miller, R. Goswami, S.-F. Cheng, S. P. Mulvaney, L. J. Whitman, V. G. Harris, *J. Appl. Phys.* **2003**, *94*, 778 – 783; c) X.-C. Sun, N. Nava, *Nano Lett.* **2002**, *2*, 765 – 769.

[114] J. K. Lim, S. A. Majetich, R. D. Tilton, *Langmuir* **2009**, *25*, 13384 – 13393.

[115] a) T. J. Daou, J. M. Grenèche, G. Pourroy, S. Buathong, A. Derory, C. Ulhaq-Bouillet, B. Donnio, D. Guillon, S. Begin-Colin, *Chem. Mater.* **2008**, *20*, 5869 – 5875; b) Q. Wang, A. Wu, L. Yu, Z. Liu, W. Xu, H. Yang, *J. Phys. Chem. C* **2009**, *113*, 19875 – 19882; c) T. J. Daou, G. Pourroy, J. M. Grenèche, A. Bertin, D. Felder-Flesch, S. Begin-Colin, *Dalton Trans.* **2009**, 4442 – 4449.

[116] P. W. Selwood, *Chemisorption and Magnetization*, Academic Press, New York, **1975**.

[117] R. van Hardefeld, F. Hartog, *Surf. Sci.* **1969**, *15*, 189.

[118] F. J. Lázaro, J. L. García, V. Schünemann, C. Butzlaff, A. Larrea, M. A. Zaluska-Kotur, *Phys. Rev. B* **1996**, *53*, 13934 – 13941.

[119] D. Fiorani in *The Time Domain in Surface and Structural Dynamics* (Eds.: G. J. Long, F. Grandjean), Kluwer Academic Publishers, Dordrecht, **1988**, p. 391 (*NATO ASI Ser. C*, *Vol. 228*).

[120] S. Thakur, S. C. Katyal, A. Gupta, V. R. Reddy, S. K. Sharma, M. Knobel, M. Singh, *J. Phys. Chem. C* **2009**, *113*, 20785 – 20794.

[121] O. Ersen, S. Bégin, M. Houllè, J. Amadou, I. Janowska, J.-M. Grenèche, C. Crucifix, C. Pham-Huu, *J. Am. Chem. Soc.* **2008**, *8*, 1033 – 1040.

[122] V. Schünemann, H. Winkler, C. Butzlaff, A. X. Trautwein, *Hyperfine Interact.* **1994**, *93*, 1427 – 1432.

[123] S. Mørup, J.-A. Dumesic, H. Topsøe in *Applications of Mössbauer spectroscopy*, *Vol. II* (Ed.: R. L. Cohen), Academic Press, New York, **1980**, pp. 1 – 53.

[124] P. H. Christensen, S. Mørup, J. W. Niemantsverdriet, *J. Phys. Chem.* **1985**, *89*, 4898 – 4900.

[125] "Mössbauer Spectroscopy": V. Schünemann, H. Paulsen in *Application of Physical Methods to Inorganic and Bioinorganic Chemistry* (Eds.: R. A. Scott, C. M. Lukehart), Wiley, Chichester, **2007**.

[126] J. Balogh, D. Kaptás, I. Vincze, K. Temst, C. Van Haesendonck, *Phys. Rev. B* **2007**, *76*, 052408.

[127] L. M. Lacava, Z. G. M. Lacava, M. F. Da Silva, O. Silva, S. B. Chaves, R. B. Azevedo, F. Pelegrini, C. Gansau, N. Buske, D. Sabolovic, P. C. Morais, *Biophys. J.* **2001**, *80*, 2483 – 2486.

[128] A. H. Morrish, *The Physical Principles of Magnetism*, R. E. Krieger Publishing Company, Huntington, New York, **1980**.

[129] E. Schloemann, *J. Phys. Chem. Solids* **1958**, *6*, 257 – 266.

[130] E. Schloemann, J. R. Zeender, *J. Appl. Phys.* **1958**, *29*, 341 – 343.

[131] F. Schmidt, T. Meeder, *Surf. Sci.* **1981**, *106*, 397 – 402.

[132] a) J. H. Moon, J. W. Shin, S. Y. Kim, J. W. Park, *Langmuir* **1996**, *12*, 4621 – 4624; b) M. Rosenholm, M. Linden, *Chem. Mater.* **2007**, *19*, 5023 – 5034; c) S. Čampelj, D. Makovec, M. Drofenik, *J. Magn. Mater.* **2009**, *321*, 1346 – 1350; d) L. Polito, M. Colombo, D. Monti, S. Melato, E. Caneva, D. Prosperi, *J. Am. Chem. Soc.* **2008**, *130*, 12712 – 12724; e) B. Panella, A. Vargas, D. Ferri, A. Baiker, *Chem. Mater.* **2009**, *21*, 4316 – 4322.

[133] a) J. Tsuji, Palladium Reagents and Catalysts, Wiley-VCH, Weinheim, **2004**; b) H.-U. Blaser, A. Indolese, A. Schnyder, H. Steiner, M. Studer, *J. Mol. Catal. A* **2001**, *173*, 3 – 18; c) V. Polshettiwar, A. Molnar, *Tetrahedron* **2007**, *63*, 6949 – 6976; d) M. Moreno-Mañas, R. Pleixats, *Acc. Chem. Res.* **2003**, *36*, 638 – 643.

[134] P. D. Stevens, G. Li, J. Fan, M. Yen, Y. Gao, *Chem. Commun.* **2005**, 4435 – 4437.

[135] P. D. Stevens, J. Fan, H. M. R. Gardimalla, M. Yen, Y. Gao, *Org. Lett.* **2005**, *7*, 2085 – 2088.

[136] Y. Zheng, P. D. Stevens, Y. Gao, *J. Org. Chem.* **2006**, *71*, 537 – 542.

[137] Z. Wang, B. Shen, Z. Aihua, N. He, *Chem. Eng. J.* **2005**, *113*, 27 – 34.

[138] Z. Yinghuai, S. C. Peng, A. Emi, S. Zhenshun, Monalisa, R. A. Remp, *Adv. Synth. Catal.* **2007**, *349*, 1917 – 1922.

[139] G. Lu, W. Mal, R. Jin, L. Gao, *Synlett* **2008**, 1418 – 1420.

[140] B. Baruwati, D. Guin, S. V. Manorama, *Org. Lett.* **2007**, *9*, 5377 – 5380.

[141] a) V. Polshettiwar, B. Baruwati, R. S. Varma, *ACS Nano* **2009**, *3*, 728 – 736; b) V. Polshettiwar, M. N. Nadagouda, R. S. Varma, *Chem. Commun.* **2008**, 6318 – 6320.

[142] J. Liu, X. Peng, W. Sun, Y. Zhao, C. Xia, *Org. Lett.* **2008**, *10*, 3933 – 3936.

[143] J. Kim, J. E. Lee, J. Lee, Y. Jang, S.-W. Kim, K. An, J. H. Yu, T. Hyeon, *Angew. Chem.* **2006**, *118*, 4907 – 4911; *Angew. Chem. Int. Ed.* **2006**, *45*, 4789 – 4793.

[144] a) B. Yoon, C. M. Wai, *J. Am. Chem. Soc.* **2005**, *127*, 17174 – 17175; b) G. Korneva, H. Ye, Y. Gogotsi, D. Halverson, G. Friedman, J.-C. Bradley, K. G. Kornev, *Nano Lett.* **2005**, *5*, 879 – 884; c) A. H. Lu, F. Schüth, *Adv. Mater.* **2006**, *18*, 1793 – 1805; d) F. L. Deepak, N. S. John, A. Govindraj, G. U. Kulkarni, C. N. R. Rao, *Chem. Phys. Lett.* **2005**, *411*, 468 – 473.

[145] H. Yoon, S. Ko, J. Jang, *Chem. Commun.* **2007**, 1468 – 1470.

[146] S. Ko, J. Jang, *Angew. Chem.* **2006**, *118*, 7726 – 7729; *Angew. Chem. Int. Ed.* **2006**, *45*, 7564 – 7567.

[147] S. Luo, X. Zheng, H. Xu, X. Mi, L. Zhang, J.-P. Cheng, *Adv. Synth. Catal.* **2007**, *349*, 2431 – 2434.

[148] a) D. Basavaiah, P. D. Rao, R. S. Hyma, *Tetrahedron* **1996**, *52*, 8001 – 8062; b) D. Basavaiah, A. J. Rao, T. Satyanarayana, *Chem. Rev.* **2003**, *103*, 811 – 891.

[149] G. Chouhan, D. Wang, H. Alper, *Chem. Commun.* **2007**, 4809 – 4811.

[150] R. B. Bedford, M. Betham, D. W. Bruce, S. A. Davis, R. M. Frost, M. Hird, *Chem. Commun.* **2006**, 1398 – 1400.

[151] a) M. Takasaki, Y. Motoyama, K. Higashi, S. H. Yoon, I. Mochida, H. Nagashima, *Org. Lett.* **2008**, *10*, 1601 – 1604; b) E. Molnár, G. Tasi, Z. Konya, I. Kiricsi, *Catal. Lett.* **2005**, *101*, 159 – 167; c) S. Miao, Z. Liu, B. Han, J. Huang, Z. Sun, J. Zhang, T. Jian, *Angew. Chem.* **2006**, *118*, 272 – 275; *Angew. Chem. Int. Ed.* **2006**, *45*, 266 – 269; d) I. S. Park, M. S. Kwon, K. Y. Kang, J. S. Lee, J. Park, *Adv. Synth. Catal.* **2007**, *349*, 2039 – 2047; e) J. M. Thomas, B. F. G. Johnson, R. Raja, G. Sankar, P. A. Midgley, *Acc. Chem. Res.* **2003**, *36*, 20 – 30.

[152] C.-H. Jun, Y. J. Park, Y.-R. Yeon, J.-R. Choi, W.-R. Lee, S.-J. Ko, J. Cheon, *Chem. Commun.* **2006**, 1619 – 1621.

[153] D. K. Yi, S. S. Lee, J. Y. Ying, *Chem. Mater.* **2006**, *18*, 2459 – 2461.

[154] D. Guin, B. Baruwati, S. V. Manorama, *Org. Lett.* **2007**, *9*, 1419 – 1421.

[155] V. Polshettiwar, B. Baruwati, R. S. Varma, *Green Chem.* **2009**, *11*, 127 – 131.

[156] B. Baruwati, V. Polshettiwar, R. S. Varma, *Tetrahedron Lett.* **2009**, *50*, 1215 – 1218.

[157] L. M. Rossi, F. P. Silva, L. L. R. Vano, P. K. Kiyohara, E. L. Duarte, R. Itri, R. Landers, G. Machado, *Green Chem.* **2007**, *9*, 379 – 385.

[158] M. J. Jacinto, P. K. Kiyohara, S. H. Masunaga, R. F. Jardim, L. M. Rossi, *Appl. Catal. A* **2008**, *338*, 52 – 57.

[159] M. J. Jacinto, O. H. C. F. Santos, R. F. Jardim, R. Landers, L. M. Rossi, *Appl. Catal. A.* **2009**, *360*, 177 – 182.

[160] Y. Wang, J.-K. Lee, *J. Mol. Catal. A* **2007**, *263*, 163 – 168.

[161] R. Abu-Reziq, D. Wang, M. Post, H. Alper, *Adv. Synth. Catal.* **2007**, *349*, 2145 – 2150.

[162] J. Zhang, Y. Wang, H. Ji, Y. Wei, N. Wu, B. Zuo, Q. Wang, *J. Catal.* **2005**, *229*, 114 – 118.

[163] U. Laska, C. G. Frost, P. K. Plucinski, G. J. Price, *Catal. Lett.* **2008**, *122*, 68 – 75.

[164] S. C. Tsang, V. Caps, I. Paraskevas, D. Chadwick, D. Thompsett, *Angew. Chem.* **2004**, *116*, 5763 – 5767; *Angew. Chem. Int. Ed.* **2004**, *43*, 5645 – 5649.

[165] A. H. Lu, W. Schmidt, N. Matoussevitch, H. Bonnemann, B. Spliethoff, B. Tesche, E. Bill, W. Kiefer, F. Schüth, *Angew. Chem.* **2004**, *116*, 4403 – 4406; *Angew. Chem. Int. Ed.* **2004**, *43*, 4303 – 4306.

[166] T.-J. Yoon, W. Lee, Y-S. Oh, J.-K. Lee, *New J. Chem.* **2003**, *27*, 227 – 229.

[167] Y. Jiang, Q. Gao, *J. Am. Chem. Soc.* **2006**, *128*, 716 – 717.

[168] R. Abu-Reziq, H. Alper, D. Wang, M. L. Post, *J. Am. Chem. Soc.* **2006**, *128*, 5279 – 5282.

[169] F. Shi, M. K. Tse, M. M. Pohl, A. Bruckner, S. Zhang, M. Beller, *Angew. Chem.* **2007**, *119*, 9022 – 9024; *Angew. Chem. Int. Ed.* **2007**, *46*, 8866 – 8868.

[170] V. Polshettiwar, R. S. Varma, *Org. Biomol. Chem.* **2009**, *7*, 37 – 40.

[171] M. Kotani, T. Koike, K. Yamaguchi, N. Mizuno, *Green Chem.* **2006**, *8*, 735 – 741.

[172] U. Schuchardt, D. Cardoso, R. Sercheli, R. Pereira, R. S. da Cruz, M. C. Guerreiro, D. Mandelli, E. V. Spinace, E. L. Pires, *Appl. Catal. A* **2001**, *211*, 1 – 17.

[173] J. Tong, L. Bo, Z. Li, Z. Lei, C. Xia, *J. Mol. Catal. A* **2009**, *307*, 58 – 63.

[174] L. Aschwanden, B. Panella, P. Rossbach, B. Keller, A. Baiker, *ChemCatChem* **2009**, *1*, 111 – 115.

[175] a) K. Kaneda, K. Ebitani, T. Mizugaki, K. Mori, *Bull. Chem. Soc. Jpn.* **2006**, *79*, 981; b) K. Yamaguchi, K. Mori, T. Mizugaki, K. Ebitani, K. Kaneda, *J. Am. Chem. Soc.* **2000**, *122*, 7144 – 7145; c) K. Mori, T. Hara, T. Mizugaki, K. Ebitani, K. Kaneda, *J. Am. Chem. Soc.* **2004**, *126*, 10657 – 10666.

[176] K. Mori, S. Kanai, T. Hara, T. Mizugaki, K. Ebitani, K. Jitsukawa, K. Kaneda, *Chem. Mater.* **2007**, *19*, 1249 – 1256.

[177] T. Arai, T. Sato, H. Kanoh, K. Kaneka, K. Oruma, A. Yanagisawa, *Chem. Eur. J.* **2008**, *14*, 882 – 885.
[178] A. Schätz, R. N. Grass, W. J. Stark, O. Reiser, *Chem. Eur. J.* **2008**, *14*, 8262 – 8266.
[179] M. Shokouhimehr, Y. Piao, J. Kim, Y. Jang, T. Hyeon, *Angew. Chem.* **2007**, *119*, 7169 – 7173; *Angew. Chem. Int. Ed.* **2007**, *46*, 7039 – 7043.
[180] S. Shylesh, J. Schweitzer, S. Demeshko, V. Schünemann, S. Ernst, W. R. Thiel, *Adv. Synth. Catal.* **2009**, *351*, 1789 – 1795.
[181] H. Tang, C. H. Yu, W. Oduoro, H. He, S. C. Tsang, *Langmuir* **2008**, *24*, 1587 – 1590.
[182] A. Corma, H. Garcia, *Chem. Rev.* **2002**, *102*, 3837 – 3892.
[183] K. Mori, K. Sugihara, Y. Kondo, T. Takeuchi, S. Morimoto, H. Yamashita, *J. Phys. Chem. C* **2008**, *112*, 16478 – 16483.
[184] D.-H. Zhang, G.-D. Li, J.-X. Li, J.-S. Chen, *Chem. Commun.* **2008**, 3414 – 3416.
[185] a) J. Seayad, B. List, *Org. Biomol. Chem.* **2005**, *3*, 719 – 724; b) D. Enders, O. Niemeier, A. Henseler, *Chem. Rev.* **2007**, *107*, 5606 – 5655.
[186] V. Polshettiwar, B. Baruwati, R. S. Varma, *Chem. Commun.* **2009**, 1837 – 1839.
[187] B. Lygo, B. I. Andrews, *Acc. Chem. Res.* **2004**, *37*, 518 – 525.
[188] M. Kawamura, K. Sato, *Chem. Commun.* **2006**, 4718 – 4719.
[189] M. Kawamura, K. Sato, *Chem. Commun.* **2007**, 3404 – 3405.
[190] a) C. J. Pedersen, *J. Am. Chem. Soc.* **1967**, *89*, 2495 – 2496; b) R. M. Izatt, K. Pawlak, J. S. Bradshaw, R. L. Bruening, *Chem. Rev.* **1995**, *95*, 2529 – 2586; c) D. Alabenese, D. Landini, A. Maia, M. Penso, *J. Mol. Catal. A* **1999**, *150*, 113 – 131.
[191] a) R. Noyori, *Adv. Synth. Catal.* **2003**, *345*, 15 – 32; b) M. Studer, H. U. Blaser, C. Exner, *Adv. Synth. Catal.* **2003**, *345*, 45 – 65; c) H. U. Blaser, C. Malan, B. Pugin, F. Spindler, H. Steiner, M. Studer, *Adv. Synth. Catal.* **2003**, *345*, 103 – 151.
[192] D. J. Cole-Hamilton, *Adv. Synth. Catal.* **2006**, *348*, 1341 – 1351.
[193] S. Luo, X. Zheng, J.-P. Cheng, *Chem. Commun.* **2008**, 5719 – 5721.
[194] O. Gleeson, R. Tekoriute, Y. K. Gun′ko, S. J. Connon, *Chem. Eur. J.* **2009**, *15*, 5669 – 5673.
[195] F. Neaţu, A. Kraynov, L. D'Souza, V. I. Parvulescu, K. Kranjc, M. Kocevar, V. Kuneser, R. Richards, *Appl. Catal. A* **2008**, *346*, 28 – 35.
[196] B. Panella, A. Vargas, A. Baiker, *J. Catal.* **2009**, *261*, 88 – 93.
[197] A. Schätz, M. Hager, O. Reiser, *Adv. Funct. Mater.* **2009**, *19*, 2109 – 2115.
[198] a) J. Lim, S. N. Riduan, S. S. Lee, J. Y. Ying, *Adv. Synth. Catal.* **2008**, *350*, 1295 – 1308; b) J. M. Fraile, J. I. Garcia, V. Martinez-Merino, J. A. Mayoral, L. Salvatella, *J. Am. Chem. Soc.* **2001**, *123*, 7616 – 7625.
[199] D. Lee, J. Lee, H. Lee, S. Jin, T. Hyeon, B. M. Kim, *Adv. Synth. Catal.* **2006**, *348*, 41 – 46.
[200] S. Kobayashi, M. Sugiura, *Adv. Synth. Catal.* **2006**, *348*, 1496 – 1504.
[201] J. Lin, Y. Zhang, D. Han, Q. Gao, C. Li, *J. Mol. Catal. A* **2009**, *298*, 31 – 35.
[202] C. S. Gill, B. A. Price, C. W. Jones, *J. Catal.* **2007**, *251*, 145 – 152.
[203] a) P. K. Mascharak, *Coord. Chem. Rev.* **2002**, *225*, 201 – 214; b) K. L. Breno, M. D. Pluth, D. R. Tyler, *Organometallics* **2003**, *22*, 1203 – 1211; c) J. H. Kim, J. Britten, J. Chin, *J. Am. Chem. Soc.* **1993**, *115*, 3618 – 3622.
[204] V. Polshettiwar, R. S. Varma, *Chem. Eur. J.* **2009**, *15*, 1582 – 1586.
[205] C. Ó Dálaigh, S. A. Corr, Y. Gun′ko, S. J. Connon, *Angew. Chem.* **2007**, *119*, 4407 – 4410; *Angew. Chem. Int. Ed.* **2007**, *46*, 4329 – 4332.
[206] Y. Lin, H.-T. Chen, S. Huh, J. W. Wiench, M. Pruski, V. S.-Y. Lin, *J. Am. Chem. Soc.* **2005**, *127*, 13305 – 13311.
[207] N. T. S. Phan, C. W. Jones, *J. Mol. Catal. A* **2006**, *253*, 123 – 131.
[208] J. D. Bass, S. L. Anderson, A. Katz, *Angew. Chem.* **2003**, *115*, 5377 – 5380; *Angew. Chem. Int. Ed.* **2003**, *42*, 5219 – 5222.
[209] a) T. Welton, *Chem. Rev.* **1999**, *99*, 2071 – 2084; b) V. V. Namboodiri, R. S. Varma, *Chem. Commun.* **2002**, 342 – 343; c) X. Mu, J. Meng, Z. Li, Y. Kou, *J. Am. Chem. Soc.* **2005**, *127*, 9694 – 9695; d) A. Riisager, R. Fehrmann S. Flicker, R. Van Hal, M. Haumann, P. Wasserscheid, *Angew. Chem.* **2005**, *117*, 826 – 830; *Angew. Chem. Int. Ed.* **2005**, *44*, 815 – 819.
[210] Y. Zhang, Y. Zhao, C. Xia, *J. Mol. Catal. A* **2009**, *306*, 107 – 112.
[211] a) A. David, M. A. Vannice, *J. Catal.* **2006**, *237*, 349 – 358; b) A. Perosa, P. Tundo, M. Selva, P. Canton, *Chem. Commun.* **2006**, 4480 – 4481; c) Y. Zhang, S. Liao, Y. Xu, *Tetrahedron Lett.* **1994**, *35*, 4599 – 4602.
[212] T. Hara, T. Kaneta, K. Mori, T. Mitsudome, T. Mizugaki, K. Ebitani, K. Kaneda, *Green Chem.* **2007**, *9*, 1246 – 1251.
[213] M. S. Kwon, I. S. Park, J. S. Jang, J. S. Lee, J. Park, *Org. Lett.* **2007**, *9*, 3417 – 3419.
[214] X. Zheng, S. Luo, l. Zhang, J.-P. Cheng, *Green Chem.* **2009**, *11*, 455 – 458.
[215] S. Ding, Y. Xing, M. Radosz, Y. Shen, *Macromolecules* **2006**, *39*, 6399 – 6405.
[216] N. T. S. Phan, C. S. Gill, J. V. Nguyen, Z. J. Zhang, C. W. Jones, *Angew. Chem.* **2006**, *118*, 2267 – 2270; *Angew. Chem. Int. Ed.* **2006**, *45*, 2209 – 2212.
[217] R. Abu-Reziq, D. Wang, M. Post, H. Alper, *Chem. Mater.* **2008**, *20*, 2544 – 2550.
[218] a) L. Zhang, J. C. Yu, *Chem. Commun.* **2003**, 2078 – 2079; b) H. Luo, C. Wang, Y. Yan, *Chem. Mater.* **2003**, *15*, 3841 – 3846; c) E. Stathatos, P. Lianos, *Adv. Mater.* **2007**, *19*, 3338 – 3341; d) M. R. Hoffmann, S. T. Martin, W. Choi, D. W. Bahnemann, *Chem. Rev.* **1995**, *95*, 69 – 96; e) S. C. Yang, D. J. Yang, J. Y. Kim, J. M. Hong, H. G. Kim, I. D. Kim, H. J. Lee, *Adv. Mater.* **2008**, *20*, 1059 – 1064.
[219] a) D. Beydoun, R. Amal, G. K.-C. Low, S. McEvoy, *J. Phys. Chem. B* **2000**, *104*, 4387 – 4396; b) B. P. Zhang, J. L. Zhang, F. Chen, *Res. Chem. Intermed.* **2008**, *34*, 375 – 379; c) T. A. Gad-Allah, S. Kato, S. Satokawa, T. Kojima, *Solid State Sci.* **2007**, *9*, 737 – 743.
[220] C. Wang, L. Yin, L. Zhang, L. Kang, X. Wang, R. Gao, *J. Phys. Chem. C* **2009**, *113*, 4008 – 4011.
[221] S. Xuan, W. Jiang, X. Gong, Y. Hu, Z. Chen, *J. Phys. Chem. C* **2009**, *113*, 553 – 558.
[222] J. Ge, T. Huynh, Y. Hu, Y. Yin, *Nano Lett.* **2008**, *8*, 931 – 934.
[223] J. Ge, Q. Zhang, T. Zhang, Y. Yin, *Angew. Chem.* **2008**, *120*, 9056 – 9060; *Angew. Chem. Int. Ed.* **2008**, *47*, 8924 – 8928.